USACERL Technical Report EC-94/19
May 1994
Noise Mitigation and Noise Impact Management Practices

Comparison of Barriers and Partial Enclosures for Rifle Range Noise Reduction

by
Larry L. Pater
Eric R. Sandeen
George Swenson, Jr.
Kenneth McK. Eldred
Raman Yousefi
Walter Alvendia

The noise from small-arms firing at Army rifle ranges can disturb the surrounding community, generating complaints and attempts to curtail necessary training activities. The U.S. Army Construction Engineering Research Laboratories (USACERL) is developing methods to reduce such noise disturbances.

This investigation experimentally and analytically compared the rifle range noise reduction of barriers and partial enclosures. The barrier was a wall located behind the firing line, and the partial enclosure was an open front shed with the firing line located within the shed. Results of the experiments showed that the shed did not outperform the rear wall, a significant outcome because walls are less expensive to build than sheds. Evidence substantiates that this is primarily a consequence of gun muzzle blast directivity.

Barrier design curves were also generated by experimental algorithm. The optimum distance from rifle to rear wall for maximum insertion loss was calculated to be about 5 m for the test configuration. An investigation into the effect of sound wave interaction with the ground on achieved noise reduction at the test site showed that excess attenuation for a propagation path close to the ground can substantially reduce achieved barrier insertion loss.

The contents of this report are not to be used for advertising, publication, or promotional purposes. Citation of trade names does not constitute an official endorsement or approval of the use of such commercial products. The findings of this report are not to be construed as an official Department of the Army position, unless so designated by other authorized documents.

DESTROY THIS REPORT WHEN IT IS NO LONGER NEEDED

DO NOT RETURN IT TO THE ORIGINATOR

REPORT DOCUMENTATION PAGE

Form Approved
OMB No. 0704-0188

1. AGENCY USE ONLY (Leave Blank)	2. REPORT DATE	3. REPORT TYPE AND DATES COVERED
	May 1994	Final

4. TITLE AND SUBTITLE
Comparison of Barriers and Partial Enclosures for Rifle Range Noise Reduction

5. FUNDING NUMBERS
4A162720
A896
NN-TU1

6. AUTHOR(S)
Larry L. Pater, Eric R. Sandeen, George Swenson, Jr., Kenneth McK. Eldred, Raman Yousefi, and Walter Alvendia

7. PERFORMING ORGANIZATION NAME(S) AND ADDRESS(ES)
U.S. Army Construction Engineering Research Laboratories (USACERL)
P.O. Box 9005
Champaign, IL 61826-9005

8. PERFORMING ORGANIZATION REPORT NUMBER
TR EC-94/19

9. SPONSORING/MONITORING AGENCY NAME(S) AND ADDRESS(ES)
Office of the Assistant Chief of Engineers (OACE)
ATTN: ENVR-E
Room 1E685, The Pentagon
Washington, D.C. 20310-2600

10. SPONSORING/MONITORING AGENCY REPORT NUMBER

11. SUPPLEMENTARY NOTES
Copies are available from the National Technical Information Service, 5285 Port Royal Road, Springfield, VA 22161.

12a. DISTRIBUTION/AVAILABILITY STATEMENT
Approved for public release; distribution is unlimited.

12b. DISTRIBUTION CODE

13. ABSTRACT (Maximum 200 words)

The noise from small-arms firing at Army rifle ranges can disturb the surrounding community, generating complaints and attempts to curtail necessary training activities. The U.S. Army Construction Engineering Research Laboratories (USACERL) is developing methods to reduce such noise disturbances.

This investigation experimentally and analytically compared the rifle range noise reduction of barriers and partial enclosures. The barrier was a wall located behind the firing line, and the partial enclosure was an open front shed with the firing line located within the shed. Results of the experiments showed that the shed did not outperform the rear wall, a significant outcome because walls are less expensive to build than sheds. Evidence substantiates that this is primarily a consequence of gun muzzle blast directivity.

Barrier design curves were also generated by experimental algorithm. The optimum distance from rifle to rear wall for maximum insertion loss was calculated to be about 5 m for the test configuration. An investigation into the effect of sound wave interaction with the ground on achieved noise reduction at the test site showed that excess attenuation for a propagation path close to the ground can substantially reduce achieved barrier insertion loss.

14. SUBJECT TERMS
firing shed
noise barriers
noise reduction
rifle ranges

15. NUMBER OF PAGES
110

16. PRICE CODE

17. SECURITY CLASSIFICATION OF REPORT	18. SECURITY CLASSIFICATION OF THIS PAGE	19. SECURITY CLASSIFICATION OF ABSTRACT	20. LIMITATION OF ABSTRACT
Unclassified	Unclassified	Unclassified	SAR

FOREWORD

This research was done for the Office of the Assistant Chief of Engineers (OACE) under Project 4A162720A896, "Environmental Quality Technology"; Work Unit No. NN-TU1, "Barriers and Structures for Weapon Noise Mitigation." The OACE technical monitor was Timothy Julious, ENVR-E.

The work was done by the Acoustics Team (ECA), Environmental Compliance Modeling and Simulation Division (EC), Environmental Sustainment Laboratory (EL), of the U.S. Army Construction Engineering Research Laboratories (USACERL). The USACERL principal investigator was Dr. Larry L. Pater. Special gratitude is owed to Dr. Michael White of USACERL for his interest, ideas, and discussion during the project. The University of Illinois, Urbana is acknowledged for allowing these experiments to be conducted at their Bondville field research site. Dr. Paul Schomer is Chief, CECER-ECA; John Bandy is Chief, CECER-EC, and Bill Goran is Chief, CECER-EL. The USACERL technical editor was William J. Wolfe, Information Management Office.

LTC David J. Rehbein is Commander of USACERL and Dr. L.R. Shaffer is Director.

CONTENTS

		Page
	FOREWORD	2
	CONTENTS	3
	LIST OF FIGURES AND TABLES	4
1	INTRODUCTION	9
	Background	9
	Objectives	10
	Approach	10
	Mode of Technology Transfer	10
2	DESIGN AND CONSTRUCTION OF NOISE MITIGATION STRUCTURE	14
3	EXPERIMENTAL ARRANGEMENT AND PROCEDURES FOR INSERTION LOSS MEASUREMENTS	16
4	EXPERIMENTAL ARRANGEMENT AND PROCEDURES FOR GROUND INTERACTION INVESTIGATION	22
5	DATA REDUCTION	27
6	DISCUSSION OF RESULTS	29
	Analytical Insertion Loss Results	29
	Experimental Insertion Loss Results	33
	Experimental Excess Ground Attenuation Results	35
	Design Charts	38
7	CONCLUSIONS	78
	REFERENCES	79
	APPENDIX A: Calculations of Insertion Loss Using a Simple Approximate Barrier Design Algorithm	A1
	APPENDIX B: An Evaluation of Insertion Loss by a Rigorous Diffraction Algorithm	B1
	APPENDIX C: Effect of Atmospheric Absorption on the Source Spectrum	C1
	DISTRIBUTION	

FIGURES

Number		Page
1	Propagation Paths and Source Locations for Firing Shed Experiments	11
2	Assumed Model for Gun Muzzle Blast Far Field Directivity	11
3	Angle From DOF to Barrier Top Edge for Shed and Wall	12
4	Firing Shed Dimensions (in Meters)	14
5	The Experimental Shed	15
6	Experimental Layout Showing Microphone Array for Insertion Loss Experiments	18
7	Condenser Microphone Instrumentation System	19
8	Condenser Microphone Arrangement	20
9	Piezoresistive Microphone Instrumentation System	21
10	Layout for the Ground Interaction Experiments	23
11	Firing Positions for the Ground Interaction Experiments	24
12	Microphone Pole Used for the Ground Interaction Experiments	25
13	Data Reduction System	28
14	Source Spectra Used for Insertion Loss Calculations, Illustrated With and Without A-Frequency Weighting	40
15	Calculated Effect of Diffraction Around Shed Roofline and of Frequency Weighting on Source Spectrum, for -1 m Gun Location and 180-Degree Azimuth	41
16	Calculated Unweighted Insertion Loss at 180-Degree Azimuth vs. Source Location, for a Structure of Infinite Length, Structure Height 7 m, Source Height 0.5 m	42
17	Calculated Unweighted Insertion Loss at 180-Degree Azimuth vs. Source Location, for Structure Length of 20 m, Structure Height of 7 m, Source Height of 0.5 m	42
18	Calculated Unweighted Insertion Loss for the -1 m Source Location, for a Gun Firing Normal to the Shed Front	45
19	Calculated A-Weighted Insertion Loss for the -1 m Source Location, for a Gun Firing Normal to the Shed Front	45

FIGURES (Cont'd)

Number		Page
20	Calculated Unweighted Insertion Loss for an Isotropic Source Located at the -1 m Source Location	46
21	Calculated Unweighted Insertion Loss for the +5 m Source Location, for a Gun Firing Normal to the Wall	46
22	A Comparison of Calculated Unweighted Insertion Loss Due to a Shed (-1 m Source Location) and a Rear Wall (+5 m Source Location) for an Isotropic Source	47
23	A Comparison of Calculated Unweighted Insertion Loss Due to a Shed (-1 m Source Location) and a Rear Wall (+5 m Source Location) for a Gun Firing Normal to the Barrier	47
24	Summary of Calculated Unweighted Insertion Loss for Various Combinations of Source Location and Source Directivity	48
25	Summary of Calculated A-Weighted Insertion Loss for Various Combinations of Source Location and Source Directivity	48
26	Calculated Unweighted Insertion Loss Results From Two Diffraction Algorithms for an Isotropic Source Shielded by a Barrier (7 m High by 14 m Width)	49
27	Calculated Unweighted Insertion Loss Results From Two Diffraction Algorithms for a Gun Firing Normal to a Barrier (7 m High by 14 m Base Width)	49
28	Shed and Wall Experimental FSEL Insertion Loss for Gun Firing Normal to Barrier (South)	56
29	Shed and Wall Experimental ASEL Insertion Loss for Gun Firing Normal to Barrier (South)	56
30	Shed and Wall Experimental FSEL Insertion Loss for Gun Firing Parallel to Barrier (West)	57
31	Shed and Wall Experimental ASEL Insertion Loss for Gun Firing Parallel to Barrier (West)	57
32	Shed and Wall Experimental FSEL Insertion Loss for Both Gun Firing Directions	58
33	Shed and Wall Experimental ASEL Insertion Loss for Both Gun Firing Directions	58
34	Analytical and Experimental A-Weighted Shed Insertion Loss for Gun Firing Normal to Shed Front	60

FIGURES (Cont'd)

Number		Page
35	Experimental FSEL for Various Propagation Paths Over Two Types of Ground Cover	64
36	Experimental ASEL for Various Propagation Paths Over Two Types of Ground Cover	64
37	Source Microphone Waveform for High Gun, Test 3, Round 1, Mic # 1 (Gun Height 2.85 m, Mic Height 1.70 m)	65
38	Source Spectra for High Gun and Low Gun, Ground Reflection Excluded, for Ground Interaction Experiment	66
39	Spectra for High Gun Over Grass for Various Microphone Heights	66
40	Spectra for Low Gun Over Grass for Various Microphone Heights	67
41	Spectra for High Gun Over Beans for Various Microphone Heights	67
42	Spectra for Low Gun Over Beans for Various Microphone Heights	68
43	Spectra at 1.22 m Microphone Height for Various Propagation Paths	68
44	Source and Barrier Edge Spectra, Ground Reflection Excluded, for Insertion Loss Experiments	71
45	Spectra at 180 Degrees, 80 m	71
46	Spectra at 180 degrees, 242 m	72
47	Spectra at 150 degrees, 279 m	72
48	Spectra at 120 degrees, 161 m	73
49	Spectra at 90 degrees, 150 m	73
50	Calculated Insertion Loss for Various Values of H (Barrier Height Above Source), for a Shed of Infinite Length With an Isotropic Source Located at S = -1 m	74
51	Calculated Insertion Loss for Various Values of H, for a Shed Length of 20 m With an Isotropic Source Located at S = -1 m	74
52	Calculated Insertion Loss for Various Values of H, for a Shed of Infinite Length With a Gun Located at S = -1 m Firing Normal to the Shed Front	75
53	Calculated Insertion Loss for Various Values of H, for a Shed Length of 20 m With a Gun Located at S = -1 m Firing Normal to the Shed Front	75

FIGURES (Cont'd)

Number		Page
54	Calculated Insertion Loss for Various Values of H, for a Shed of Infinite Length With a Gun Located at S = -1 m Firing Normal to the Shed Front	76
55	Calculated A-Weighted Insertion Loss for Various Values of H, for a Shed of Infinite Length With a Gun Located at S = -1 m Firing Normal to the Shed Front	76
56	Calculated Insertion Loss for Various Values of H, for a Wall of Infinite Length With a Gun Located at S = +5 m Firing Normal to the Barrier	77
57	Calculated A-Weighted Insertion Loss for Various Values of H, for a Wall of Infinite Length With a Gun Located at S = +5 m Firing Normal to the Barrier	77
B1	Plan and Elevation Diagrams of a Spherical Acoustic Shelter	B2
B2	Assumed Small Arms Spectrum	B4
B3	Assumed Rifle Directivity Pattern and Step Approximations	B4
B4	Structural Directivity Patterns for the Composite Isotropic Source	B5
B5	Structural Directivity Patterns for the Composite Directional Source	B5
B6	Structural Insertion Loss for the Isotropic Source	B6
B7	Structural Insertion Loss for the Directional Source	B6
C1	Effect of Atmospheric Absorption on Source Spectrum at Several Distances	C2

TABLES

1	Microphone Locations for Insertion Loss Measurements	13
2	Mean Propagation Path Heights for Ground Interaction Experiments	26
3	Calculated Results From Appendix A for Insertion Loss to the Rear for Infinite Length Barrier	43
4	Calculated Results From Appendix A for Insertion Loss to the Rear for 20 m Long Finite Barrier	44
5	Typical Detailed Sound Level Data From Insertion Loss Experiment	50
6	Insertion Loss Experiments	51
7	Measured Shed Insertion Loss for Gun Firing South	52

TABLES (Cont'd)

Number		Page
8	Measured Wall Insertion Loss for Gun Firing South	53
9	Measured Shed Insertion Loss for Gun Firing West	54
10	Measured Wall Insertion Loss for Gun Firing West	55
11	Mean Experimental Insertion Loss to the Rear	59
12	The Effect of Excess Attenuation on Measured Shed Insertion Loss for Gun Firing South (Data of Table 7)	61
13	The Effect of Excess Attenuation on Measured Wall Insertion Loss for Gun Firing South (Data of Table 8)	62
14	Ground Interaction Experiments	63
15	Overall Summary of Ground Interaction Experimental Results	69
16	Effect of Path Height on Measured Noise Level	70
A1	Calculated Barrier Insertion Loss for the - 1 m Gun Location	A5
A2	Summary of Calculated Results for Various Combinations of Gun Location, Direction of Fire and Frequency Weighting	A16
A3	Insertion Loss at 180° vs. Source Location, for Structure of Infinite Length, Structure Height 7 m, Source Height 0.5 m	A19
A4	Insertion Loss at 180° vs. Source Location, for Structure Length of 20 m, Structure Height 0.5 m	A20
C1	Attenuation Due to Atmospheric Absorption for Several Propogation Distances, T= 20 °C, 70% Relative Humidity, Standard Sea L	C2

COMPARISON OF BARRIERS AND PARTIAL ENCLOSURES FOR RIFLE RANGE NOISE REDUCTION

1 INTRODUCTION

Background

Small arms (rifles and pistols) are fired extensively at rifle ranges for military and law enforcement training, and for recreational and competitive shooting. The noise of such firing can disturb the surrounding community, which can lead to noise complaints and attempts to curtail the firing activity. The Environmental Acoustics Team of the U.S. Army Construction Engineer ıg Research Laboratories (USACERL) is developing methods to reduce such noise disturbance.

A number of noise events are associated with gunfire. Minor contributors to far field noise include propellant gas escaping at locations other than the muzzle, bullet wake noise, noise from actuating gun mechanisms, and noise due to a projectile hitting a target. The most important noise events for small arms are normally the muzzle blast noise and a bow shock (sonic boom) associated with a supersonic projectile. The projectile bow shock noise is important only in a portion of the noise field forward of the gun unless structures are present that reflect the bow shock noise to the rear (Pater 1981). The noise event of primary interest to this investigation was the muzzle blast noise to the rear of a rifle range.

One way to reduce noise exposure is to use a noise barrier. Figure 1* shows sound propagation paths from source to receiver with and without a barrier. The amount of sound energy diffracted to a receiver located in the shadow zone depends on the frequency of the sound, the size of the barrier, and the juxtaposition of source, receiver, and barrier. At lower frequencies, more sound energy is diffracted around a barrier of given size, yielding less noise reduction. Noise shielding structures such as partial enclosures and walls can be useful for small arms because the acoustic energy is concentrated at higher frequencies, so that barriers of moderate size can provide effective noise shielding.

The quantity used to characterize the amount of noise reduction achieved by a noise barrier is "insertion" loss, defined as the difference in sound levels before and after the installation of a sound-reducing structure (American National Standards Institute [ANSI] S12.9-1987). In general, a noise barrier is not characterized by a single value of insertion loss; rather, the insertion loss due to diffraction effects will vary with azimuth and with distance. In addition, sound wave propagation and ground interaction conditions can cause substantial variation in the achieved insertion loss of a given barrier for a given noise source.

A previous USACERL study investigated the noise from small arms rifle ranges (McBryan 1978), and a more recent study suggested possible methods to mitigate this noise (Eldred 1990). One technique that seemed promising for reducing noise in the region to the rear of the range was to partially enclose the firing line in an open-front shed. A recent study found that a firing shed that partially encloses the firing line can provide significant noise reduction in the region behind the firing line; but also indicated that source directivity must also be considered (Pater 1992). Directivity refers to the fact that some sources do not radiate acoustic power equally in all directions. Figure 2 shows that, at a given distance, a gun typically exhibits its greatest noise level directly ahead of the gun, and noise levels that decrease

* All figures and tables are included at the end of their associated chapter.

at increasing angles from the direction of fire, to a minimum level directly behind the gun (Schomer 1979; Pater 1981).

Preliminary calculations for nondirective sources showed that the partial enclosure should provide significantly more insertion loss than the wall. However, for source directivity typical of rifles, the calculations predicted that the shed and a simple rear wall of similar height would yield approximately equal insertion loss (Pater 1992). In this situation, gun directivity causes the field strength at the barrier edge to be greater than that of a nondirective source having equal field strength in the direct-to-receiver direction, resulting in reduced insertion loss. This increase in field strength at the barrier edge is greater for the partial enclosure than for the rear wall because of the smaller angle between the direction of fire and the azimuth to the barrier edge (Figures 2 and 3), so that the directivity causes a larger reduction in insertion loss for the shed than for the wall. This information, combined with the fact that a wall is less expensive to construct than a firing shed, indicated a need for further investigation of these two noise-reduction methods.

Objectives

The ultimate motivation for this rifle range noise mitigation effort is to help preserve Army training capability. The specific objectives of this study were to experimentally test and compare the rifle range noise reduction performance of a partial enclosure of the firing line (open front firing shed) with that of a simple wall barrier located behind the firing line.

Approach

Theoretical insertion loss values of the shed and wall were calculated by two analytical techniques: a method based on the Federal Highway Administration (FHWA) highway barrier design algorithm, and a classical diffraction analysis in a spherical coordinate system. A direct experimental comparison was also made of the insertion loss of the two structures. A partial-enclosure firing shed was designed and constructed. Measurements were made of the insertion loss due to the shed, using the muzzle blasts of 5.56 mm rifles as sound sources. To minimize differences in site characteristics for the shed and the wall, the shed was also used as a wall barrier by relocating the rifle an appropriate distance forward of the front of the shed.

The resultant experimental data were analyzed to determine the relative noise reduction successes of the two structures, and to compare calculated values with experimental measurements of insertion loss. Sound attenuation as a function of sound path height above the ground was also experimentally studied at the field site to help evaluate the insertion loss results.

Mode of Technology Transfer

The results of this study will be used in planning and design of rifle ranges. The information will be furnished to the Army Environmental Hygiene Agency (AEHA) to help Army installations resolve specific noise mitigation problems. These results will also be disseminated through technical papers and journal articles, and will be incorporated into a planned handbook of noise mitigation techniques for Army noise sources.

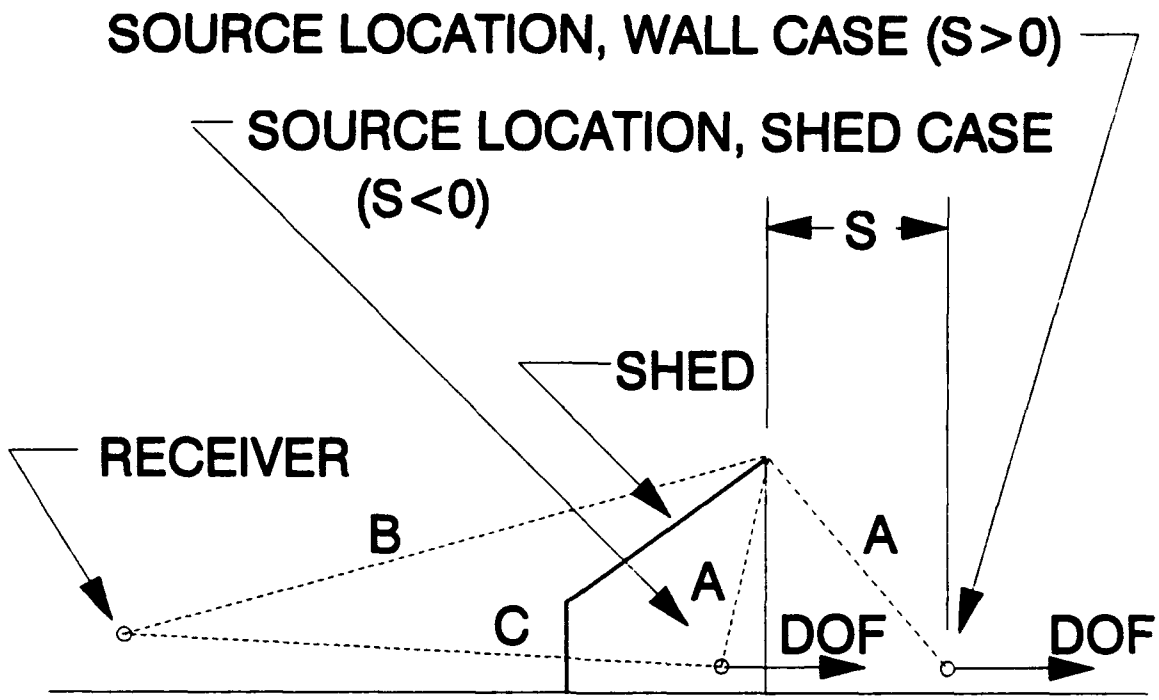

Figure 1. Propagation Paths and Source Locations for Firing Shed Experiments.

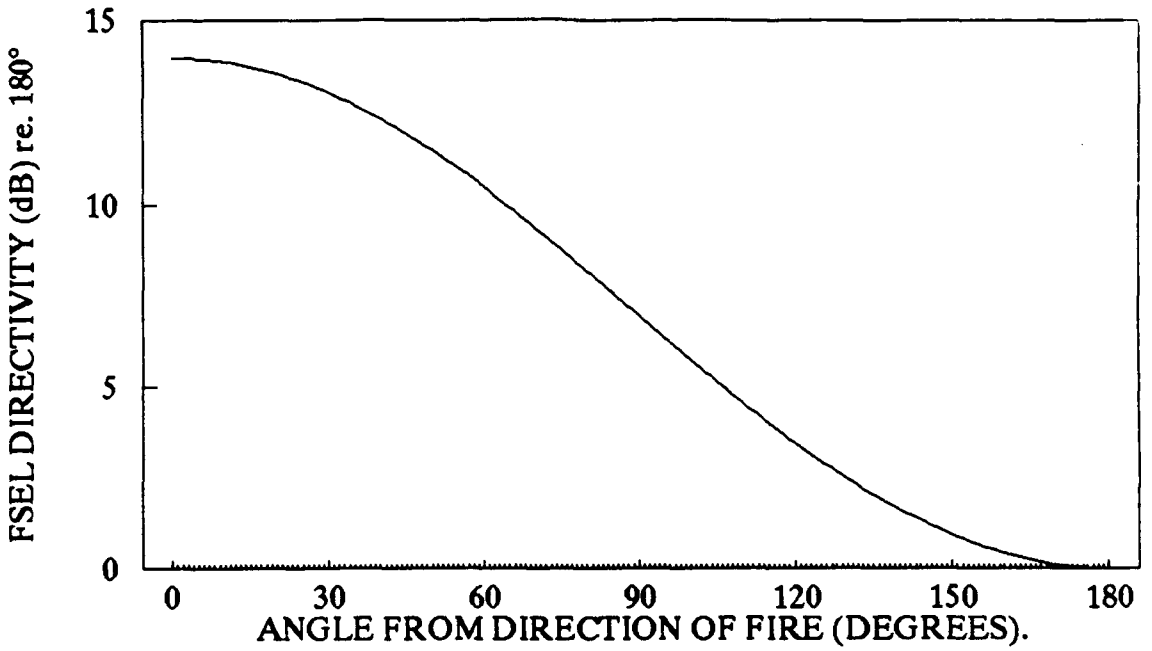

Figure 2. Assumed Model for Gun Muzzle Blast Far Field Directivity.

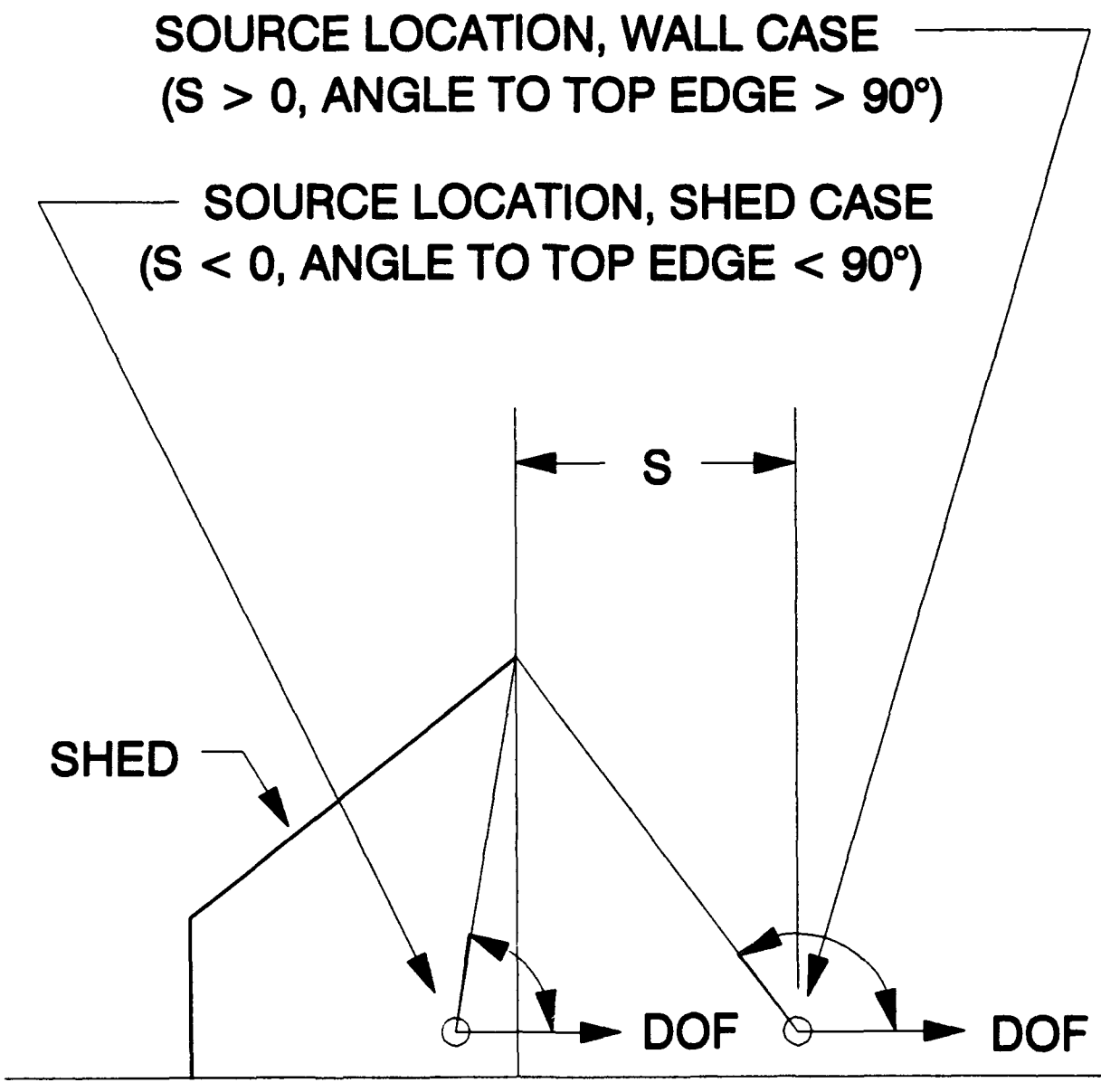

Figure 3. Angle From DOF to Barrier Top Edge for Shed and Wall.

Table 1

Microphone Locations for Insertion Loss Measurements

	Microphone Location (Azimuth, Range) Relative to:							
	"A"* Gun @-1m		"B" Gun @-1m		"A" Gun @+5m		"B" Gun @+5m	
Mic. No.	Θ (°)**	R (m)	Θ (°)	R (m)	Θ (°)	R (m)	Θ (°)	R (m)
1(S)***	ND	ND	1 m Fwd of Roofline		ND	ND	1 m Fwd of Roofline	
2	ND	ND	89.6	150	ND	ND	91.9	150
3	89.6	150	ND	ND	91.9	150	ND	ND
4	ND	ND	180	80	ND	ND	180	86
5	180	80	119.6	161	180	86	121.5	164
6	119.6	161	ND	ND	121.5	164	ND	ND
7	ND	ND	180	242	ND	ND	180	248
8	180	242	149.9	279	180	248	150.5	284
9	149.9	279	ND	ND	150.5	284	ND	ND
10(S)	ND	ND	90	1.25 (Above)	ND	ND	90	1.25 (Above)
11(S)	90	1.25 (Above)	ND	ND	90	1.25 (Above)	ND	ND

* "A" Gun is the unshielded gun, "B" Gun is the shielded gun.
** Azimuth angle Θ is measured counterclockwise from south, which is the basic direction of fire.
*** Source mic.
ND "Not a data location."

2 DESIGN AND CONSTRUCTION OF NOISE MITIGATION STRUCTURE

The experimental shed had a depth of 6 m, a rear wall height of 3 m, a roof front lip height of 7 m, and side walls splayed outward to avoid internal flutter echo (Figures 4 and 5). The gun muzzle was located 5 m from the rear wall to accommodate the gunners, safety officers, and troop movement behind the firing line. The gun muzzle was located 1 m behind the front plane of the shed. The height of the rear wall of the shed (3 m) was chosen to accommodate movement of troops carrying rifles. On an actual rifle range, a firing shed would have to be very long to house the entire firing line. (Some outdoor rifle ranges are as wide as 500 m.) For cost consideration, the experimental shed was constructed 20 m long.

The experimental shed was of pole building construction, with walls and roof sheathed with 16 mm thick tongue-and-groove waterproof chipboard sheets. The surface mass of the sheathing was about 10 kg/m^2. To prevent sound leakage, the walls extended about 0.1 m below grade and were backfilled with earth and sand, and all openings and cracks in the roof and walls were covered and caulked. The interior of the shed was covered with 0.05 m (2 in.) thick, 48 kg m^3 (3 lb per cu ft) density, Owens-Corning Type 703 fiberglass board sound absorption material for these experiments. Lining the shed with sound absorption material helps minimize sound exposure for the shooters and also minimizes additional sound energy radiated from the shed due to reflections from the interior surfaces.

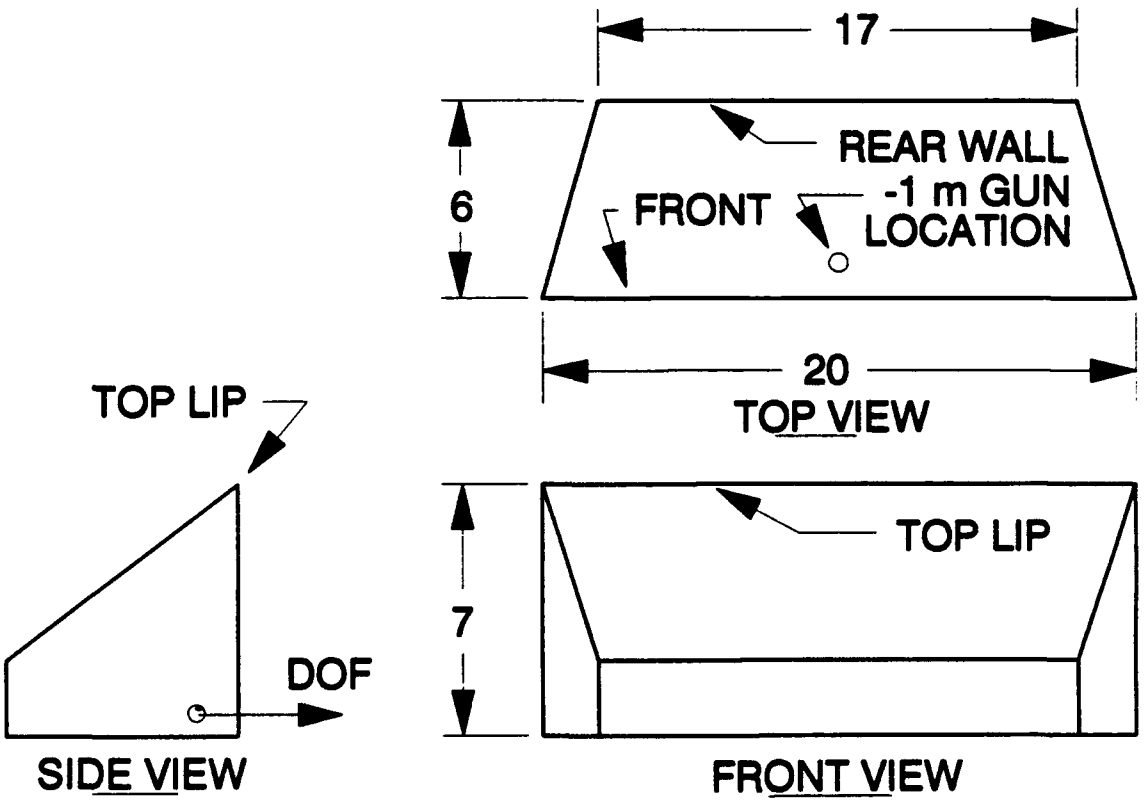

Figure 4. Firing Shed Dimensions (in Meters).

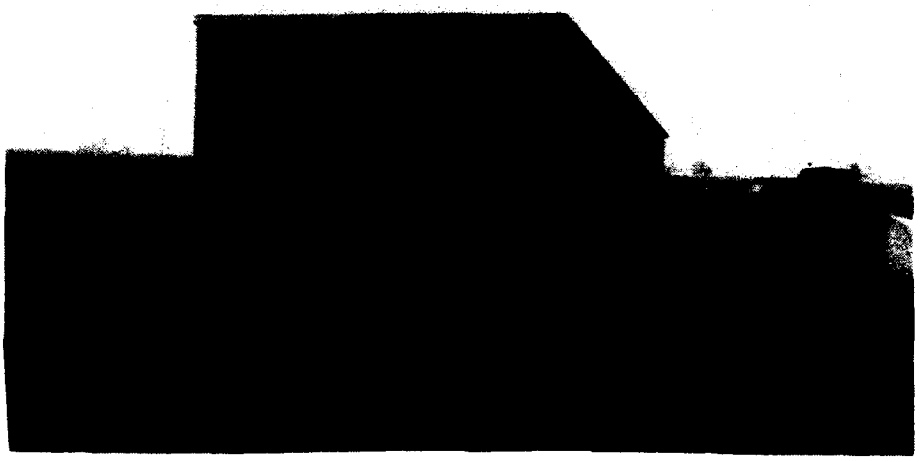

Figure 5. The Experimental Shed.

3 EXPERIMENTAL ARRANGEMENT AND PROCEDURES FOR INSERTION LOSS MEASUREMENTS

Actual guns were used as the noise sources in this investigation because gunfire exhibits source directivity, source strength, and a transient waveform that are difficult to simulate. The noise sources were identical 5.56 mm Ruger Mini-14 rifles, firing recently produced commercial ammunition randomly selected from a single production lot. These weapons produce the same noise signature as the Army M-16 rifle.

For safety, the bullets were fired into bullet traps during all of the experiments. The bullet traps were wooden boxes about 0.5 m square by 0.7 m long, filled with fine dry sand, with a steel rear wall safety stop (which was never impacted) and a thin wood front panel to minimize impact noise. The front surface of each bullet trap was covered with a double layer of the same noise absorption material used to line the shed to reduce noise reflected from the face of the bullet traps.

Other safety precautions used during the experiments included provisions for hearing protection, communications among field personnel and the laboratory base station via portable radios, and a cellular telephone for emergency communications. Rifle range safety procedures were stringently enforced. The gunners were experienced riflemen who fired at the test director's order.

The measured insertion loss was computed as the difference between the received noise level for shielded and unshielded noise sources. The noise level was measured for shielded and unshielded noise sources under conditions as nearly identical as practical. The experiments were carried out in a large, level, open field (Figure 6). The shed and the microphones were located on grass-covered strips about 30 m wide, separated by about 110 m wide strips of cropland. Microphones were arrayed to measure the noise level at locations of interest. An unshielded noise source identical to the shielded noise source was located nearby, with a matching array of microphones. Both guns were fired in the same compass direction to minimize wind effect differences on propagation. Care was taken to attain ground characteristics and cover as similar as possible for corresponding propagation paths for the two guns. At the time of the experiments the recently mowed grass was 0.1 to 0.2 m tall and the cropland was covered by a thick growth of soybean plants of about 0.8 m height. There were no trees or other structures near enough to the setup to affect the sound propagation.

The experimental arrangement was designed to determine and compare the small arms noise reduction of the firing shed and a wall of similar size located behind the firing line. The shed was used as a wall by moving the gun forward to a location 5 m in front of the shed (Figure 3). This procedure provided a "wall" the same size as the front opening of the shed and also provided for essentially identical propagation paths and ground characteristics for the "wall" and the shed. It was assumed that the shed used as a wall would produce substantially the same noise reduction as an actual wall covered with sound absorption material.

The lateral location of the shielded gun within the shed was halfway between the ends of the shed. For the shed case, the gun was located 1 m behind the front plane of the shed (the "-1 (minus one) meter" gun location). For the "wall" case, the gun was located 5 m forward of the front plane of the shed (to the "+5 meter" gun location). Table 1 lists details of the microphone locations relative to the shielded and unshielded guns for both gun locations. The azimuth of microphone location is specified relative to the intended direction of fire, which is perpendicular to the front of the shed (south). The gun muzzles were located at a height of 0.5 m above the ground surface. The actual position of a gun muzzle was only known within several centimeters because of gun recoil. A small wooden rod driven into the ground was used to provide the gunners a reference for locating the gun muzzle for each shot. When the location of

the shielded gun was changed, from the -1m to the +5m location, the unshielded gun was moved an equal distance to maintain identical microphone locations for the two guns. A bullet trap was located a distance of 8 to 10 m in front of each gun location for most of the experiments.

As Figure 6 shows, the basic direction of fire was south, perpendicular to the plane of the barrier. To experimentally demonstrate the effect of a change in source directivity, the guns were also fired to the west, i.e., parallel to the front plane of the shed. This changes the effect of source directivity on the field strength pattern at the barrier edges, as is discussed in more detail later in this report. For the shielded gun firing west, the bullet trap was located only 1 m forward of the muzzle to minimize the bow shock, since for this case, the bow shock could intersect with and diffract around the edges of the roof and walls and introduce complicating anomalous noise.

During data acquisition for the design direction of fire (south), the shielded and unshielded guns were fired alternately at intervals of about 5 to 10 seconds until a total of 21 rounds (11 unshielded, 10 shielded) had been fired, to obtain sensibly identical average atmospheric propagation conditions. For the west direction of fire, the 5 to 10-second interval could not safely be maintained because it would have placed personnel downrange of a loaded gun. Instead, a series of 10 rounds was fired from one gun, and the other gun was fired as soon as the personnel could move into position (typically a few minutes).

Figures 7 and 8 show the instrumentation arrangement used to measure the noise event at microphone locations 2 through 9. The 1/2-in. condenser microphones were mounted with axis vertical with the diaphragm located 1.22 m above the ground surface. The sound level meter shown in Figure 7 was used to measure sound level at selected mic locations during the experiment; the values were recorded by hand for field judgment of data validity and for later comparison with the results of the data reduction.

Each noise event was also measured by piezoresistive microphones used as source mics located about 1 m above each gun muzzle (mic locations 10 and 11) and also at a location 1 m forward of the roofline of the shed (mic location 1). Table 1 lists details of these microphone locations. Figure 9 shows the piezoresistive microphone system used at these locations.

The noise events were recorded on digital audio tape (DAT) for later detailed analysis. A pistonphone calibration for each microphone was recorded on tape before and after a series of experiments to provide a reference during later data reduction. A pistonphone was also used to check the system calibration periodically during the experiments and any time a system was moved or disturbed.

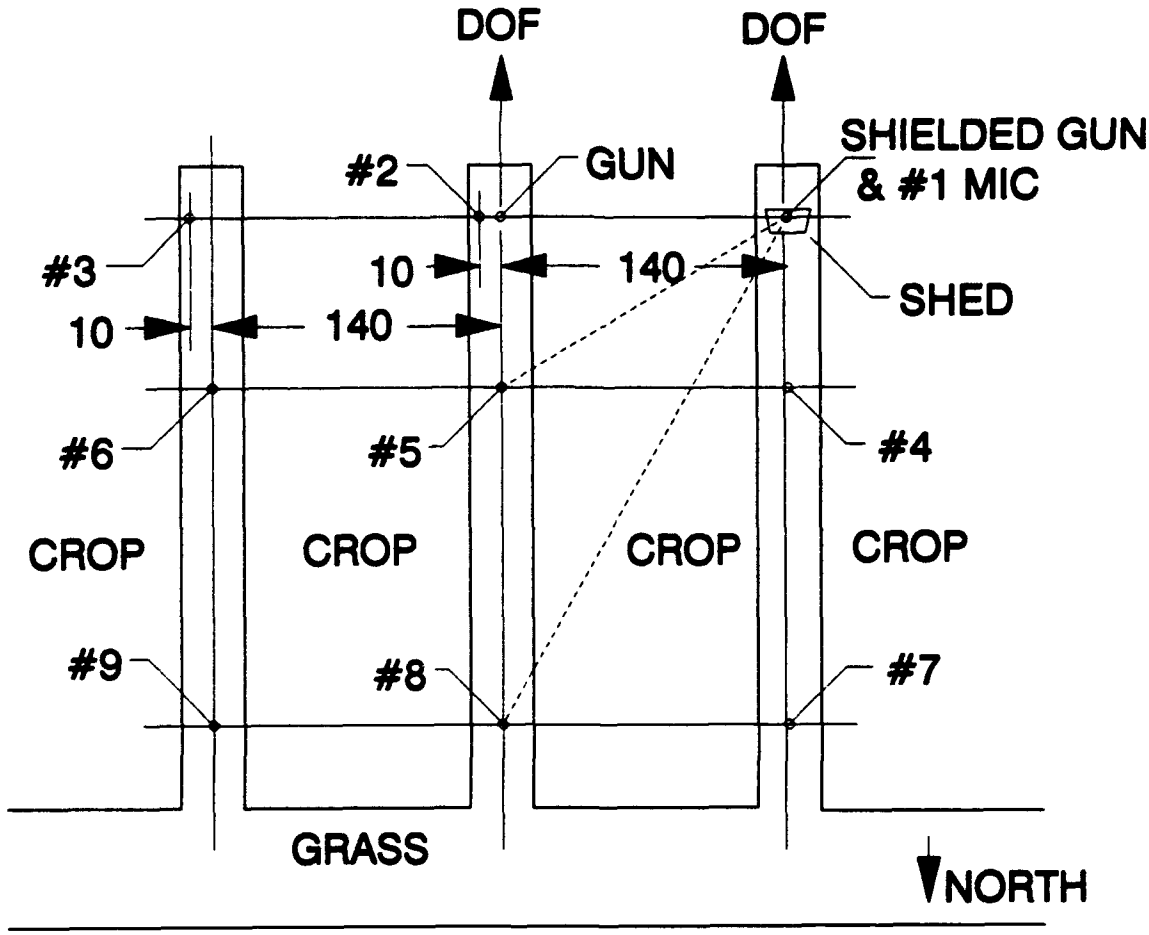

Figure 6. Experimental Layout Showing Microphone Array for Insertion Loss Experiments.

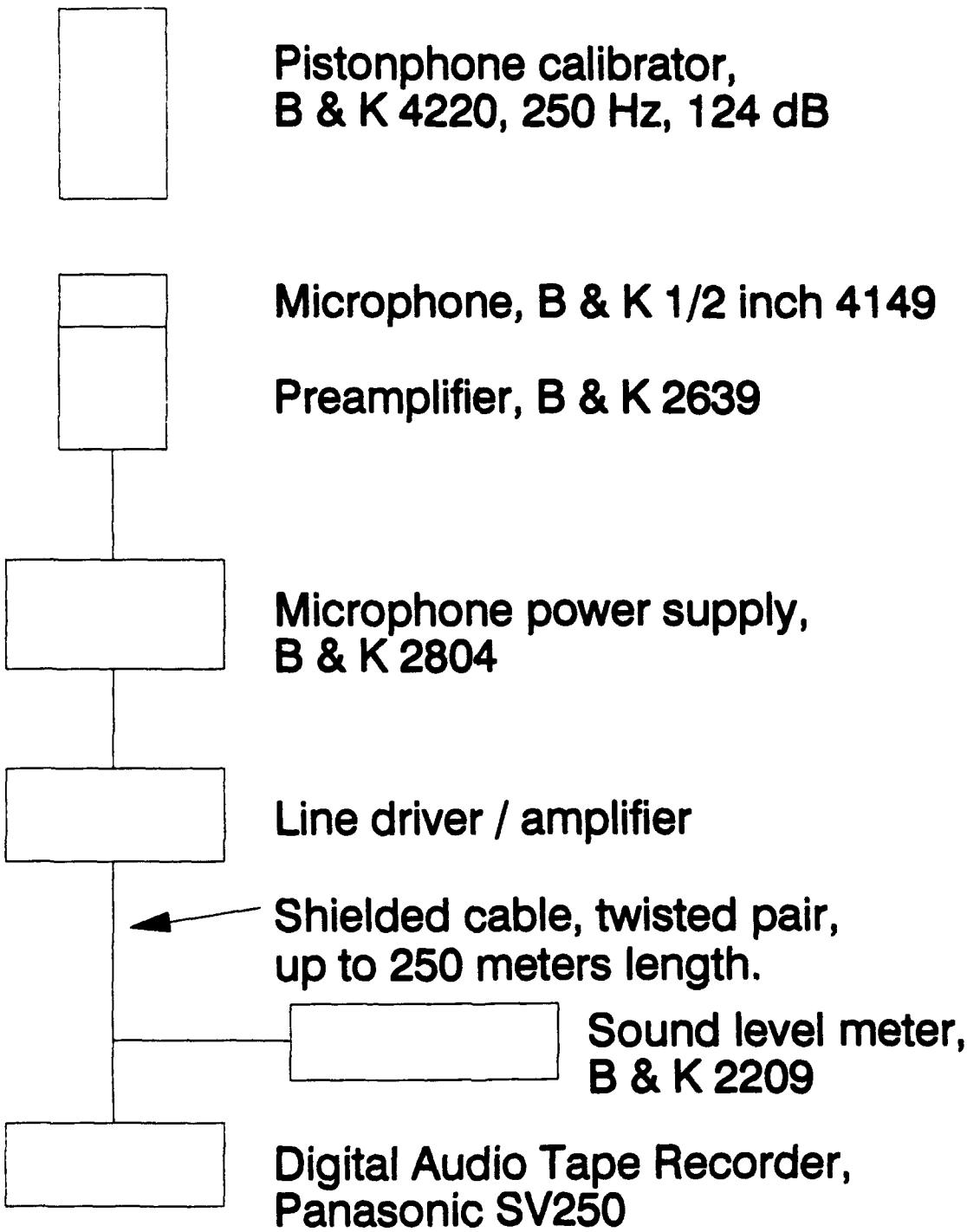

Figure 7. Condenser Microphone Instrumentation System.

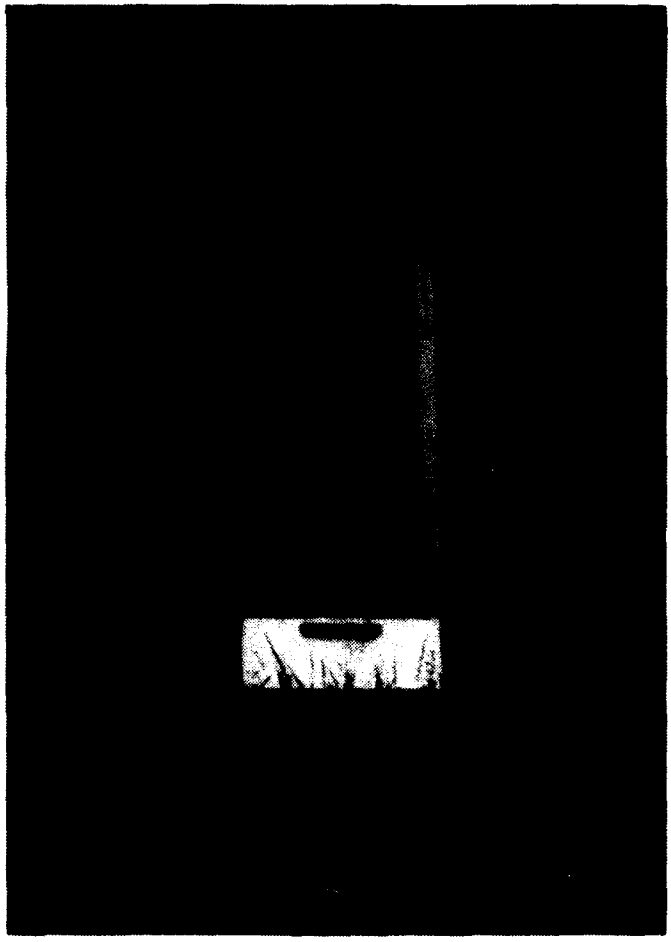

Figure 8. Condenser Microphone Arrangement.

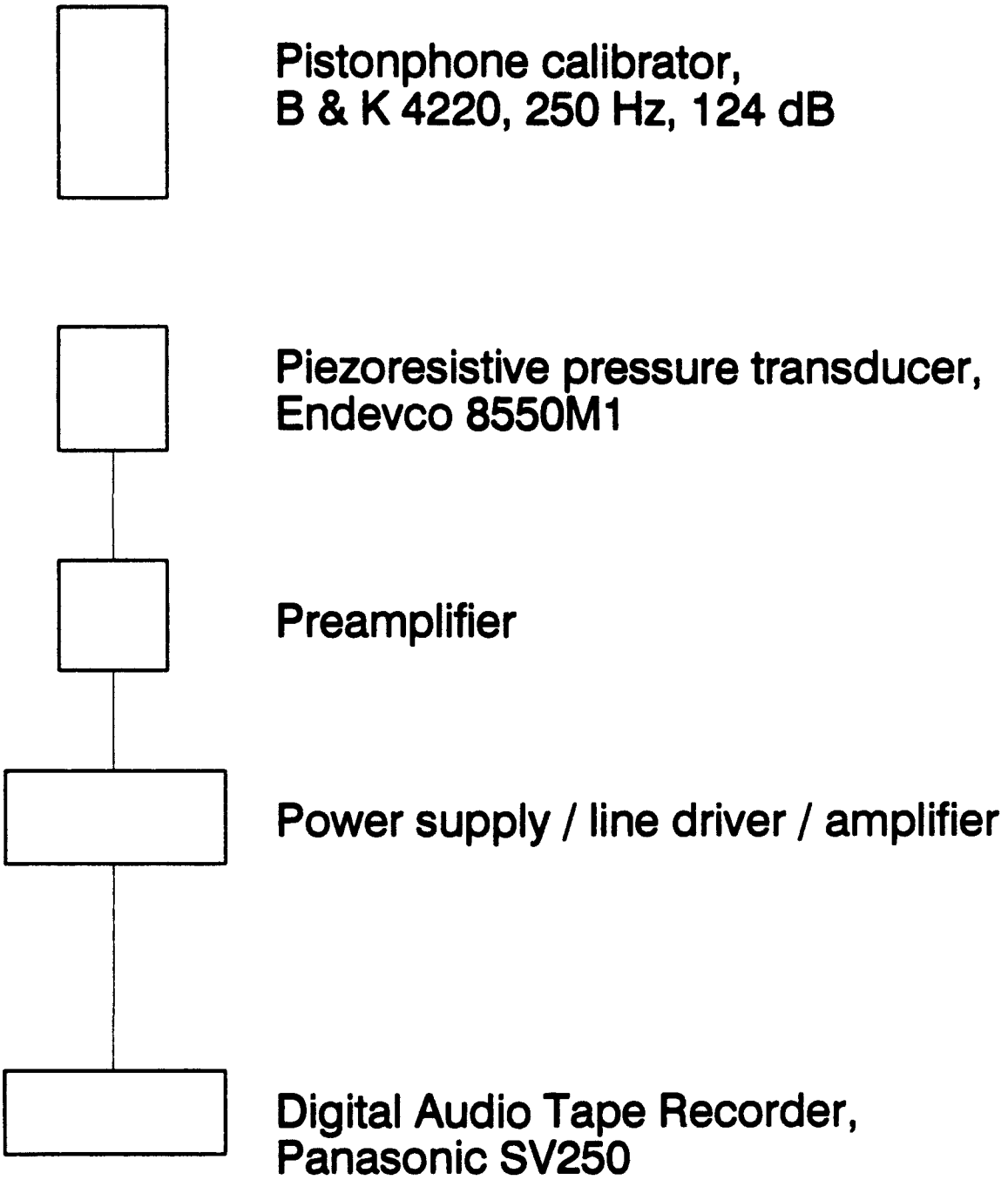

Figure 9. Piezoresistive Microphone Instrumentation System.

4 EXPERIMENTAL ARRANGEMENT AND PROCEDURES FOR GROUND INTERACTION INVESTIGATION

It is well known that the amount of attenuation of sound energy depends on the height of the propagation path above the ground and on the type and condition of soil and ground cover and also on meteorological conditions (Embleton, 1982). The propagation path for the sound diffracted around the roofline of the shed is higher above the ground than the direct line-of-sight propagation path for the unshielded gun (Figure 1). Often the higher path experiences less attenuation than the lower path, resulting in a reduction in insertion loss compared to what would occur if attenuation due to ground interaction were small or were not accounted for in calculations.

An experiment was performed to obtain information regarding the effect of sound path height and ground cover at the experimental site. The arrangement was designed to provide a line of sight from the gun to the microphone at several different heights above the ground, over both grass and soybeans. Figure 10 shows both layouts. The direction of fire was south for both ground cover cases. Data were thereby obtained at 90 degrees from the line of fire over beans and over grass.

The soybean plants were mature but still green at the time of the experiment (1 August 1991), with an average height of about 0.8 m, and were thick and luxuriant. The grass was about 0.1 to 0.2 m high between the mic pole and the gun, with a patch of clover about 0.25 m high located midway between the gun and mic pole. The ground surface was generally quite flat and level, except for a rise of several centimeters midway between the gun and mic pole for the grass ground cover area.

Various sound path heights were obtained by using four microphone heights and two gun heights. Figure 11 shows the two gun muzzle heights above the ground, 0.5 m and 2.84 m, and Figure 12 shows a typical wooden pole on which the microphones were mounted. The four different microphone heights used were: 0.5 m (19 in.), 1.22 m (48 in.), 1.32 m (52 in.) and 3.05 m (120 in.). Table 2 lists the resulting mean path heights from gun to mic. Condenser microphone systems used to take these measurements (Figure 7). The 1.22 m and 1.32 m (48 in. and 52 in.) mic heights were selected to investigate the effect of errors in microphone placement at the nominal height used at the insertion loss field measurement locations. The piezoresistive mic systems (Figure 9) were used as source mics, and were typically located approximately 1.2 m above the low gun and below the high gun.

A total of 10 rounds, spaced at intervals of a few seconds, were fired for each combination of gun height and ground cover. The noise level data for the 10 rounds were averaged during data analysis since short-term variations in propagation conditions can cause considerable scatter in noise level for the very short duration impulse noise of rifles. Bullets traps were used at a distance of approximately 15 m for all configurations.

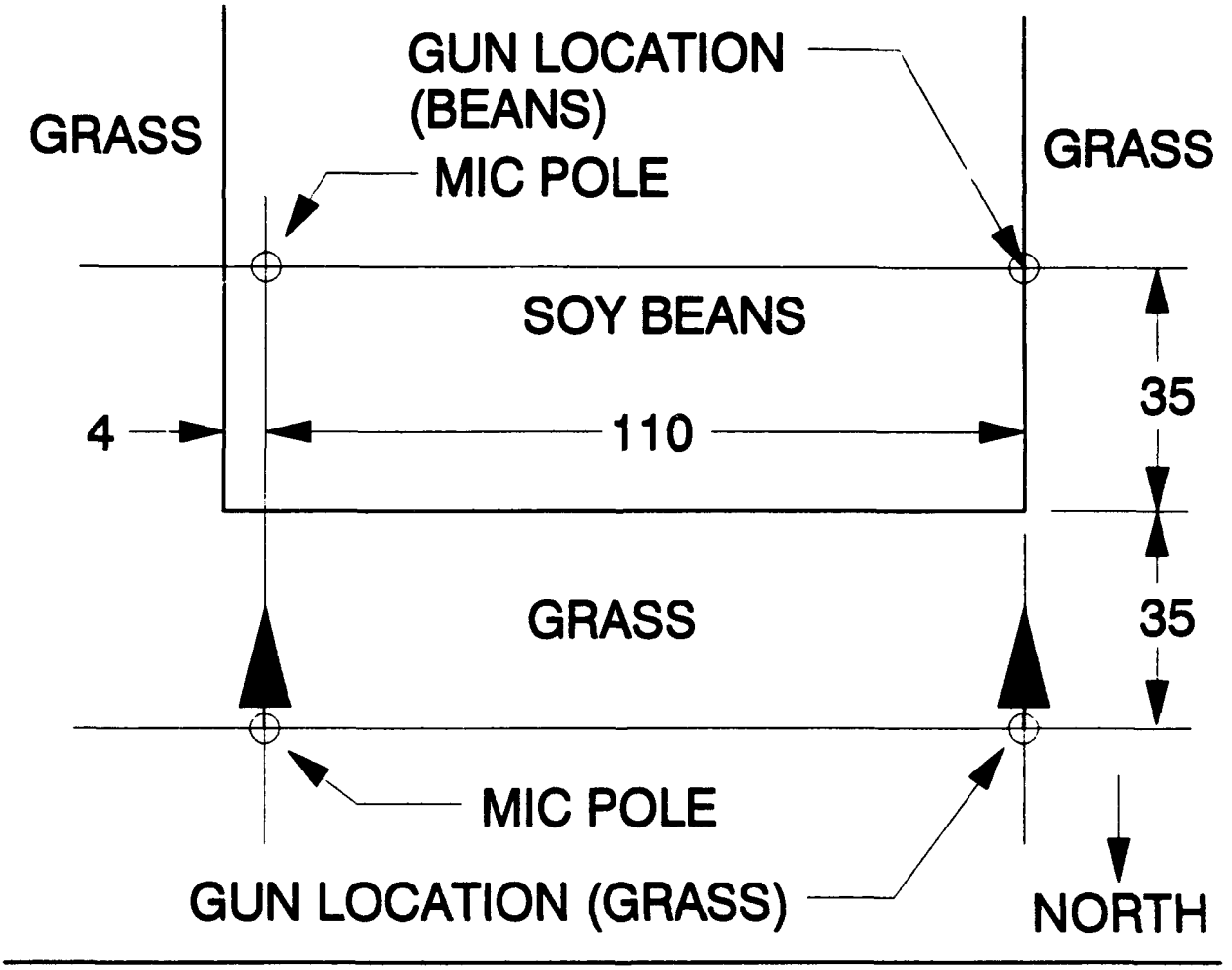

Figure 10. Layout for the Ground Interaction Experiments.

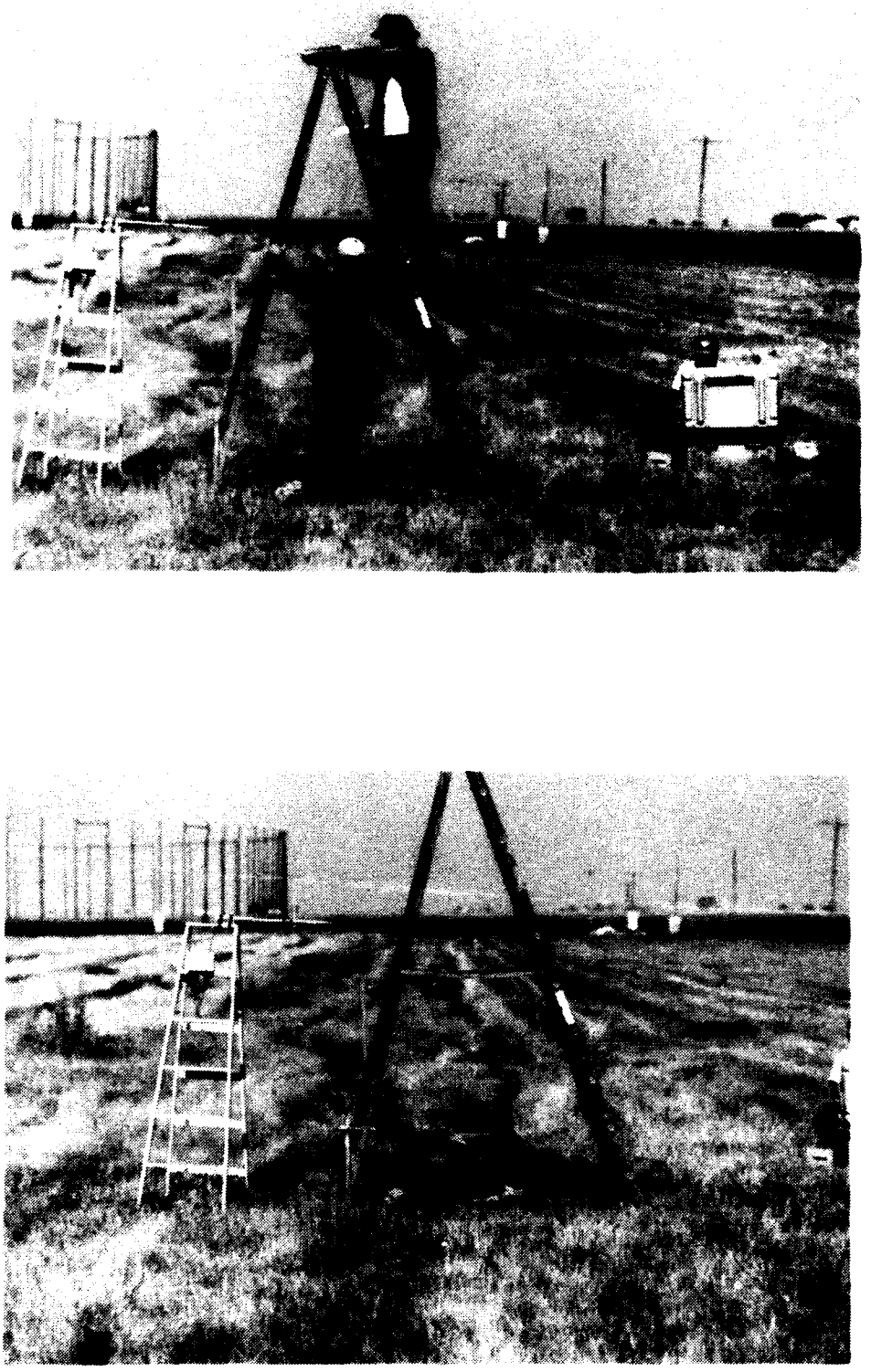

Figure 11. Firing Positions for the Ground Interaction Experiments.

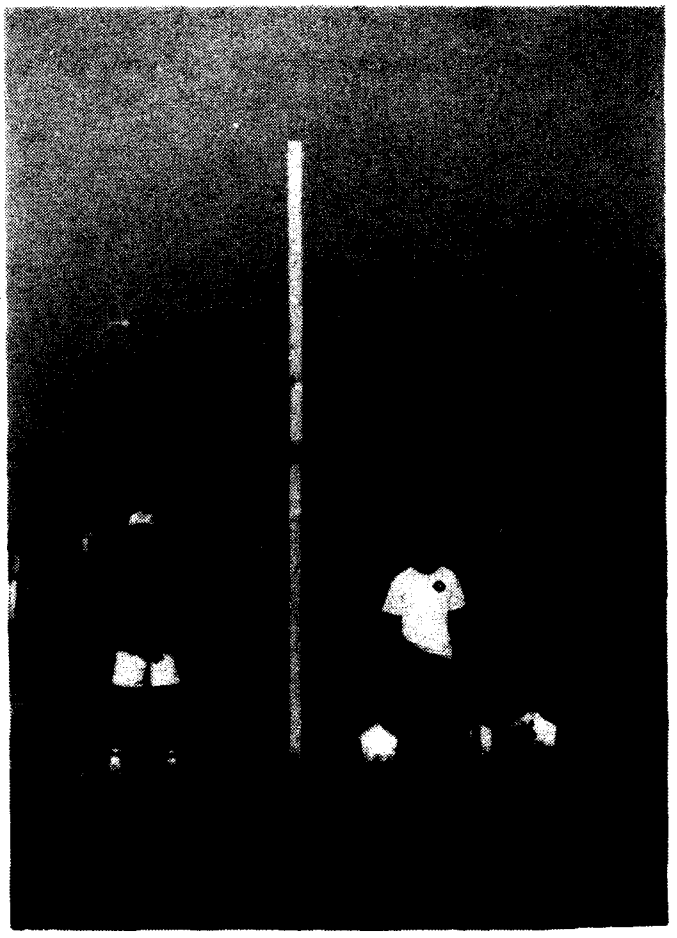

Figure 12. Microphone Pole Used for the Ground Interaction Experiments.

Table 2

Mean Propagation Path Heights for Ground Interaction Experiments

Mic Height (m)	Gun Height (m)	Mean Path Height (m)
0.5	0.5	0.5
1.22	0.5	0.86
1.32	0.5	0.91
3.05	0.5	1.78
0.5	2.84	1.67
1.22	2.84	2.03
1.32	2.84	2.08
3.05	2.84	2.95

Note: Distance from gun to mic pole 110 m.

5 DATA REDUCTION

The sound level parameters used were peak flat sound pressure level (PSPL), A-weighted sound exposure level (ASEL) and flat (unweighted) sound exposure level (FSEL), with 20 microPascals as the reference for sound pressure level (ANSI S1.4-1983). Sound exposure is defined as the time integral of the squared pressure, which is taken to represent the total acoustic energy of an impulsive noise waveform.

Figure 13 shows the data reduction system. The digitizing transient waveform analyzer (TWA) was remotely controlled with a computer program written for the purpose, via an IEEE-488 interface. Sound pressure level values were measured by playback of the DAT-recorded waveform into the TWA, where the waveform was captured and digitized. Typical capture parameters included sample intervals of 5 microseconds and 4K samples, for a time window length of about 20 milliseconds, which was longer than the duration of any of the events recorded. A-weighting was obtained when desired by passing the signal through an appropriate filter before entry into the TWA. Utilities built into the TWA were used to extract the peak value and also to calculate sound exposures by squaring and integrating the digitized records (flat and A-weighted). The resulting values were sent via the 488 bus to the computer where the level was computed for each event. The recorded standardized pistonphone signal for each microphone was used as the reference level for calculating sound levels. The computer program also calculated mean levels for each block of data. All calculation of mean sound levels was done on an energy basis, that is, using the square root of the average of pressure squared values.

The same data reduction system was used to obtain spectra. An FFT (fast Fourier transform) algorithm built in to the TWA was used to obtain a narrow band power spectrum for a specific digitized waveform record. The resulting narrow band spectrum digital file was transmitted via the 488 bus to the computer, where it was transformed into an approximate 1/3 octave spectrum (ANSI S1.6-1967) from 31.5 Hz to 16 kHz by appropriately adding the narrow band power values (using a commercial spreadsheet program). This procedure results in only an approximate 1/3 octave band spectrum since the edges of the standard 1/3 octave frequency bands do not coincide exactly with the edges of the constant width narrow bands. Typical parameter values used were a sample interval of 20 microseconds and 16K samples, which resulted in a time window length of 0.384 seconds, which yielded a narrow band power spectrum with bandwidth of about 3 Hertz and an upper limit of 25 KHZ. This upper limit is adequate since human response requires consideration of frequencies only up to about 20 KHz. The narrow band spectrum bandwidth of about 3 Hz allowed accurate approximation of 1/3 octave bandwidths.

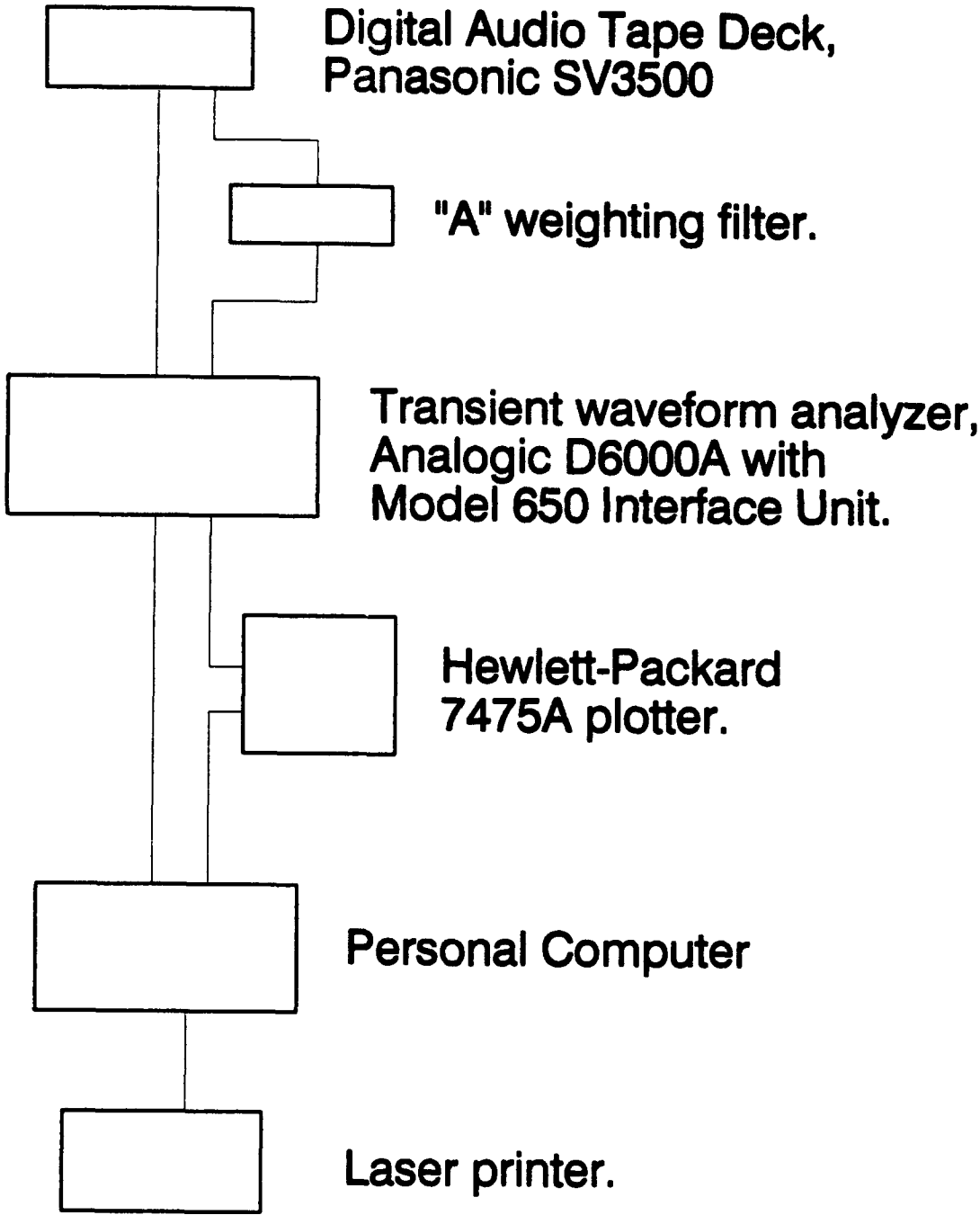

Figure 13. Data Reduction System.

6 DISCUSSION OF RESULTS

Analytical Insertion Loss Results

Calculated results done for a previous study (Pater 1992), obtained using an approximate diffraction algorithm adapted from the Federal Highway Administration (FHWA) barrier design algorithm, indicated that source directivity can have a significant effect on the insertion loss of barriers and partial enclosures. The calculated results indicated that, for a nondirectional source, the shed provides about 4 dB more insertion loss to the rear than does the wall. The indicated effect of rifle directivity was an 8 dB reduction in shed insertion loss and a 3 dB reduction in wall insertion loss; the net effect is that, for rifles, the wall yields 1 dB more insertion loss than does the shed.

These previously reported calculated results used a source sound exposure level (SEL) spectrum assumed to be representative of small arms. This spectrum was obtained from experimental data at about 100 m from the gun over sandy soil. The calculations were repeated as part of the current investigation, using a source spectrum obtained during the current investigation that more accurately represents the source spectrum as it appears at the barrier edge. Figure 14 shows the two source spectra as relative spectra, that is, each band sound exposure is normalized by the total broad band sound exposure. The spectra are presented both with and without "A" frequency weighting.

Appendix A gives the FHWA diffraction algorithm and modifications that were made to the algorithm to account for source directivity and finite barrier length. Appendix A also presents tables of calculated results obtained using the new spectrum. Unless otherwise noted, all calculations are for a structure height of 7 m, source height of 0.5 m, and receiver height of 1.22 m (equal to the values used in the experiments). A brief description of the algorithm and representative results are presented and discussed below.

The algorithm models attenuation as a function of nondimensional path length difference, which is the difference between the direct and diffracted paths from source to receiver (Figure 1). For purposes of the calculations, it was assumed that the spectral energy distribution, which is the relative source spectrum given in Figure 14, does not change with azimuth from the direction of fire. That is, directivity is assumed to consist of change with azimuth of broadband SEL, but the spectral energy distribution is assumed to be invariant. The validity of this assumption is uncertain due to lack of pertinent information. Directivity was accounted for simply by modifying the value of received broadband acoustic energy according to the difference in broadband source strength (expressed in terms of sound exposure level) due to directivity for the directions of the direct and diffracted paths. Note that this procedure is not rigorously correct in general and must be used with caution. It can be used with some measure of confidence for cases that have been corroborated experimentally or by some other rigorous analytical techniques.

The algorithm strictly applies to barriers of infinite length. It is used here to calculate insertion loss of finite barriers such as the experimental structure by first calculating the insertion loss due to each edge as if it were of infinite length. A value for the overall insertion loss of the finite structure is then obtained by summing the spectral band intensities for all three (infinitely long) edges (Appendix A). This procedure is tantamount to assuming that the most important contribution to the sound intensity arriving at the receiver around each infinite edge is due to a portion of that edge that is present in the finite structure. This may be a reasonable assumption when the receiver is far from the barrier and the source is close to the barrier. The effect of directivity on the distribution of field strength along a barrier edge is also of potential importance. This procedure is an approximation and could conceivably lead to inaccurate results if not used judiciously.

Figure 15 shows calculated effects on the assumed source spectrum due to "A" frequency weighting and due to diffraction of the sound around the top edge of an infinitely long shed, for 180-degree azimuth. The attenuation due to diffraction increases with frequency. The effect of "A" frequency weighting on calculated insertion loss is of particular interest, since A weighting is generally used to emphasize those frequencies to which the human auditory system is most sensitive.

The A-weighted insertion loss is the difference in A-weighted noise level with and without the barrier. Examination of calculated results presented in Appendix A and in the text below, for both an infinitely long and a 20-m long structure, will show that A-weighted insertion loss to the rear is generally about 2.2 dB greater than unweighted insertion loss. Figure 15 explains this. The A-weighted source spectrum of Figure 15 has a total broadband SEL (sound exposure level) that is 0.5 dB lower than that of the unweighted source spectrum. The diffracted spectrum has a different spectral energy distribution, with the result that the A-weighted diffracted spectrum broadband SEL is 2.8 dB lower than that of the unweighted diffracted spectrum. The difference, 2.3 dB, is the amount by which A-weighted insertion loss exceeds unweighted insertion loss. Bear in mind that spectral energy distribution can also be affected by other phenomena, such as interaction of sound waves with the ground, and the attenuation, scattering, and refraction that occur during propagation of sound waves through the atmosphere. These can likewise cause changes in the acoustic power spectrum that result in differences between A-weighted and unweighted insertion loss values.

A set of calculations were carried out to determine the effect of location of the source relative to the barrier. Summary presentations of calculated insertion loss results (unweighted) at 180-degree azimuth for a wide range of gun locations, for both isotropic and gun directivity sources, taken from Tables A3 and A4 (Appendix A), are shown in Figure 16 for a shed of infinite length, and in Figure 17 for a shed of finite (20 m) length. The calculations are for a barrier height of 7 m and source height of 0.5 m. In these figures, the abscissa is the source axial location referenced to the shed front plane, a directed distance represented by the symbol "S." A value greater than zero corresponds to a wall located behind the gun, while a value less than zero represents the gun located within the shed.* The source directivity causes a reduction in insertion loss compared to that of a nondirective source. The magnitude of the effect of directivity diminishes as the gun is located further downrange from the barrier, because the angle from the line of fire to the receiver becomes more nearly equal to the angle from the line of fire to the barrier edge, i.e., directivity causes very little increase in the field strength at the barrier edge (Figure 2). The diffraction model may not be valid for large magnitude negative values of S, for which the configuration begins to resemble a source located in a duct. Note that the optimum juxtaposition of gun and barrier, at least for this particular barrier height and assumed source directivity, is in the vicinity of S = 5m, that is, a wall located 5 m behind the gun.

The calculated results of immediate interest for comparison with experimental results are for S = +5m (wall) and -1m (shed), for the experimental barrier and source parameter values. The calculated results for these two cases (nondirective and gun directivity sources) for the 180-degree azimuth (directly to the rear), are detailed in Appendix A and summarized in Table 3 for a structure of infinite length, and in Table 4 for a structure of 20m length. Calculations were carried out for two distances along the 180-degree azimuth, corresponding to microphone locations of the experiments. The results for the two distances were virtually identical in all cases. Recall that, in one of the experimental configurations the gun was fired in a direction parallel to the shed front, to demonstrate experimentally that a change in source directivity can affect insertion loss. Insertion loss calculations were therefore performed for both gun-firing directions (perpendicular to and parallel to the barrier).

---

* To be physically meaningful, of course, the shed depth must be greater than the distance the gun is located behind the shed front.

The calculated insertion loss values for a structure of infinite length (Table 3) are generally about 3 to 4 dB higher than for a structure 20m long (Table 4). This result seems reasonable, since the reduction of insertion loss would be about 5 dB (shielded case insonification increased by a factor of 3) if the contribution to total intensity at the receiver were equal for each of the three edges. Since the field strength at the two endwall edges should be somewhat smaller than at the top edge, the actual reduction in insertion loss should be somewhat smaller.

The calculated effect of directivity on insertion loss for the gun firing *perpendicular* to the shed are similar for the infinite length and the 20-m length configurations. These results agree well with the results of the previous investigation described in the first paragraph of this chapter, which were obtained for a somewhat different source spectrum. Reiterating, the shed yields about 4 dB more insertion loss for a nondirective source. For a source with the assumed rifle directivity, the wall yields about 1 dB more than the shed. The indicated effects of directivity are to reduce the insertion loss of the shed by about 8 dB and of the wall by about 3 dB.

The results of this algorithm may not be valid when applied to the case of a gun firing parallel to the barrier since the model was not developed for this case. For the gun firing parallel to the barrier, the field strength varies along the top edge of the barrier in a nonsymmetrical way relative to the mid-length point. That is, the point of maximum field strength along the barrier edge does not lie on the shortest path around the barrier edge from source to receiver. Table 3, the infinite-length shed case, indicates insertion loss values equal to the nondirective source values. The results of Table 4, for the finite length shed, indicate that this case yields insertion loss values that lie between those of the other two directivity cases.

The insertion loss is of course of interest at azimuths other than 180 degrees. Figures 18 to 25 show a variety of calculated results from Table A2 of Appendix A, for the azimuths used in the experiments. These graphs all show the variation of calculated insertion loss vs. azimuth angle measured from the intended firing direction, which is the direction perpendicular to the front plane of the shed. Calculated insertion loss results are presented for each edge of the structure, treated as if it were the edge of an infinitely long barrier. Approximate values for the overall insertion loss of the finite structure were obtained by summing the spectral band intensities for all three (infinitely long) edges, as discussed earlier. Comparing the curves shows the relative influence of each edge on the overall insertion loss at each azimuth. The finite barrier length must be considered during interpretation of these results. The azimuth to the vertical edge of the end wall of the structure is 84.3 degrees for the -1m gun location (shed case) and 116.6 degrees for the +5m location (wall case).

Figure 18 shows unweighted insertion loss results for the -1m gun location (the experimental shed configuration) with the gun firing perpendicular to the front of the shed, and Figure 19 presents the A-weighted results for the same case. These predict the insertion loss to be approximately constant from 120 to 180 degrees azimuth, at a value of 16 to 17 dB unweighted and about 19 dB A-weighted. The insertion loss is lower at 90 degrees because less shielding is provided by the endwall. The unweighted and A-weighted insertion loss values at 90 degrees are different by only 1 dB because diffraction effects on the spectrum are smaller.

Figure 20 presents results for the experimental shed configuration for a nondirective source. Insertion loss values are about 8 dB higher at 180 degrees compared to the gun firing perpendicular to the shed front, as discussed earlier; the difference is progressively less as the azimuth angle decreases toward 90 degrees since the effect of gun directivity becomes smaller.

Figure 21 presents results for the +5m gun location (the experimental wall case) for the gun firing perpendicular to the wall. Here the insertion loss is zero for the 90-degree azimuth since the receiver does not lie in or near the acoustic shadow of the wall. The insertion loss is small at 120 degrees since this

azimuth lies near the line of sight to the end of the wall. At 180 degrees, the insertion loss is about 18 dB, or about 1.5 dB higher than for the shed case, as discussed earlier. At 150 degrees, the insertion loss is approximately the same as for the shed.

More direct comparisons of the wall and shed are made in Figures 22 and 23, for a nondirective source and gun directivity source respectively. The influence of the end wall can be clearly seen at azimuths of 90 and 120 degrees. At 150 and 180 degrees, the previous conclusions are evident; that is, for the nondirective source, the shed yields more insertion loss, but for the gun firing perpendicular, the wall yields a slightly greater insertion loss.

Figures 24 and 25 show a comparison of the flat and A-weighted calculated insertion loss for the finite shed and wall, for a nondirective source and for both gun-firing directions. The gun firing parallel to the shed front always yielded insertion loss values between those for the nondirective source and the gun firing in the perpendicular direction.

A radically different analytical investigation of the noise reduction of the shed and wall is detailed in Appendix B to this report. This analysis accounts for finite size of the structure in a considerably more rigorous way than does the analysis of Appendix A, and also accounts for source directivity in an approximate but basically rigorous way. The analysis was used to model the cases of a nondirective source and of source directivity representative of the gun firing perpendicular to the front plane of the barrier. (The case of the gun firing parallel to the barrier cannot be modeled because the analysis is restricted to axially symmetric situations.) The analysis is carried out in spherical coordinates and represents the shed as a hemispherical shell of 14m diameter and 7m height with a semicircular aperture and with the source located at the center of the sphere, which for a 90-degree aperture angle, places the source at the front plane (S = 0m). The wall is represented as a portion of a spherical surface with a semicircular outline, located 5m to the rear of the source. The results of this analysis should at least indicate the results for the actual rectangular structures since diffraction results tend to depend more on the size of the diffracting structure than on the detailed shape. Summary results of that analysis, in terms of unweighted insertion loss, are shown as the solid lines in Figures 26 and 27 for the nondirective and directive sources respectively. The results show sharply reduced insertion loss at 180 degrees. This is a characteristic diffraction feature (known in optics as Poisson's bright spot) due to constructive interference of waves that have diffracted around the edges of a normal circular barrier and that arrive in phase. For a rectangular barrier, this "bright" spot would be considerably less bright, that is, insertion loss at a 180-degrees azimuth would not decrease nearly as much. For the nondirective source (Figure 26), the maximum shed insertion loss is about 21 dB at 145 degrees, while the maximum for the wall is about 17 dB at about 160 degrees. These results indicate that the shed yields about 4 dB more insertion loss to the rear than the wall for a nondirective source. For source directivity typical of a rifle (Figure 27), the results show the maximum insertion loss to be about 15 dB for the shed and about 14 dB for the wall, so that the shed yields 1 dB more insertion loss than the wall.

It is useful to make a direct and detailed comparison of the results of the two algorithms. The analytical results from Appendix B (Figure 26 and 27) were obtained using the source spectrum used in the previous investigation (Peter 1992), and shown in Figure 14. It is therefore more appropriate to compare the results of the Appendix B's analysis with results of the analysis of Appendix A using the same source spectrum (Figures 26 and 27). The Appendix B calculated results were obtained for a semicircular barrier of 7 m radius. Appendix A calculated results are for a rectangular barrier 14 m wide and 7 m high relative to the source, with the source located at the shed frontplane, S = 0. The two algorithms yield similar conclusions regarding the relative noise reduction of the shed and the wall. For the nondirective source (Figure 26) both algorithms agree that the shed provides about 4 dB more maximum insertion loss in the region generally to the rear than does the wall. For the simulated rifle source, both algorithms show the shed and wall to yield about the same (within about 1 dB) maximum

insertion loss, although they disagree as to which yields slightly larger insertion loss. The agreement is not good directly to the rear (near 180 degrees), where the two algorithms would not be expected to agree since wave interference effects would be different for the two barrier profile shapes (semicircular vs. rectangular). Also, the simplified model of Appendix A does not account for some details of wave interference. It should also be noted that one would not expect perfect agreement between the two analyses since they model barriers of differing shape, perimeter and area. Another significant difference is that the field strength along the barrier edge is uniform for the semicircular barrier, even for the modeled directive source, while the field strength along the edges of the rectangular barrier is not uniform.

In summary, the calculated results of both analytical methods show the shed to offer about 4 dB more insertion loss than the wall for a nondirective source, but the two structures offer about the same (within 1 dB) insertion loss for a source with directivity similar to that of a rifle firing perpendicular to the plane of the barrier. It is worth noting that, although the shed and wall offer about the same maximum insertion loss for gunfire noise, the shed offers that insertion loss over a significantly greater portion of the region to the rear. This is the result of the sound path around the ends of the short wall; a longer wall or a wall with a section at the end that extends forward would offer protection over a greater portion of the region to the rear.

Experimental Insertion Loss Results

Table 5 lists a typical set of detailed data values for one microphone location. This table shows the measured value of each sound level parameter for each round fired, and also (at the bottom of the table) gives the mean values and the maximum deviations from the means. The data scatter shown in this table is typical of most of the experiments. This type of data table was generated during data reduction for each microphone location of each configuration investigated.

Table 6 lists the insertion loss experiments for which data are presented in this report. These consist of the gun firing normal to and parallel to the barrier for the two gun locations used to represent the shed and the wall. No experimental data were obtained for a nondirective source.

Summary data tables (Tables 7 through 10) list mean data values for each of the insertion loss experiments. The summary tables show the mean measured noise levels and the resulting measured insertion loss in terms of several noise metrics. The upper portion of each table shows the averaged data values for the unshielded gun; the middle portion shows the values for the shielded gun; and the bottom portion shows the difference between the shielded and unshielded guns, which is the measured insertion loss of the barrier. The microphone locations are identified in the first three columns of each table by number, azimuth angle, and distance from the gun muzzle. The data presented in these tables are discussed in detail below.

Table 7 presents measured noise levels and insertion loss values for each microphone location for the shed (-1 m gun location) with the rifle firing in the direction perpendicular to the front plane of the shed (south). Table 8 gives the same data for the wall (+5m gun location) case. These two sets of results can be compared to determine the relative noise reduction of the shed and the wall, essentially exclusive of propagation effects since care was taken to keep the propagation conditions identical. This comparison is shown graphically in Figures 28 and 29 in terms of FSEL (unweighted) and ASEL respectively. Note that the abscissa identifies receiver (microphone) locations in terms of azimuth and range, and that there are two 180-degree azimuth receiver locations. The data must be interpreted carefully, taking into account the effect of finite barrier length. The azimuth to the vertical edge of the end wall of the structure is 84.3 degrees for the -1m gun location (shed case), and 116.6 degrees for the +5m location (wall case). Since the 90-degree azimuth does not lie in the acoustic shadow of the wall, the wall provides little or no

insertion loss for this azimuth. The 120-degree azimuth lies just inside the acoustic shadow of the wall, but well within the acoustic shadow of the shed, so it is not surprising that the shed provides larger insertion loss. To the rear, at 150 and 180 degree, the experimental data shows that the wall and shed provide nearly identical insertion loss in terms of FSEL, though ASEL insertion loss values are different by about 2 dB at one of the 180-degree locations. (Recall that, from Figure 6 and Table 1, there were two microphone locations at two different distances along the 180-degree azimuth.)

Tables 9 and 10 and Figures 30 and 31 give the data for the experimental configurations in which the rifles were fired in a direction parallel to the front of the shed, to the west. This configuration provides a different source directivity pattern relative to the barrier, to demonstrate experimentally the significant effect that source directivity can have on insertion loss. For a wall or shed of infinite length, one might argue that this arrangement should yield insertion loss more similar to that which would be obtained for an isotropic source, since the angle between the direction of fire and the minimum length propagation path around the barrier is 90 degrees for the top edge of both the shed and the wall and also for the direct line of sight to the observer for the unshielded case. However, source directivity could still be expected to have some effect even for barriers of infinite length since the field strength along the top edge of the barrier would be affected. For the experimental finite length barrier, source directivity also has considerable effect on the field strength at the edges of the side walls of the structure. The data show that, for this case, the shed yields greater insertion loss than does the wall in the region to the rear of the structure, by a margin of about 8 dB. Indeed, the shed is shown to offer superior insertion loss at all azimuths for which noise levels were measured. Note that, at 90 degrees the wall insertion loss is negative; that is, the shielded gun was measured to be louder than the unshielded gun.

Figures 32 and 33 give the combined experimental results for the two directions of fire. Table 11 summarizes the measured insertion loss averaged over both 180-degree locations (to obtain improved statistical significance) for each of the four combinations of shed vs. wall, and the two firing directions. These data clearly show the experimental answer that the present study was designed to provide. For the gun firing perpendicular to the barrier (south), the wall and shed provide approximately the same insertion loss to the rear. This experimental result for relative noise reduction performance of the wall and shed agrees well with the analytical results of both Appendices A and B.

For the gun firing parallel to the barrier (west), the agreement between calculated and experimental results for relative noise reduction performance is not good. The experimental data show the shed providing about 7 dB more insertion loss to the rear than the wall, while the analytical data from Appendix A show the shed providing only about 2 dB more. This may be an indication that the calculation algorithm of Appendix A is not adequate to correctly account for the complicated diffraction around all three edges for this case, perhaps because source directivity can strongly affect the distribution of field strength along the barrier edges, with consequences that are not accounted for by the model. The problem may be that the algorithm procedure assumes that the diffraction is characterized by the path length difference for the shortest path from source to receiver around the barrier edge. The algorithm has been well substantiated for isotropic sources. For the gun firing normal to the barrier, the location of greatest field strength along the barrier edge does not change. For the gun firing parallel to the barrier, this is no longer true.

The above paragraphs compared only the shed and wall insertion loss *difference*. This was done specifically to estimate the relative noise reduction performance of the shed and wall exclusive of propagation and attenuation effects. The magnitude of insertion loss, rather than the difference between shed and wall, is of primary interest for rifle range noise mitigation. The previous investigation (Pater 1992) concluded that experimental insertion loss agreed fairly well with calculated values in the region directly to the rear of the shed and at 90 degrees, but not at intermediate angles. This conclusion is modified here, for reasons shown below.

Figure 34 summarizes the analytical and experimental A-weighted insertion loss results from both the current and previous investigations for the gun firing normal to the barrier from the -1m gun location (the shed case). (Unweighted experimental insertion loss was not measured in the previous investigation; thus the overall comparison can only be made in terms of A-weighted insertion loss.) The calculated results of Appendix A and of the previous investigation used the same algorithm, the only difference being the source spectrum, as discussed earlier. The effect on calculated results of changing to the new source spectrum was an increase in A-weighted insertion loss to the rear of about 2 dB. The solid curve in Figure 34 represents the calculated results using the algorithm of Appendix B, which used the spectrum of the previous investigation, a semicircular barrier and a source located at S = 0. (This configuration was discussed earlier in comparing the calculated results shown in Figures 26 and 27.) The agreement of this calculated curve with the calculated results of the previous investigation is quite good, there are differences in the gun location and barrier shape and size, discussed in detail earlier. Figures 26 and 27 show a more valid comparison of the two algorithms.

Figure 34 shows that the shed insertion loss values measured in the present study were generally significantly smaller than predicted by the diffraction algorithm calculations. They also do not agree very well with the experimental results of the previous investigation, particularly directly to the rear of the wall. The experimental data were all obtained at the same site and for the same shed structure; differences were that during the previous investigation the shed had not been lined with sound absorption material, and that the measurements were made in the month of November after the crops had been harvested, rather than during the summer. The lack of agreement between these two experimental data sets is a graphic example of the potential effect of propagation effects on achieved insertion loss. An algorithm for predicting atmospheric, meteorological and ground interaction effects would help produce more accurate prediction of barrier insertion loss.

Experimental Excess Ground Attenuation Results

The term "excess attenuation" refers to attenuation of sound in excess of that which can be attributed to spherical spreading. One cause of excess attenuation is absorption of sound energy by the atmosphere. The amount of excess attenuation due to atmospheric absorption for the spectrum shown in Figure 15 at the distances from which noise measurements were made is small (Appendix C). "Excess ground attenuation" is the excess attenuation due to the proximity of the ground. These effects include dissipative and reactive effects of ground impedance, wave interference effects of the direct and ground reflected waves, and refractive and scattering effects resulting from turbulence and boundary layer profiles of wind velocity and temperature.

The effect of excess ground attenuation on measured insertion loss can be partially determined by examining the experimental insertion loss data. The experimental data for the gun firing normal to the shed and wall (Tables 7 and 8) are re-examined in Tables 12 and 13 respectively. Noise levels were measured at two distances along the 180-degree azimuth. The spherical spreading attenuation from the first to the second distance is shown for each case. The difference between spherical spreading attenuation and measured attenuation is the excess attenuation that occurred from the first to the second distance for both the shielded and unshielded guns (Tables 12 and 13). The excess attenuation values were used to correct the data values at the second location for the effect of excess attenuation that occurred between the two locations (but not for excess attenuation that occurred between the source and the first distance). The resulting insertion loss at the second location, corrected for effects of excess attenuation, is also shown for each case. Note that the excess attenuation for the shielded gun is larger than for the unshielded gun; this is probably the result of larger excess ground attenuation for the lower path. The effect of excess attenuation on insertion loss is due entirely to excess ground attenuation, since the effect of atmospheric attenuation should be essentially the same for both guns, and thus subtracts out. Note that the correction

for excess ground attenuation brings the insertion loss values at the two distances into much better agreement. It is reasonable to expect that the effect of excess ground attenuation from the source to the first distance would also be substantial, as it would be for the paths from the source to the other microphone locations. Correction of the measured insertion loss for excess ground attenuation would thus increase the measured value of insertion loss for all microphone locations. This would no doubt improve the agreement between theoretical values of insertion loss, which did not take excess ground attenuation into account, and experimental values.

Table 14 lists the experiments performed specifically to investigate the possible effects of sound wave interaction with the ground at the test site. The experiments over grass were done both before and after the experiments over beans to reveal any changes in experimental conditions. At the time of the experiment the beans were about 0.8 m high; thus the lowest, 0.5 m, height microphone was submerged in the soybean plants. Also, the low gun for the experiments over beans was located immediately beside the edge of the beans plot and at a height of 0.5 m, i.e., lower than the beans.

The averaged ASEL and FSEL data for all microphones for all ground interaction experiments listed in Table 14 were compiled into a summary sheet (Table 15). ASEL is useful to judge human response to the noise, while FSEL (unweighted) gives a clearer picture of the total sound energy present in the blast noise that arrives at the microphone location. Table 15 is arranged to ease assessment of the effect of the type of ground cover (grass or soybeans) and the height of the path from source to microphone (various combinations of gun height and mic height). Selected data are shown in Figures 35 and 36. These data clearly show that there were substantial attenuation effects due to the proximity of the ground. Bear in mind that the same noise source was used for all of the experiments. It is clear that a higher line of sight results in less attenuation. It is also clear that there was a reduction in received sound level during the test (possibly a result of refraction resulting from solar heating of the ground), evidenced by the fact that the repeated experiments over grass yielded somewhat lower sound levels. The effect of type of ground cover, i.e. grass vs beans, is more subtle. The broadband FSEL and ASEL values were generally somewhat lower (perhaps 0 to 2 dB) for beans than for grass, although there were exceptions.

Detailed sound exposure level spectra of selected data rounds for several ground interaction experimental configurations were obtained to help interpret noise level data. Figure 37 shows typical source waveform (for the high gun), and Figure 38 shows source spectra for both gun heights. The source mic was located about 1.24 m above the low gun and about 1.14 m below the high gun, which may be responsible for the differences in the spectra for the two gun locations (the same gun was used). Representative spectra for the microphones mounted on the pole located 110 meters from the source are presented in various combinations in Figures 39 through 43. A source spectrum is included in each plot, arbitrarily reduced 30 dB in magnitude, for comparison of shape. Some change in the shape of the source spectrum with distance is to be expected, due for example to atmospheric absorption and refraction, as well as to ground interaction, so that care must be used in drawing conclusions from comparison of the shape of source and 110 m spectra, especially for the high propagation paths. The 110 m spectra for soybeans exhibit strong local maxima in attenuation of sound energy (minima in the sound exposure spectra) between 125 and 250 Hz. The spectra for propagation over grass show somewhat less pronounced local maxima in attenuation over frequencies from below 250 Hz to above 500 Hz. The 110-m spectra show evidence of considerable attenuation at higher frequencies, with the attenuation increasingly greater for propagation paths closer to the ground. Generally the beans exhibited more attenuation of higher frequencies than did grass. Both the beans and the grass seem to show significant absorption at frequencies as low as the 63 Hz band. Noted that there is a consistent difference of 1 to 2 dB between the sound exposure level for the 1.22 and 1.33-m mic heights, which may be due to a consistent measurement error between the two mics, or may indicate that measured sound level can be affected significantly by relatively small (0.1 m) errors in microphone placement.

Data shown in Table 15 and Figures 35 through 43 show note that ASEL and FSEL are not very much different for high propagation paths (high gun and high mic), but are substantially different for low propagation paths. For high propagation paths, a large portion of the sound energy occurs at frequencies in the vicinity of 1 KHz that are not strongly attenuated by the A-weighting filter. For propagation paths closer to the ground, for which much of the higher frequency portion of the acoustic energy has been attenuated, the ASEL and FSEL differ by a wider margin since proportionally more of the sound energy is located at the low frequencies that are strongly attenuated by A weighting.

Table 16 presents selected data from Table 15 for two of the 110-m long propagation paths. This table more clearly shows that seemingly modest differences in path height can result in significant differences in sound attenuation. The difference in attenuation was over 10 dB FSEL and over 20 dB ASEL.

A close look at the data presented in Table 16 gives some indication of the effect of ground interaction on measured insertion loss of the firing shed. The data for the low gun noise (mic height of 1.22 m) should be fairly representative of the unshielded gun in the insertion loss experiments. For sound diffracted around the 7-m high roofline of the shed in the insertion loss experiments, the average height of the propagation path is 4.11 m, which is somewhat represented by the average propagation height of 2.95 m for the high (2.85-m) gun, and 3.05-m mic height in the ground interaction experiment. For identical sources, for both grass and beans ground cover, the ground interaction experiments showed at least 10 dB FSEL and at least 20 dB ASEL more attenuation for the lower sound path compared to the higher path.

Since insertion loss is defined as the difference between sound level with and without the shielding structure present, the above situation would seemingly result in a reduction in measured insertion loss of similar amount due to ground interaction. This estimate cannot however be directly applied to the insertion loss experimental data for several reasons. One is that the spectrum of the unshielded gun, and thus the effects of ground interaction, may differ with azimuth. Another is that varying distance and the presence of both grass and beans for part of the path from source to receiver, as was the case for the insertion loss measurements, may influence the results. Also, the spectrum of the energy diffracted around the edges of the shed will be different from the source spectrum since diffraction is a function of frequency. Specifically, the diffracted (high path) sound spectrum should have proportionally more low frequency energy than the source spectrum, so that ground interaction would have less effect on the high path than was shown in the experiment, but A-weighting would have a greater effect. It is possible that, for some combination of source-barrier-receiver juxtaposition, source directivity, and/or source spectrum, the received noise level could be higher with the barrier in place than without the barrier.

In summary, these tests show that ground interaction can result in a substantial change in measured insertion loss when compared to calculated insertion loss values that do not account for ground interaction, or when compared to experimental data for which there is different attenuation due to ground interaction. Such a difference might occur if measurements were taken over bare earth or in winter, frozen ground and again over extensive vegetation cover in the summer. An accurate estimate of the effect of ground interaction on insertion loss is difficult to make without detailed knowledge of the spectrum of the noise diffracted around the edge of the barrier. A useful experimental procedure would be to locate a microphone behind and near to the structure at the height of the propagation path of interest, in addition to the mic located near the edge of the barrier. More information on how the gun spectrum might vary with azimuth would also be helpful.

Another difficulty arises in determining how to characterize propagation conditions and the ground to accurately predict propagation effects on insertion loss. The current ground interaction experiment

clearly demonstrated the possible effect of ground interaction at the test site but could not predict the effects of ground interaction on insertion loss.

It is instructive to examine spectra from the insertion loss experiments in some detail. Figure 44 shows spectra measured near the gun and also at the shed roofline. Figures 45 through 49 show the spectra (absolute, rather than relative) for the microphone locations of the insertion loss experiments. The spectra are generally quite similar for shed and wall for each gun, but the spectra for the unshielded (A) and shielded (B) guns are notably different in some respects. In the spectra for propagation over grass, Figures 45 and 46, the dip in the spectral curves in the vicinity of 500 Hz, previously seen in the results of the ground interaction experiment (Figure 40), is clearly present, especially for the unshielded (A) gun. Note that the A gun is at the same source height as the low gun in the ground interaction experiments. Careful comparison of the spectra in Figure 45 for the two guns reveals the diffraction attenuation of higher frequency energy in the spectrum of the shielded gun. The difference is not as great as predicted by calculations (Figure 15), probably because there is relatively more higher frequency ground interaction attenuation for the lower propagation path of the A gun. This trend should continue, causing the higher frequency portion of the spectra of the two guns to become more similar at greater distances; this can indeed be seen in Figure 46, by comparing the relative level at, say, 200 and 2000 Hz in Figures 45 and 46. The effect would diminish at still greater distances as the two paths become more nearly equal in elevation. One would also expect the mid-frequency (around 500 Hz) notch to become less prominent at greater distances because of higher frequency attenuation, due not only to ground interaction but also to other effects such as atmospheric absorption, scattering and refraction. The spectra of Figures 47 through 49 show similar general trends, but the details are more complicated because propagation is partly over grass and partly over soybean plants, with possible diffraction effects at the boundary between the two.

Effective noise mitigation would be greatly facilitated by the ability to make accurate predictions of noise levels at both large and small distances for both shielded and unshielded noise sources under a wide variety of propagation conditions. One aspect of this is an accurate, relatively simple to use, prediction algorithm that can account for source characteristics and barrier size and shape to predict the insertion loss of barriers for some useful situations. The analytical techniques used in this investigation are good candidates for this purpose. The results of the diffraction algorithm must be extended to large distances for practical propagation scenarios. Site measurements can possibly be used to calibrate parameter values in available ground interaction models. Available models for atmospheric attenuation and representative propagation conditions can be used to further refine the accuracy of predictions.

Design Charts

This study measured the relative insertion loss of the shed and wall for one particular value of barrier height. Figures 50 through 57 show the effects of changing barrier height. These charts were generated using the algorithm of Appendix A for a variety of source and barrier parameters. In these charts, the parameter H is the height of the barrier relative to the source; the algorithm takes no account of the effect of the source height above the ground. Propagation and ground interaction effects are not accounted for. The general trend is that a higher barrier yields larger insertion loss.

It is also interesting to examine how barrier height influences the degree to which other parameter changes affect insertion loss. Comparing Figures 50 and 51 shows that, for an isotropic source, a shed 20-m long yields 2 to 5 dB less insertion loss than an infinitely long shed; the change is larger for higher barriers. For a source with gun directivity, the change ranges from 0.5 to 5 dB (cf. Figures 52 and 53).

The effect of source directivity on insertion loss of an infinitely long shed (S < 0) may be determined by comparing the curves of Figures 50 and 52. These show that gun directivity causes an 8 to 14 dB decrease (less noise reduction) in the insertion loss of an infinitely long shed, with the largest reduction occurring for small values of H, for which the angle between the directions to the shed roofline and the receiver is large.

A comparison of Figures 52 and 54 shows how the spectral distribution of source acoustic energy can affect insertion loss for the spectra of the current and previous investigations respectively. Figure 14 shows these spectra. The unweighted insertion loss is 3 to 4 dB larger for a source with the "new" spectrum, because a larger proportion of the acoustic energy occurs at higher frequencies, which are attenuated more strongly by diffraction. Examination of calculated results not included here for various values of H show that the increase in A-weighted insertion loss is about 2 dB, as was noted for the results shown in Figure 34.

The primary topic of the current investigation is the relative rifle range insertion loss of the shed and wall. Comparison of Figures 52 and 56 reveals how barrier height affects the relative noise reduction performance of these two structures. Directly to the rear, at an 180-degree azimuth, the calculated insertion loss values are no more than about 2 dB different for all barrier height values presented, and are equal for H = 1.5. For smaller azimuth angles, e.g., in the vicinity of 120 degrees from the direction of fire, these calculated results indicate somewhat different conclusions. For large barrier heights, the insertion loss values for the two structures remain quite similar, i.e., they are different by no more than about 2 dB. However, for smaller structure heights, the shed yields significantly higher insertion loss than a wall of equal height at azimuths in the general vicinity of 120 degrees.

The effect of "A" frequency weighting may be seen by comparing the curves of Figures 52 and 55 for the shed and of Figures 56 and 57 for the wall. Generally the A-weighted insertion loss values are about 2 dB larger than the unweighted, as expected from the earlier discussion of Figure 15. The effect of A weighting is smaller for small barrier heights or for lines of sight near a barrier edge, for which diffraction has less effect on the spectral energy distribution.

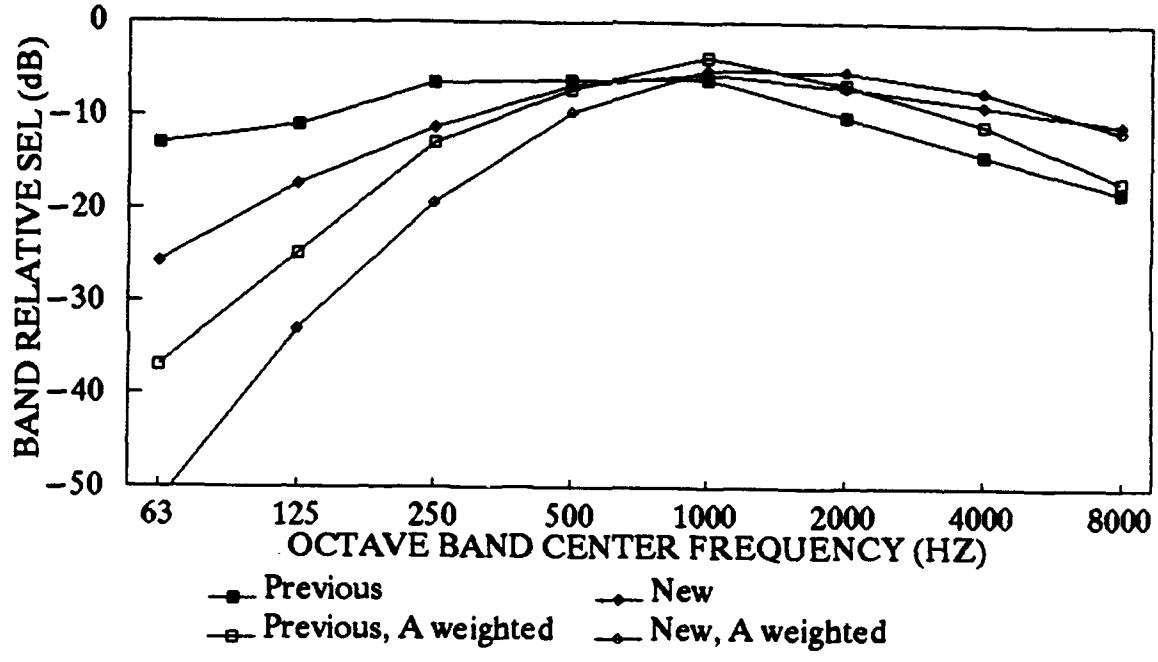

Figure 14. **Source Spectra Used for Insertion Loss Calculations, Illustrated With and Without A-Frequency Weighting.**

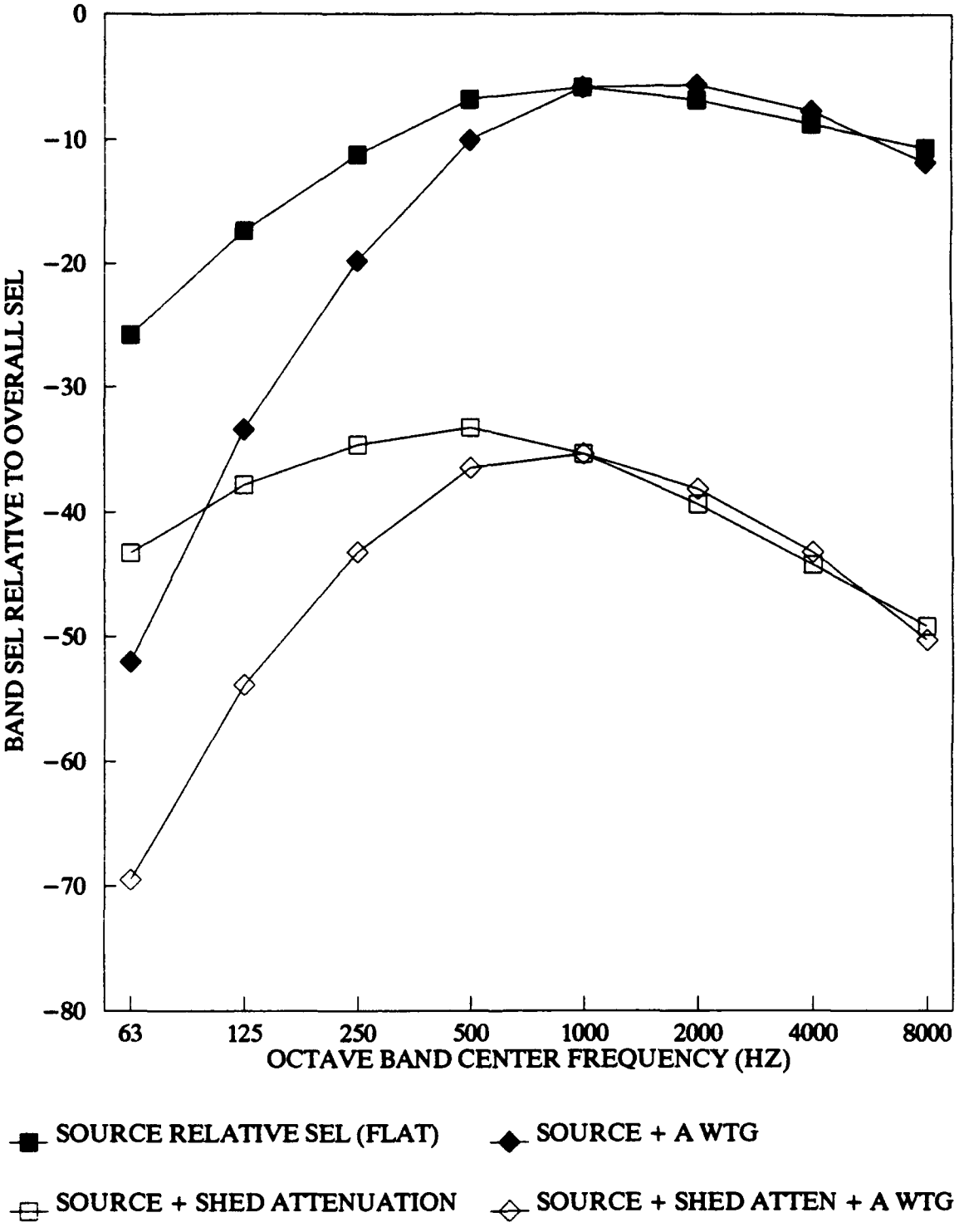

Figure 15. **Calculated Effect of Diffraction Around Shed Roofline and of Frequency Weighting on Source Spectrum, for -1 m Gun Location and 180-Degree Azimuth.**

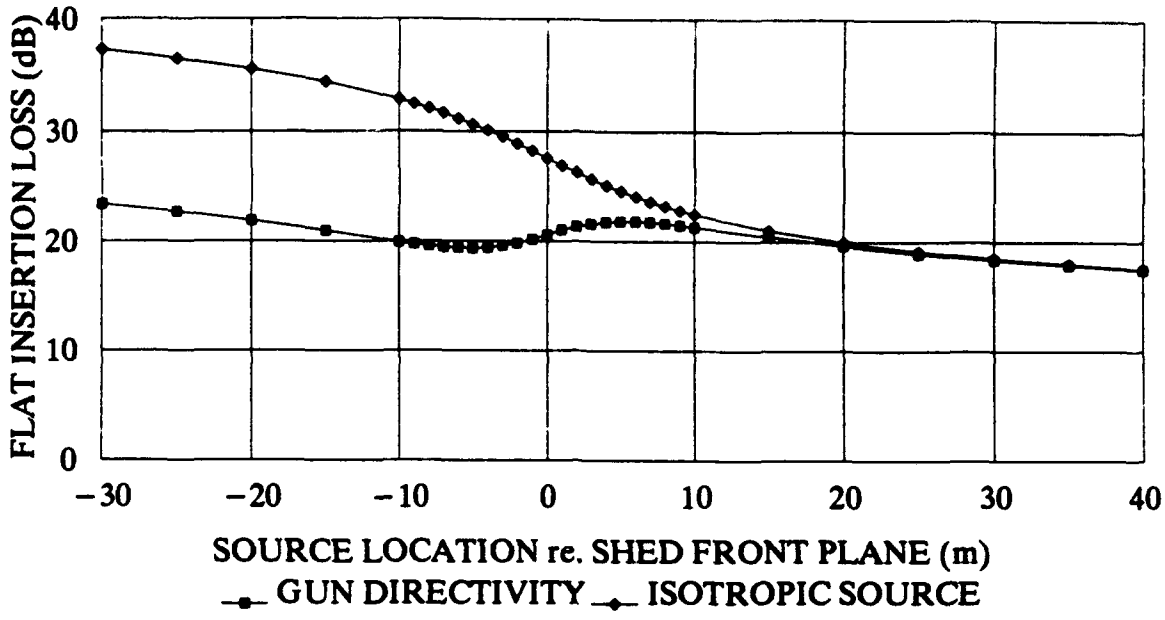

Figure 16. **Calculated Unweighted Insertion Loss at 180-Degree Azimuth vs. Source Location, for a Structure of Infinite Length, Structure Height 7 m, Source Height 0.5 m.**

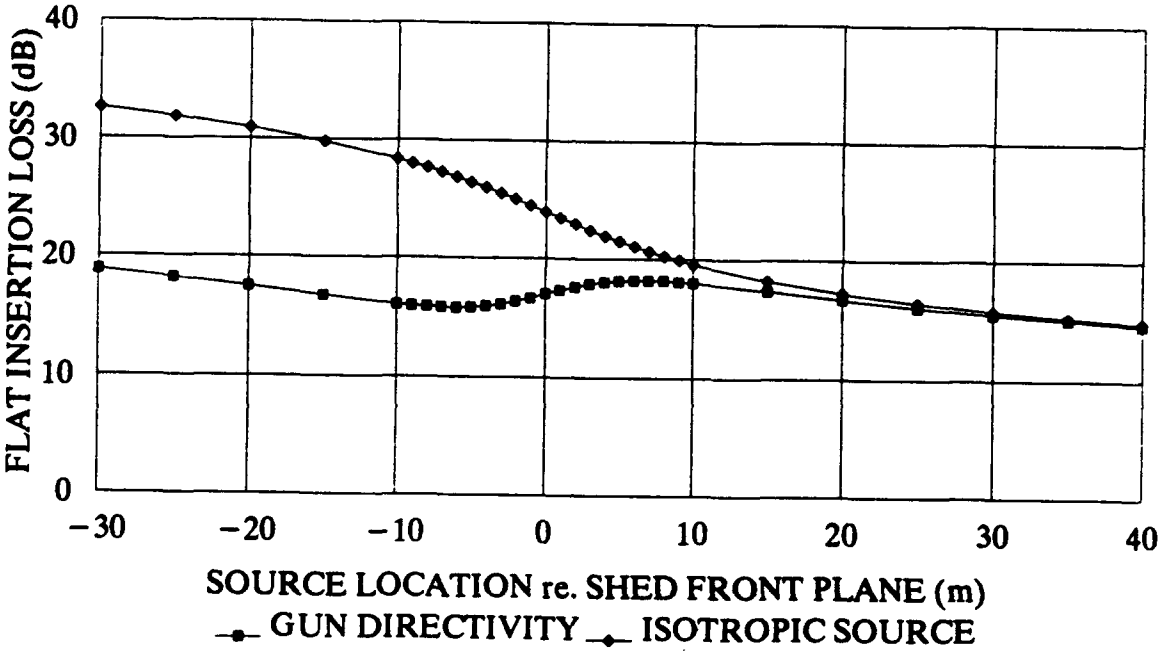

Figure 17. **Calculated Unweighted Insertion Loss at 180-Degree Azimuth vs. Source Location, for Structure Length of 20 m, Structure Height of 7 m, Source Height of 0.5 m.**

Table 3

Calculated Results From Appendix A for Insertion Loss to the Rear for Infinite Length Barrier

Configuration	Insertion loss (dB) @ 180°	
	Flat	A wtd
Shed (-1 m), isotropic source	28.3	30.5
Wall (+5 m), isotropic source	24.6	26.8
Shed (-1 m), gun firing perpendicular	20.2	22.5
Wall (+5 m), gun firing perpendicular	21.9	24.1
Shed (-1 m), gun firing parallel	28.3	30.5
Wall (+5 m), gun firing parallel	24.6	26.8
Effect on insertion loss of moving gun location from -1 m (shed) to +5 m (wall) for:		
Isotropic source	-3.7	-3.7
Gun firing perpendicular	+1.7	+1.6
Gun firing parallel	-3.7	-3.7
Effect of source directivity on insertion loss for:		
Shed (-1 m), gun firing perpendicular	-8.1	-8.0
Wall (+5 m), gun firing perpendicular	-2.7	-2.7
Shed (-1 m), gun firing parallel	0.0	0.0
Wall (+5 m), gun firing parallel	0.0	0.0

Table 4

Calculated Results From Appendix A for Insertion Loss to the Rear for 20 m Long Finite Barrier

Configuration	Insertion loss (dB) @ 180°	
	Flat	A wtd
Shed (-1 m), isotropic source	24.5	26.8
Wall (+5 m), isotropic source	21.5	23.8
Shed (-1 m), gun firing perpendicular	16.7	18.9
Wall (+5 m), gun firing perpendicular	18.2	20.4
Shed (-1 m), gun firing parallel	21.7	24.0
Wall (+5 m), gun firing parallel	19.4	21.7
Effect on insertion loss of moving gun location from -1 m (shed) to +5 m (wall) for:		
Isotropic source	-3.0	-3.0
Gun firing perpendicular	+1.5	+1.5
Gun firing parallel	-2.3	-2.3
Effect of source directivity on insertion loss for:		
Shed (-1 m), gun firing perpendicular	-7.8	-7.9
Wall (+5 m), gun firing perpendicular	-3.3	-3.4
Shed (-1 m), gun firing parallel	-2.8	-2.8
Wall (+5 m), gun firing parallel	-2.1	-2.1

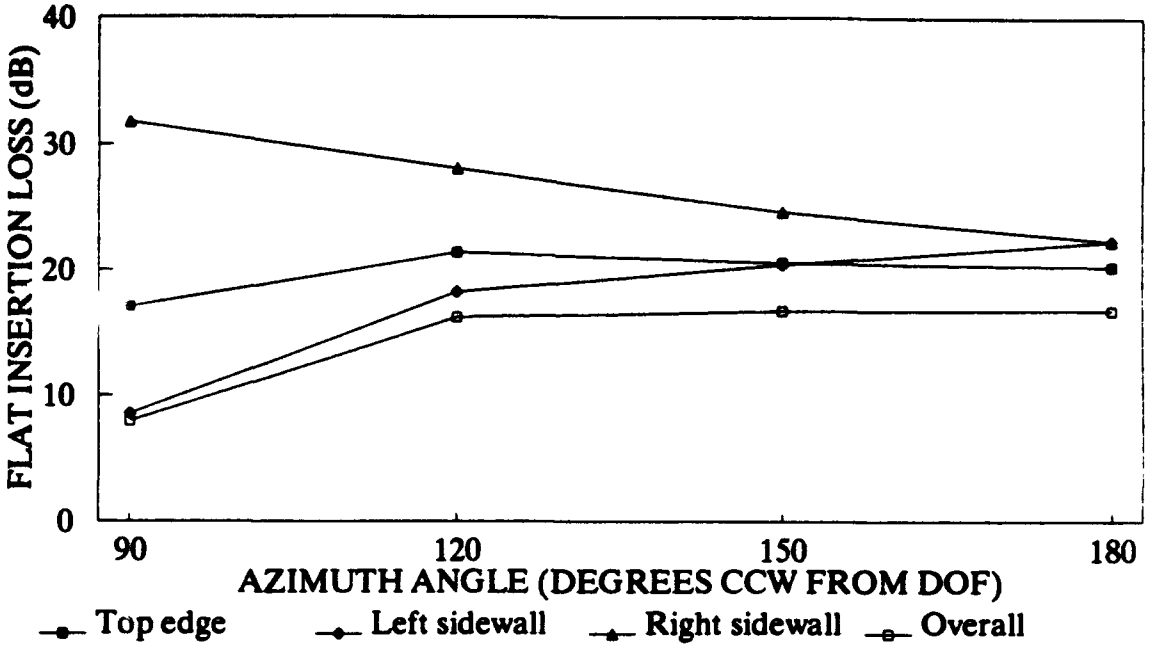

Figure 18. **Calculated Unweighted Insertion Loss for the -1 m Source Location, for a Gun Firing Normal to the Shed Front.**

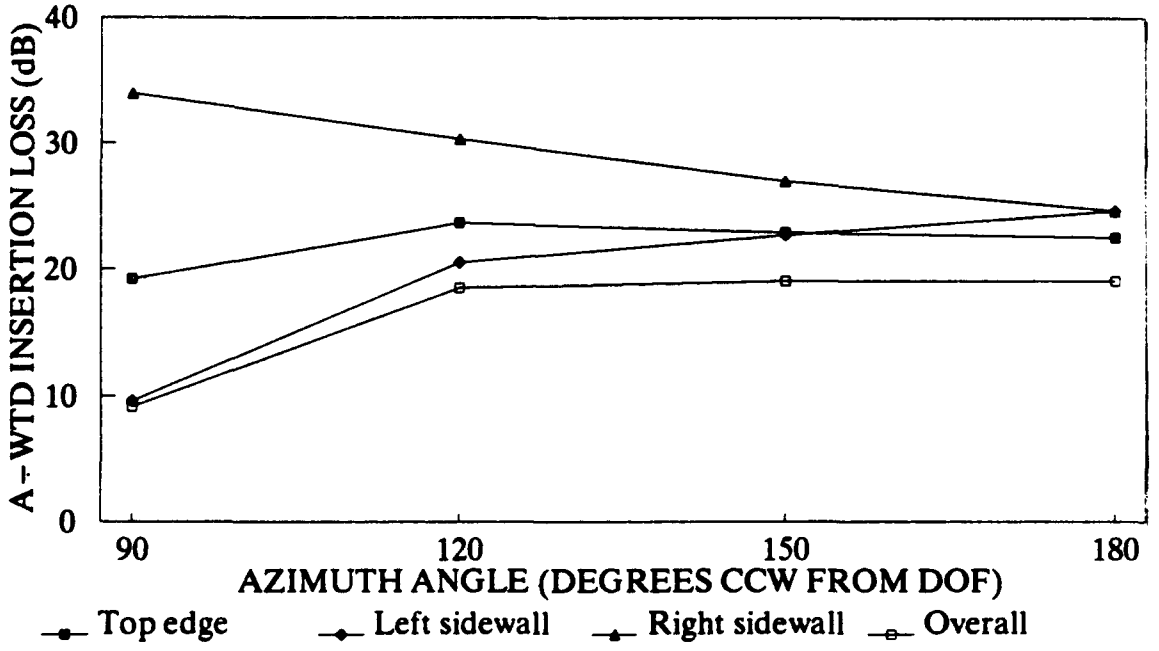

Figure 19. **Calculated A-Weighted Insertion Loss for the -1 m Source Location, for a Gun Firing Normal to the Shed Front.**

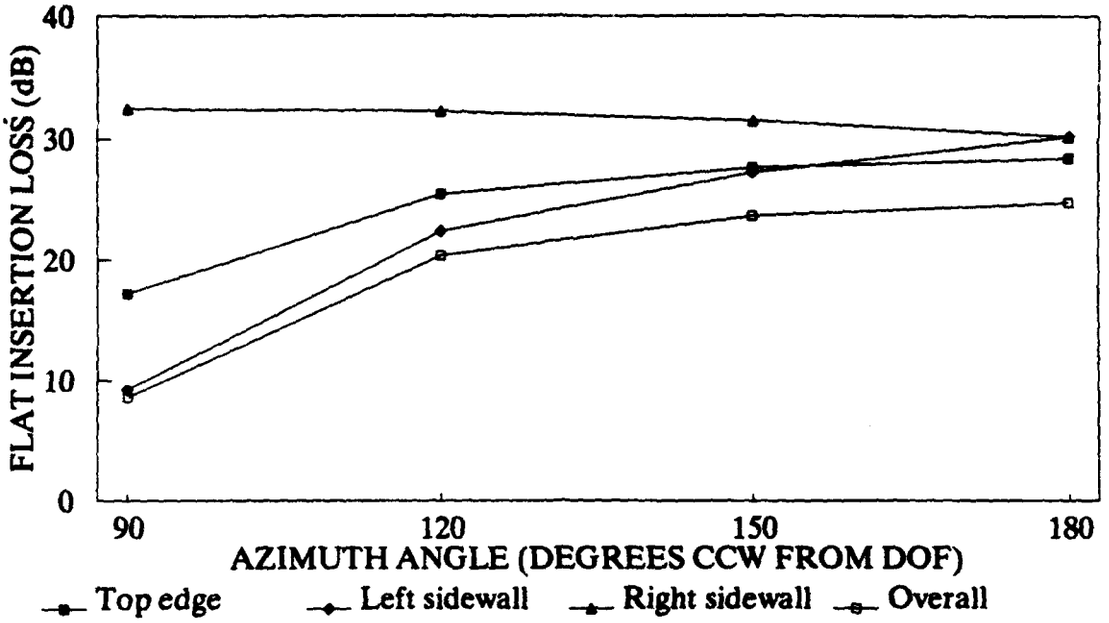

Figure 20. **Calculated Unweighted Insertion Loss for an Isotropic Source Located at the -1 m Source Location.**

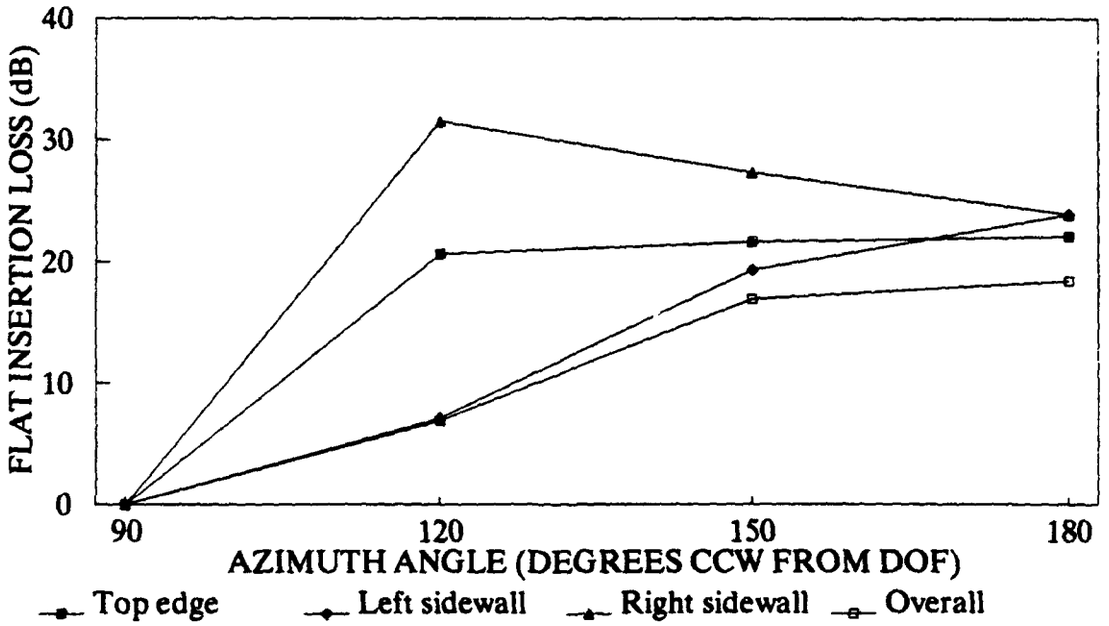

Figure 21. **Calculated Unweighted Insertion Loss for the +5 m Source Location, for a Gun Firing Normal to the Wall.**

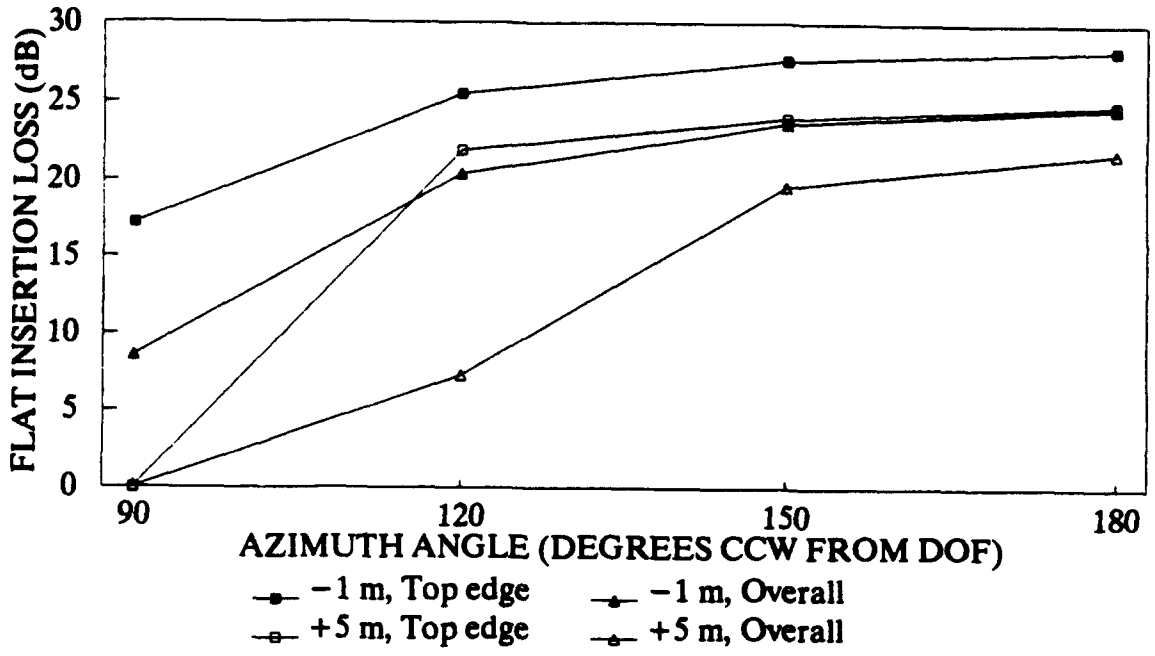

Figure 22. **A Comparison of Calculated Unweighted Insertion Loss Due to a Shed (-1 m Source Location) and a Rear Wall (+5 m Source Location) for an Isotropic Source.**

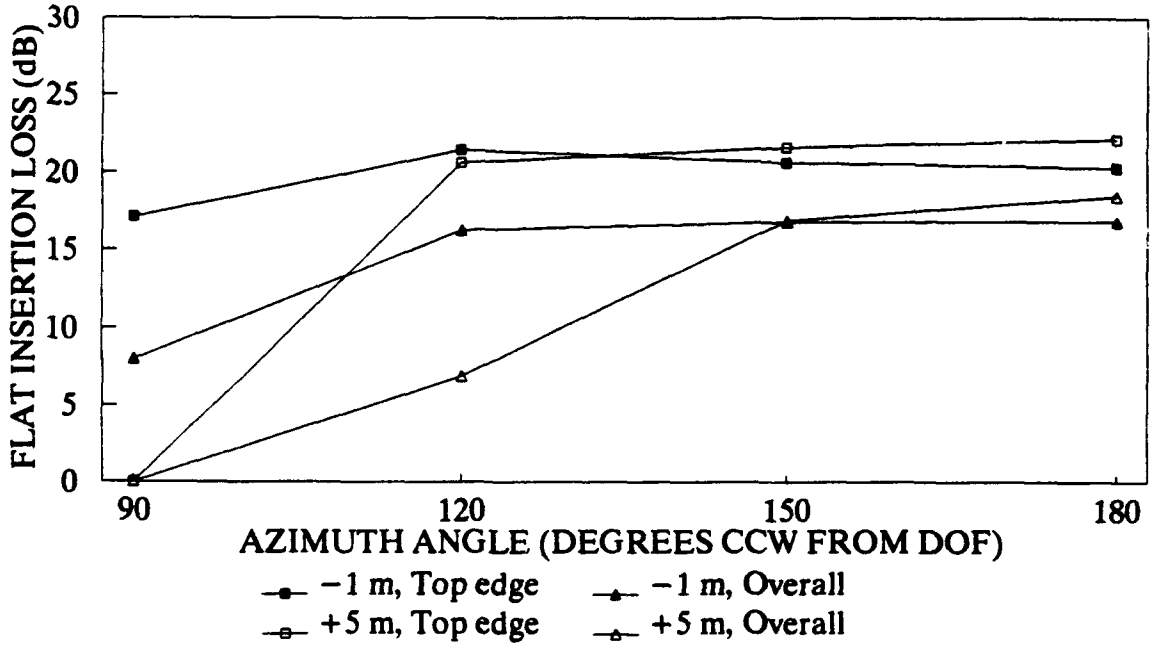

Figure 23. **A Comparison of Calculated Unweighted Insertion Loss Due to a Shed (-1 m Source Location) and a Rear Wall (+5 m Source Location) for a Gun Firing Normal to the Barrier.**

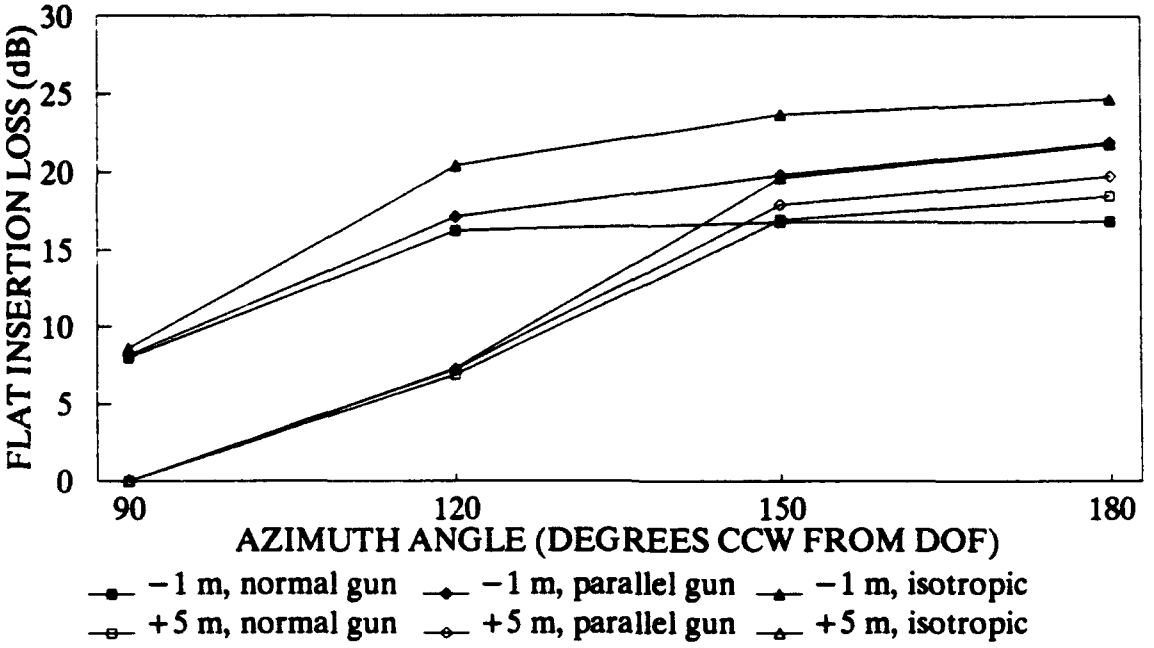

Figure 24. **Summary of Calculated Unweighted Insertion Loss for Various Combinations of Source Location and Source Directivity.**

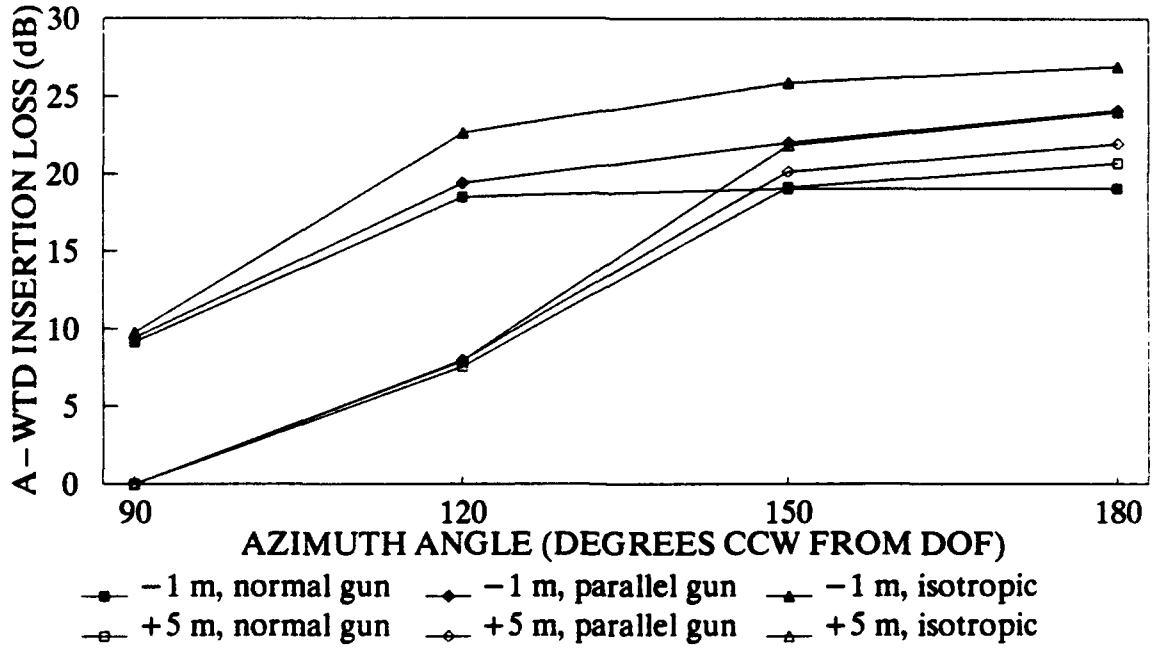

Figure 25. **Summary of Calculated A-Weighted Insertion Loss for Various Combinations of Source Location and Source Directivity.**

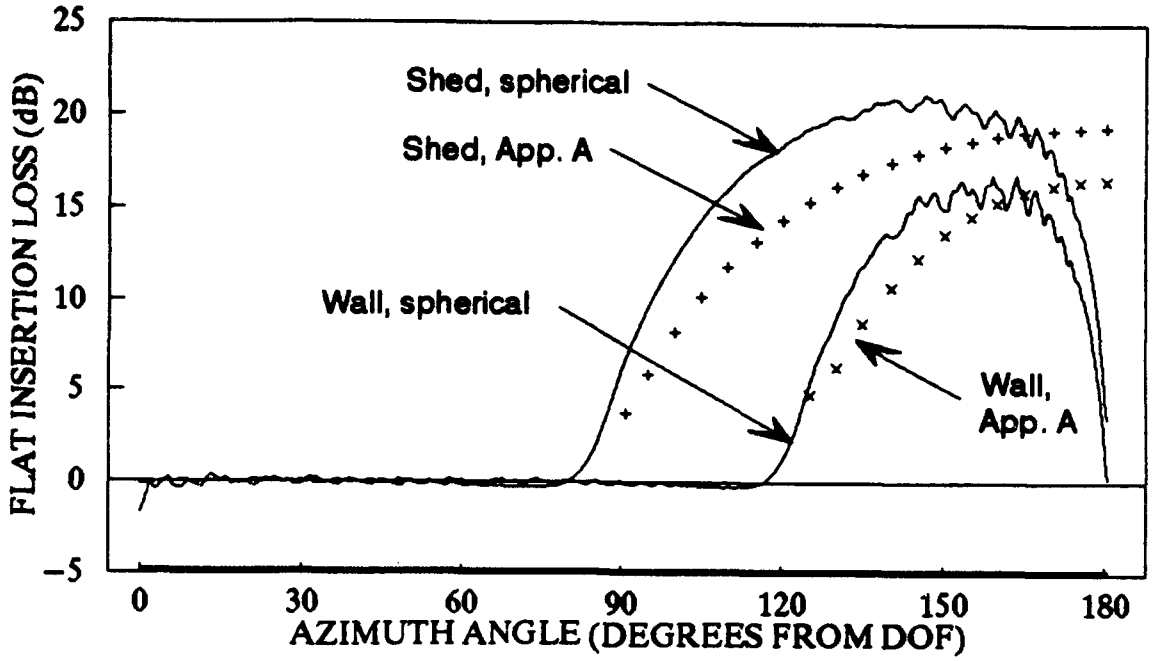

Figure 26. **Calculated Unweighted Insertion Loss Results From Two Diffraction Algorithms for an Isotropic Source Shielded by a Barrier (7 m High by 14 m Width).**

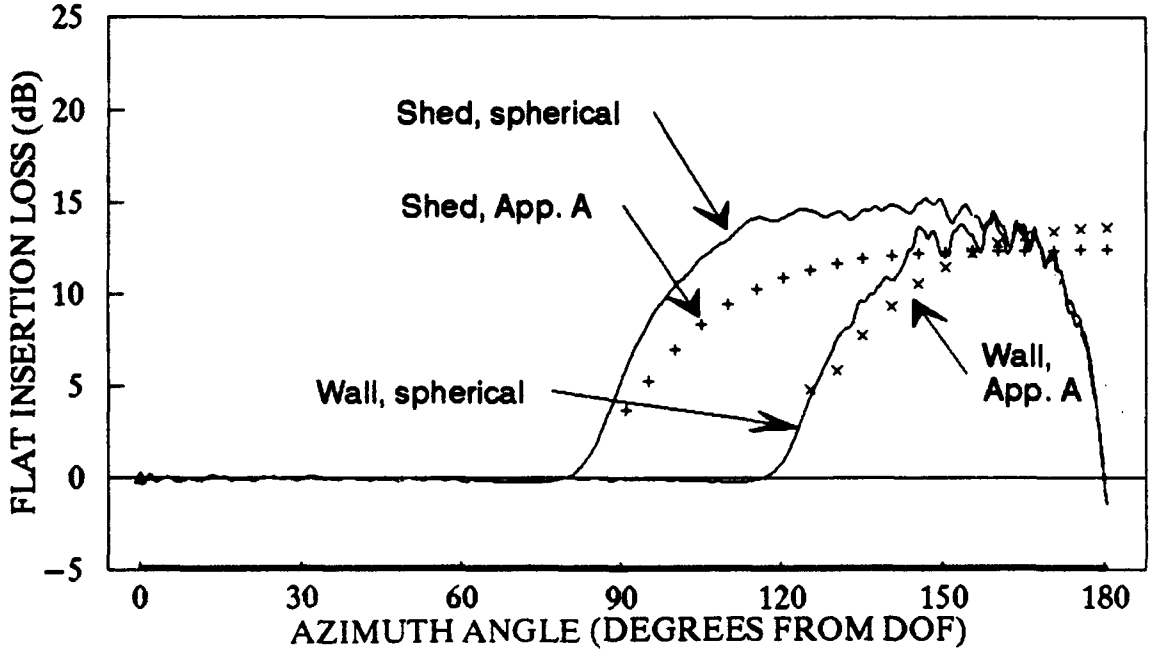

Figure 27. **Calculated Unweighted Insertion Loss Results From Two Diffraction Algorithms for a Gun Firing Normal to a Barrier (7 m High by 14 m Base Width).**

Table 5

Typical Detailed Sound Level Data From Insertion Loss Experiment

Round#	Gun	PSPL (dB)	ASEL (dB)	SEL (dB)
1	A	108.1	72.6	76.9
2	B	77.1	41.8	57.3
3	A	109.0	73.4	77.2
4	B	75.3	42.5	56.8
5	A	106.5	71.1	76.6
6	B	80.8	41.2	60.0
7	A	105.3	70.0	76.1
8	B	80.6	41.9	59.5
9	A	105.8	70.6	76.4
10	B	76.6	43.3	57.3
11	A	105.5	69.9	76.1
12	B	78.6	43.0	56.6
13	A	108.6	73.0	77.1
14	B	77.6	40.4	55.2
15	A	110.9	74.1	77.7
16	B	79.2	42.5	58.1
17	A	108.2	71.8	76.8
18	B	81.6	42.8	62.4
19	A	106.2	69.3	76.2
20	B	82.1	41.8	60.5
21	A	106.1	69.7	76.0
Mean	A	107.5	71.7	76.7
+Dev	A	3.4	2.4	1.0
-Dev	A	-2.2	-2.4	-0.6
Mean	B	79.2	42.2	58.9
+Dev	B	2.9	1.1	3.5
-Dev	B	-3.9	-1.8	-3.7

Microphone location: 5
Date: 8-7-91
Remarks: Test 3

Table 6

Insertion Loss Experiments

Test	Gun*	Location	Direction of Fire	Time	Wind**	Date
3	A&B	-1m	south	0845	0-3, 60	8-7-91
4	A&B	+5m	south	0858	3-6, 60	8-7-91
5.1	B	+5	west	0916	0-6, 60	8-7-91
5.2	A	+5	West	0920	0-6, 60	8-7-91
5.3	A	-1	West	0925	0-5, 60	8-7-91
5.4	B	-1	West	0929	0-7, 60	8-7-91

* "A" is unshielded gun; "B" is shielded
** MPH, from deg ccw re south

Table 7

Measured Shed Insertion Loss for Gun Firing South

Mic #	Angle (deg)	Distance (m)	PSPL (dB)	ASEL (dB)	FSEL (dB)
Unshielded Gun					
5	180.0	80	107.5	71.7	76.7
8	180.0	242	90.8	55.7	64.3
9	149.9	279	82.6	44.4	58.3
6	119.6	161	92.0	52.9	68.4
3	89.6	150	97.1	57.4	72.2
11	90.0	1.2	165.9	125.7	126.8
(Source)		Above			
Shielded Gun (B Gun)					
4	180.0	80	94.0	62.5	66.8
7	180.0	242	83.4	49.5	56.1
8	149.9	279	78.1	38.0	55.3
5	119.6	161	79.2	42.2	59.5
2	89.6	150	92.6	53.5	68.7
10	90.0	1.2	167.7	127.6	128.6
(Source)	74.0	Above	152.5	112.6	114.5
1		6.8			
(Roofline)		Above			
Insertion Loss					
	180.0	80	13.5	9.2	9.9
	180.0	242	7.4	6.2	8.2
	149.9	279	4.5	6.4	3.0
	119.6	161	12.8	10.7	8.9
	89.6	150	4.5	3.9	3.5
Mean insertion loss for 180o			10.5	7.7	9.1

Expt: Shed, insulated, 5.56 mm gun, Bondville site.
Date: 8-7-9 Test 3
Gun@: -1 m Firing south.
Met: Wind 60ø ccw re south @ 0-3 mph. Partly cloudy.

Table 8

Measured Wall Insertion Loss for Gun Firing South

Mic #	Angle (deg)	Distance (m)	PSPL (dB)	ASEL (dB)	FSEL (dB)
Unshielded gun (A Gun)					
5	180.0	86	103.7	69.1	75.6
8	180.0	248	90.8	56.0	64.0
9	150.5	284	81.1	44.8	58.2
6	121.5	164	92.0	53.8	67.2
3	91.9	150	96.8	56.8	71.5
11	90.0	1.2	167.2	126.6	127.6
(Source)		Above			
Shielded gun (B Gun)					
4	180.0	86	95.9	62.0	66.1
7	180.0	248	85.1	49.4	55.5
8	150.5	284	79.0	40.5	54.0
5	121.5	164	86.8	46.4	62.7
2	91.9	150	96.1	56.1	72.2
10	90.0	1.2	166.9	125.8	127.0
(Source)	121.6	Above	147.3	107.3	108.8
1		7.6			
(Roofline)		Above			
Insertion loss					
	180.0	86	7.8	7.1	9.5
	180.0	248	5.7	6.6	8.5
	150.5	284	2.1	4.3	4.2
	121.5	164	5.2	7.4	4.5
	91.9	150	0.7	0.7	-0.7
Mean insertion loss for 180°:			6.8	6.8	9.0

Expt: Wall, insulated, 5.56 mm gun, Bondville site.
Date: 8-7-91 Test 4
Gun @: +5 m Firing south.
Met: Wind 60° ccw re south @ 3-6 mph. Partly cloudy.

Table 9

Measured Shed Insertion Loss for Gun Firing West

Mic #	Angle (deg)	Distance (m)	PSPL (Db)	ASEL (Db)	FSEL (Db)
Unshielded Gun (A Gun) Test 5.3					
5	180.0	80	112.2	74.7	83.0
8	180.0	242	96.8	59.4	71.0
9	149.9	279	84.2	46.9	61.9
6	119.6	161	90.0	51.2	66.1
3	89.6	150	89.7	50.8	65.1
11 (Source)	90.0	1.2 Above	166.7	126.8	127.9
Shielded Gun (B Gun) Test 5.4					
4	180.0	80	91.5	61.5	65.7
7	180.0	242	79.4	45.1	51.9
8	149.9	279	75.5	35.9	53.5
5	119.6	161	80.4	43.1	59.2
2	89.6	150	94.6	51.7	65.5
10 (Source)	90.0	1.2 Above	166.9	126.1	127.3
1 (Roofline)	74.0	6.8 Above	151.1	112.5	113.9
Insertion Loss					
	180.0	80	20.7	13.2	17.3
	180.0	242	17.4	14.3	19.1
	149.9	279	8.7	11.0	8.4
	119.6	161	9.6	8.1	6.9
	89.6	150	-4.9	-0.9	-0.4
Mean insertion loss for 180°:			19.1	13.8	18.2

Expt: Shed, insulated, 5.56 mm gun, Bondville site.
Date: 8-7-91 Tests 5.3 & 5.4.
Gun @: -1 m Firing west.
Met: Wind 60° ccw re south @ 0-5 mph variable.

Table 10

Measured Wall Insertion Loss for Gun Firing West

Mic #	Angle (deg)	Distance (m)	PSPL (dB)	ASEL (dB)	FSEL (dB)
Unshielded Gun (A Gun) Test 5.2.					
5	180.0	86	112.3	74.5	83.0
8	180.0	248	97.3	60.4	71.9
9	150.5	284	84.9	47.4	62.4
6	121.5	164	89.6	50.7	66.3
3	91.9	150	90.5	51.3	65.6
11	90.0	1.2	165.8	125.8	126.8
(Source)		Above			
Shielded Gun (B Gun) Test 5.1.					
4	180.0	86	101.5	68.5	72.5
7	180.0	248	90.3	55.2	60.9
8	150.5	284	78.7	43.5	58.0
5	121.5	164	83.8	46.6	65.1
2	91.9	150	90.8	56.4	73.4
10	90.0	1.2	166.6	125.8	127.3
(Source)	121.6	Above	150.3	111.7	113.3
1		7.6			
(Roofline)		Above			
Insertion Loss					
	180.0	86	10.8	6.0	10.5
	180.0	248	7.0	5.2	11.0
	150.5	284	6.2	3.9	4.4
	121.5	164	5.8	4.1	1.2
	91.9	150	-0.3	-5.1	-7.8
Mean Insertion Loss for 180°			8.9	5.6	10.8

Expt: Wall, insulated, 5.56 mm gun, Bondville site.
Date: 8-7-91; Test 5.1 & 5.2
Gun @: +5 m; Firing west
Met: Wind 60° ccw re south @ 3-6 mph variable

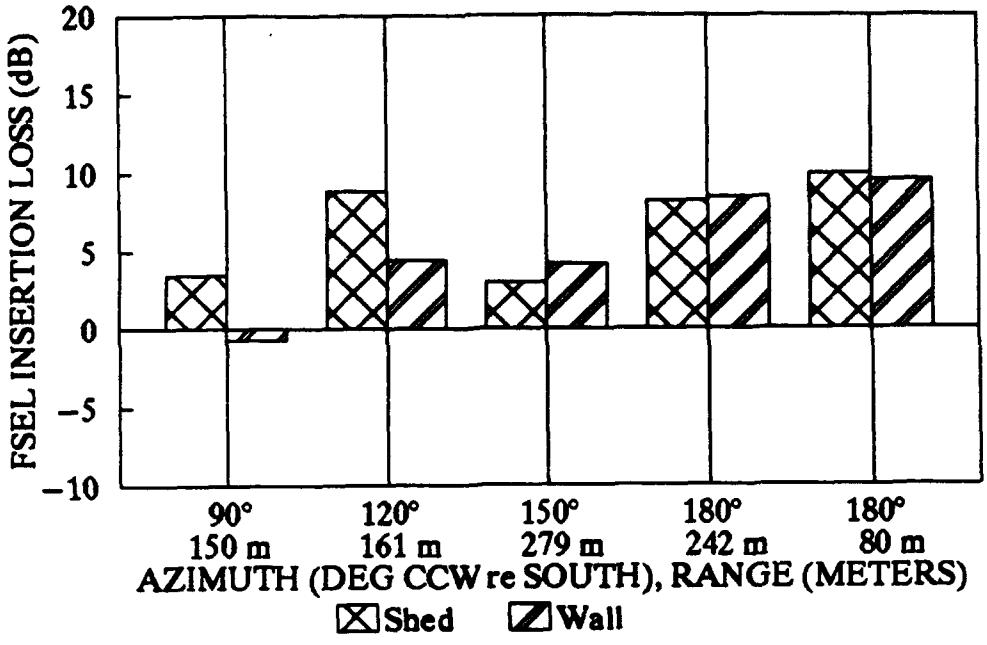

Figure 28. **Shed and Wall Experimental FSEL Insertion Loss for Gun Firing Normal to Barrier (South).**

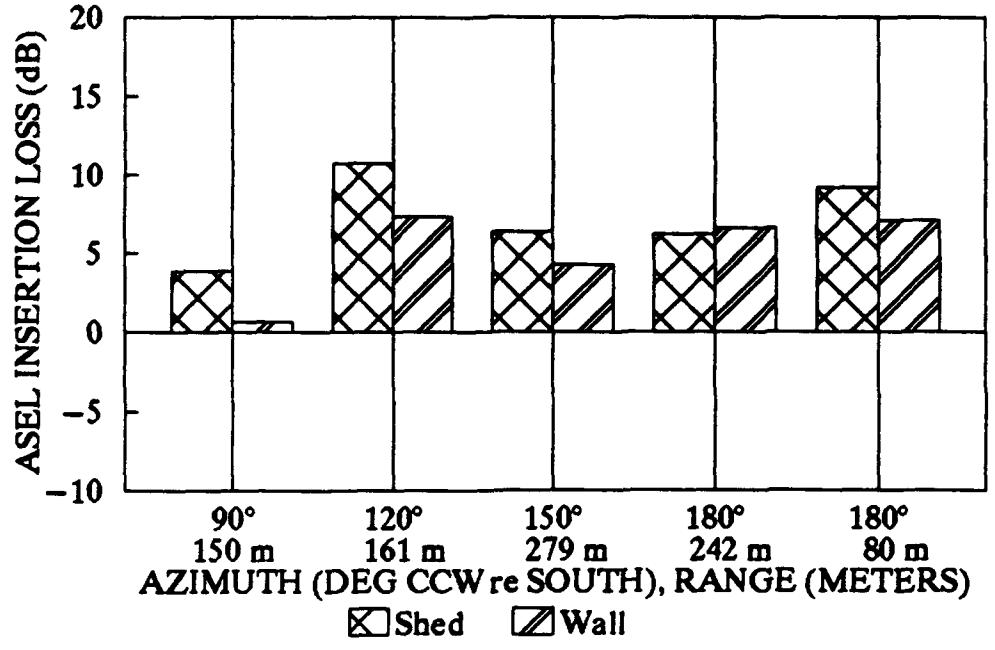

Figure 29. **Shed and Wall Experimental ASEL Insertion Loss for Gun Firing Normal to Barrier (South).**

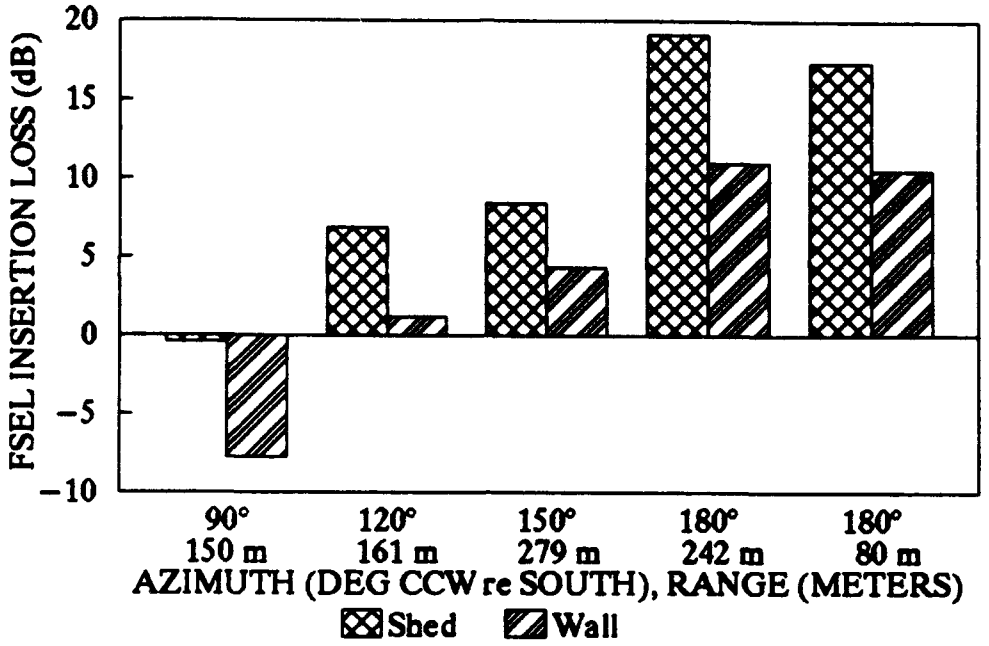

Figure 30. **Shed and Wall Experimental FSEL Insertion Loss for Gun Firing Parallel to Barrier (West).**

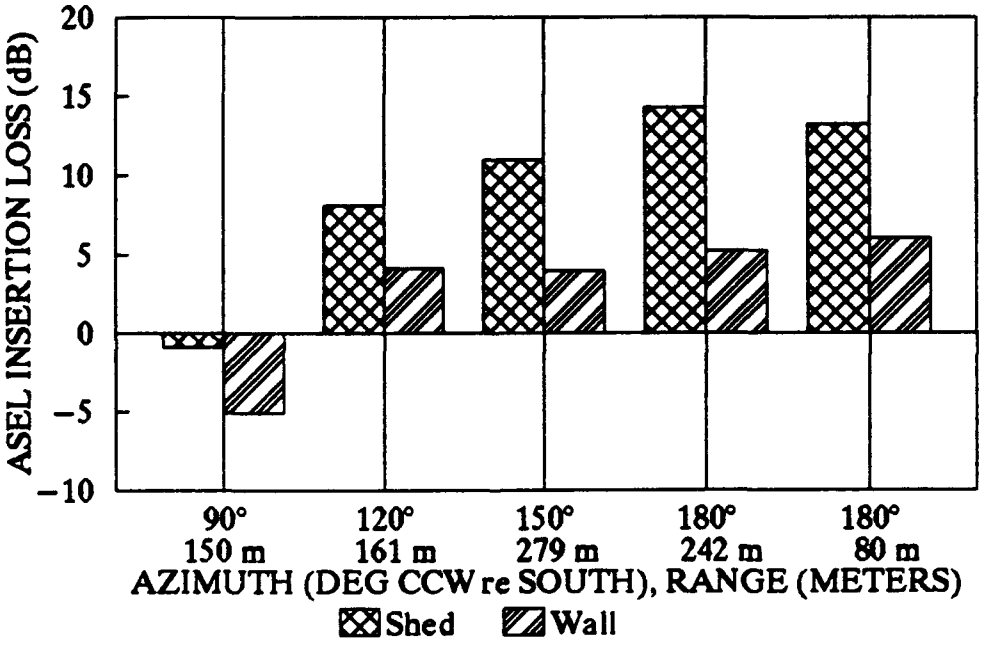

Figure 31. **Shed and Wall Experimental ASEL Insertion Loss for Gun Firing Parallel to Barrier (West).**

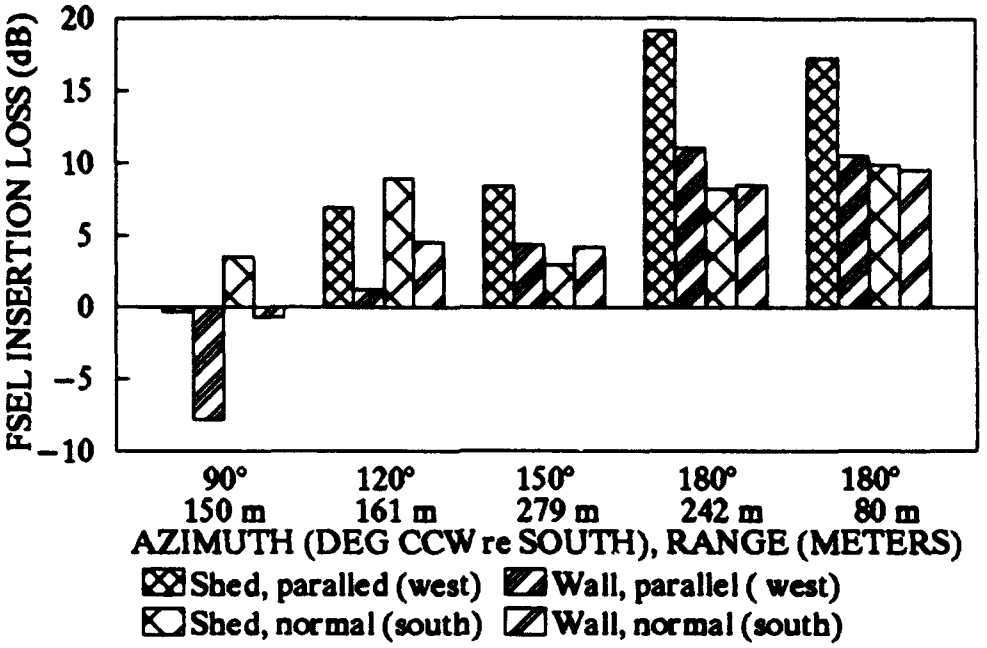

Figure 32. **Shed and Wall Experimental FSEL Insertion Loss for Both Gun Firing Directions.**

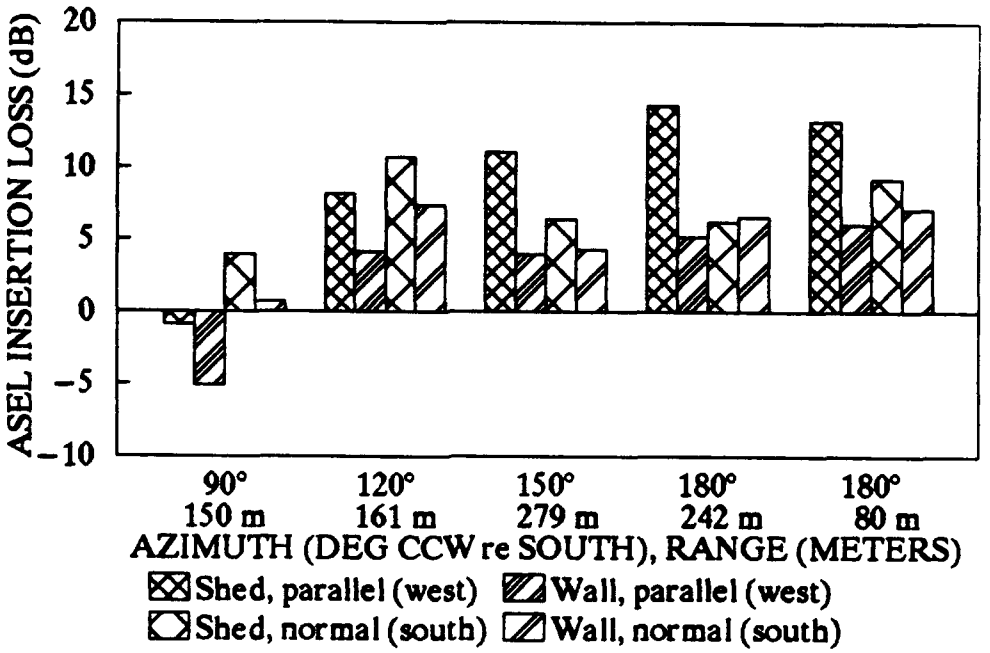

Figure 33. **Shed and Wall Experimental ASEL Insertion Loss for Both Gun Firing Directions.**

Table 11

Mean Experimental Insertion Loss to the Rear

Configuration	Mean Insertion Loss (dB)	
	ASEL @ 180°	SEL @ 180°
Shed, Gun @ -1 m, firing south	7.7	9.1
Wall, Gun @ +5 m, firing south	6.8	9.0
Shed, Gun @ -1 m, firing west	13.8	18.2
Wall, Gun @ +5 m, firing west	5.6	10.8
Shed-Wall Difference, gun firing south	0.9	0.1
Shed-Wall Difference, gun firing west	8.2	7.4

Azimuth angle is measured ccw from south

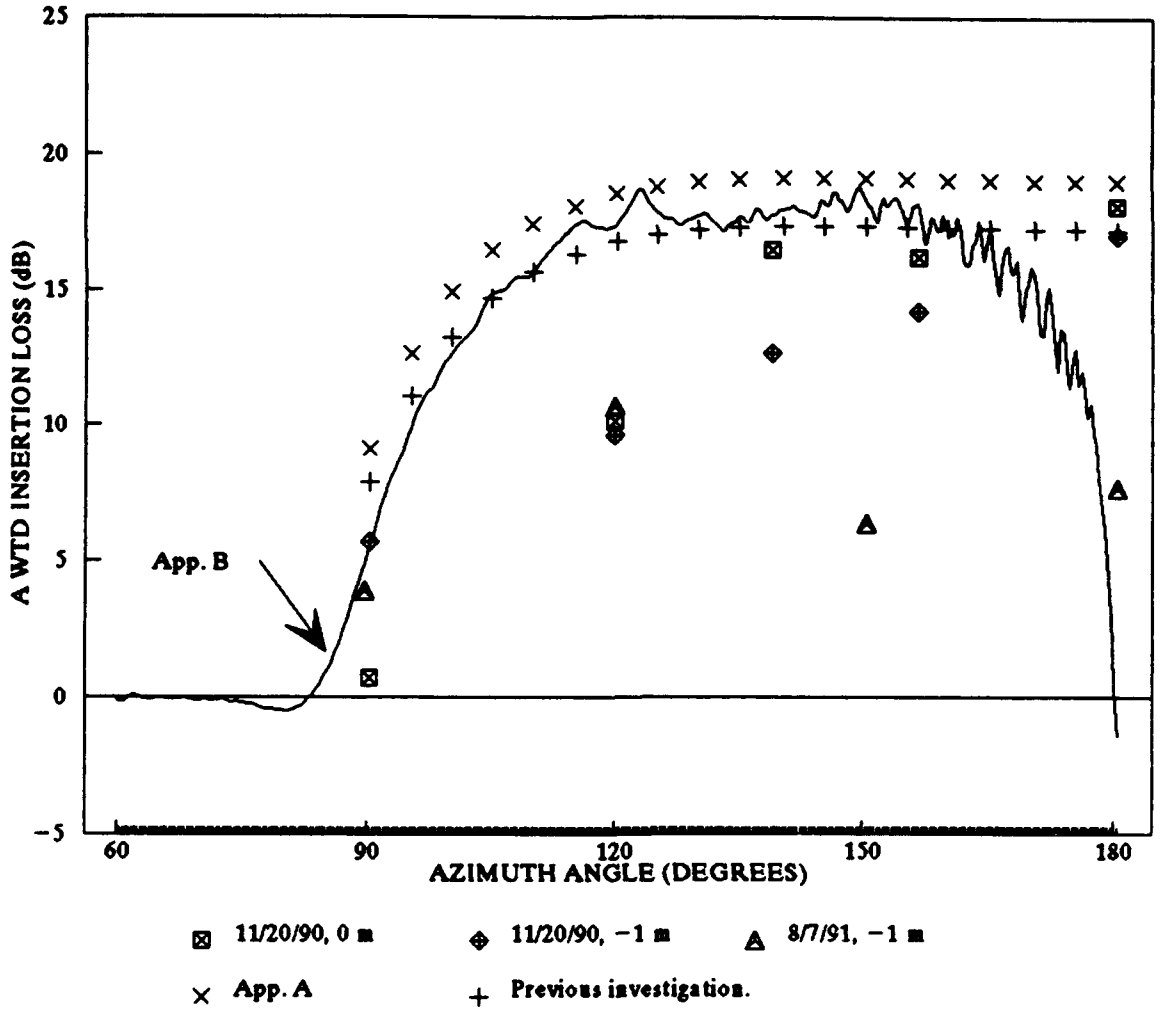

Figure 34. **Analytical and Experimental A-Weighted Shed Insertion Loss for Gun Firing Normal to Shed Front.**

Table 12

The Effect of Excess Attenuation on Measured Shed Insertion Loss for Gun Firing South (Data of Table 7)

Experimental Parameters	PSPL (dB)	ASEL (dB)	FSEL (dB)
Unshielded Gun (A Gun)			
Level @ mic # 5 (180°, 80 meters)	107.5	71.7	76.7
Level @ mic # 8 (180°, 242 meters)	90.8	55.7	64.3
Difference:	16.7	16.0	12.4
Spherical spreading: 20 log (242/80)	9.6	9.6	9.6
Excess Attenuation:	7.1	6.4	2.8
Mic # 8 corrected level:	97.9	62.1	67.1
Shielded Gun (B Gun)			
Level @ mic # 4 (180°, 80 meters)	94.0	62.5	66.8
Level @ mic # 7 (180°, 242 meters)	83.4	49.5	56.1
Difference:	10.6	13.0	10.7
Spherical spreading: 20 log (250/88)	9.1	9.1	9.1
Excess Attenuation:	1.5	3.9	1.6
Mic # 7 corrected level:	84.9	53.4	57.7
Insertion Loss			
Uncorrected @ 180°, 80 meters:	13.5	9.2	9.9
Uncorrected @ 180°, 242 meters:	7.4	6.2	8.2
Corrected @ 180°, 242 meters:	13.0	8.7	9.4
Effect of Excess Attenuation:	-5.6	-2.5	-1.2

Expt: Shed, insulated, 5.56 mm gun, Bondville site
Date: 8-7-91, Test 3
Gun @: -1 m, Firing south
Met: Wind 60° ccw re south @ 0-3 mph. Partly cloudy

Table 13

The Effect of Excess Attenuation on Measured Wall Insertion Loss for Gun Firing South (Data of Table 8)

Experimental Parameters	PSPL (dB)	ASEL (dB)	FSEL (dB)
Unshielded gun (A gun)			
Level @ mic # 5 (180°, 86 meters)	103.7	69.1	75.6
Level @ mic # 8 (180°, 248 meters)	90.8	56.0	64.0
Difference:	12.9	13.1	11.6
Spherical spreading: 20 log (248/86)	9.2	9.2	9.2
Excess attenuation:	3.7	3.9	2.4
Mic # 8 corrected level:	94.5	59.9	66.4
Shielded gun (B gun)			
Level @ mic # 4 (180°, 86 meters)	95.9	62.0	66.1
Level @ mic # 7 (180°, 248 meters)	85.1	49.4	55.5
Difference:	10.8	12.6	10.6
Spherical spreading: 20 log (251/89)	9.0	9.0	9.0
Excess Attenuation:	1.8	3.6	1.6
Mic # 7 corrected level:	86.9	53.0	57.1
Insertion loss			
Uncorrected @ 180°, 80 meters:	7.8	7.1	9.5
Uncorrected @ 180°, 242 meters:	5.7	6.6	8.5
Corrected @ 180°, 242 meters:	7.6	6.9	9.3
Effect of excess attenuation:	-1.9	-0.3	-0.8

Expt: wall, insulated, 5.56 mm gun, Bondville site.
Date: 8-7-91 Test 4
Gun @: +5 m, firing south.
Met: wind 60° ccw re south @ 3-6 mph; partly cloudy.

Table 14

Ground Interaction Experiments

Test	Time	Gun	Ground Cover	Wind (MPH, from)	Mic Azimuth (deg) re DOF*
3	0703	High	Grass	1-2, 0°	90
4	0709	Low	Grass	1-2, 0°	90
10	0834	High	Beans	1-2, 0°	90
11	0839	Low	Beans	1-2, 0°	90
14	0912	High	Grass	1-2, 0°, gusts 5	90
15	0916	Low	Grass	0-2,–60°, gusts 5	90

*Azimuth angles are measured ccw from south, which was the direction of fire

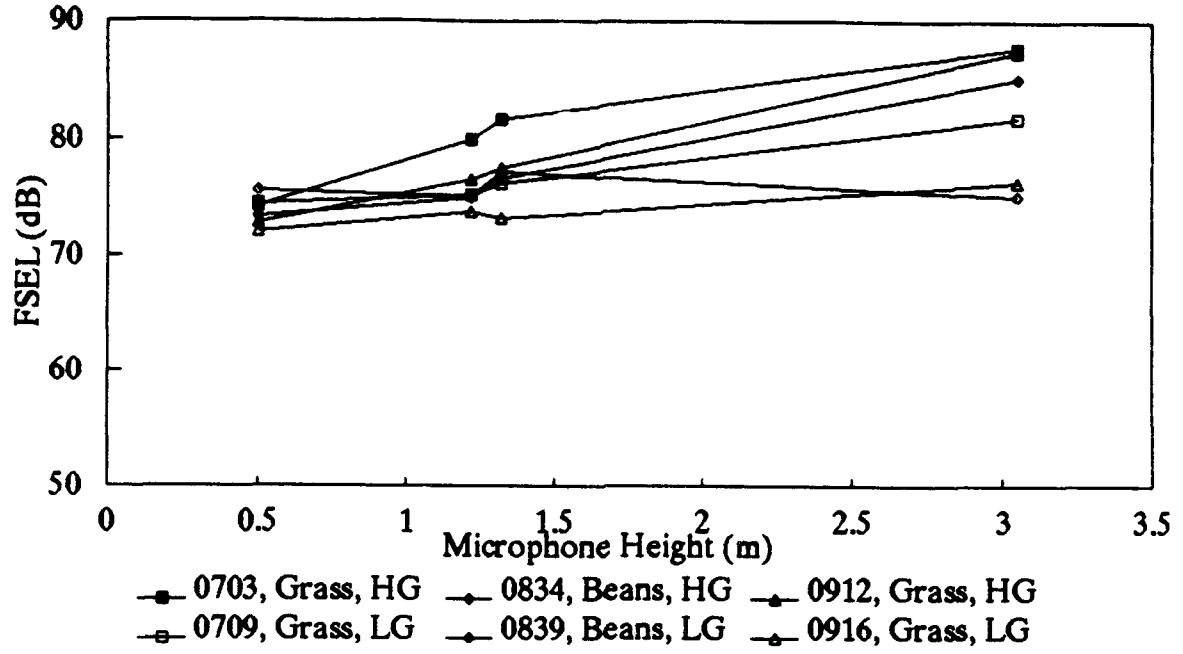

Figure 35. **Experimental FSEL for Various Propagation Paths Over Two Types of Ground Cover.**

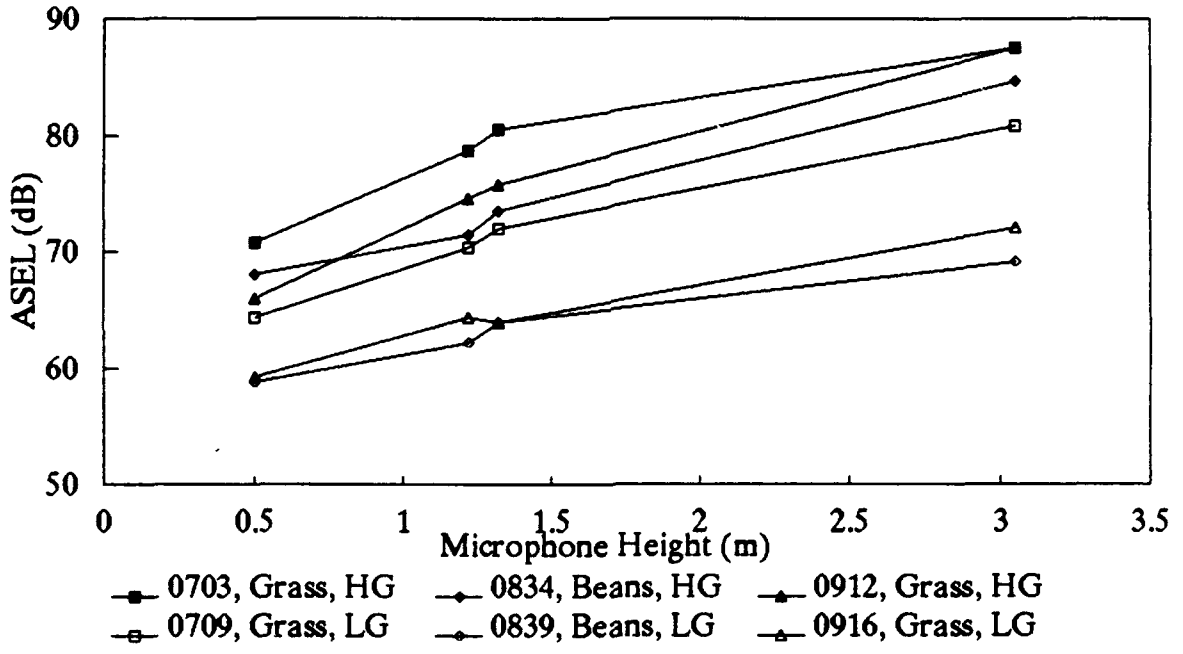

Figure 36. **Experimental ASEL for Various Propagation Paths Over Two Types of Ground Cover.**

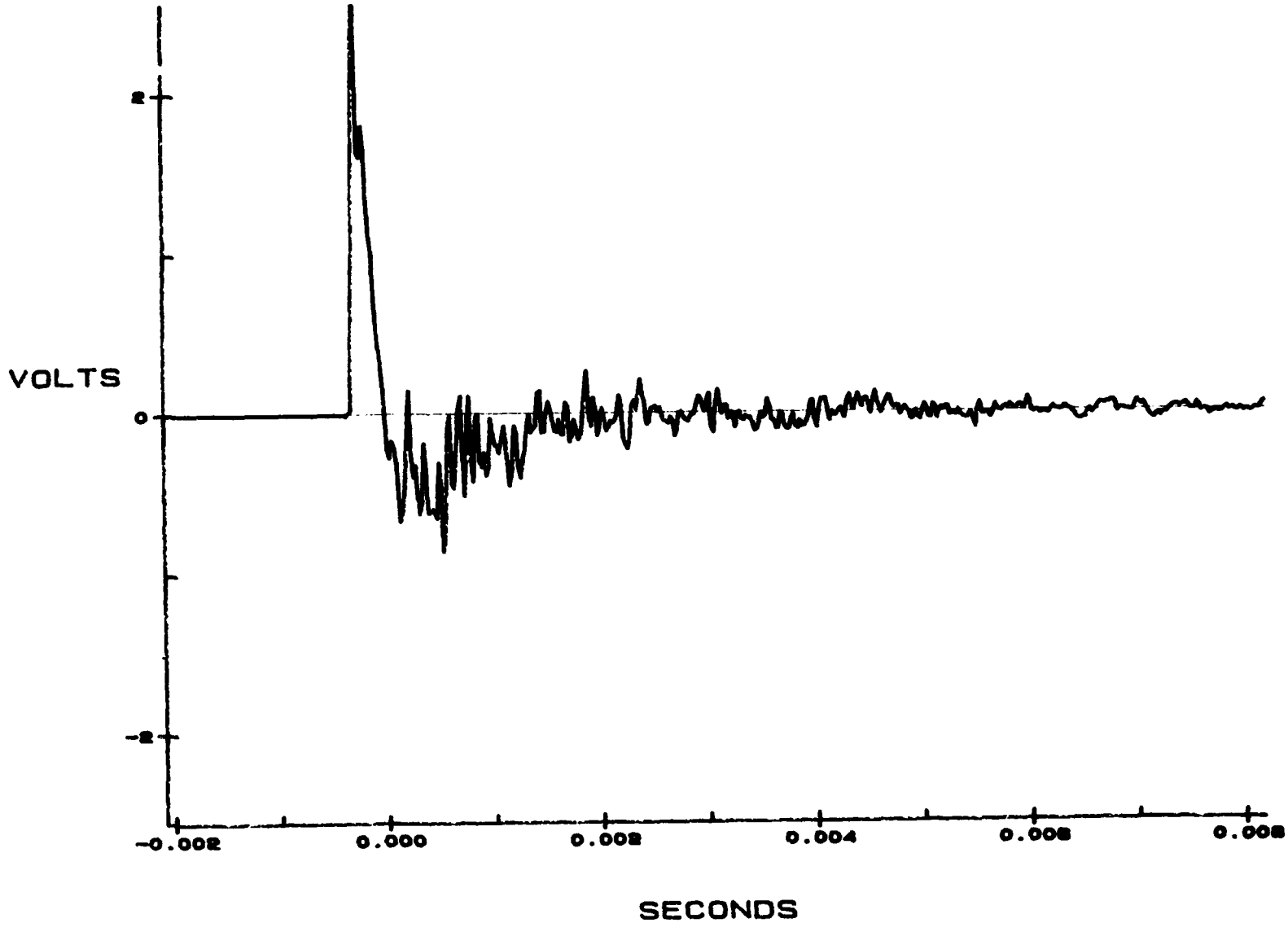

Figure 37. Source Microphone Waveform for High Gun, Test 3, Round 1, Mic # 1 (Gun Height 2.85 m, Mic Height 1.70 m).

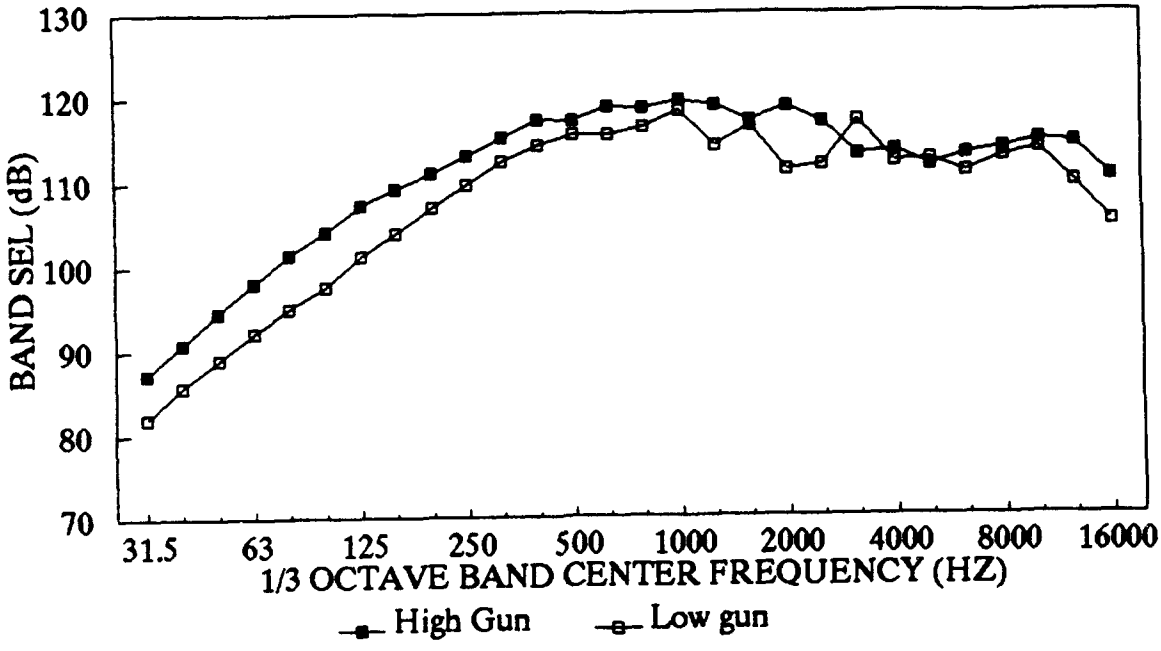

Figure 38. **Source Spectra for High Gun and Low Gun, Ground Reflection Excluded, for Ground Interaction Experiment.**

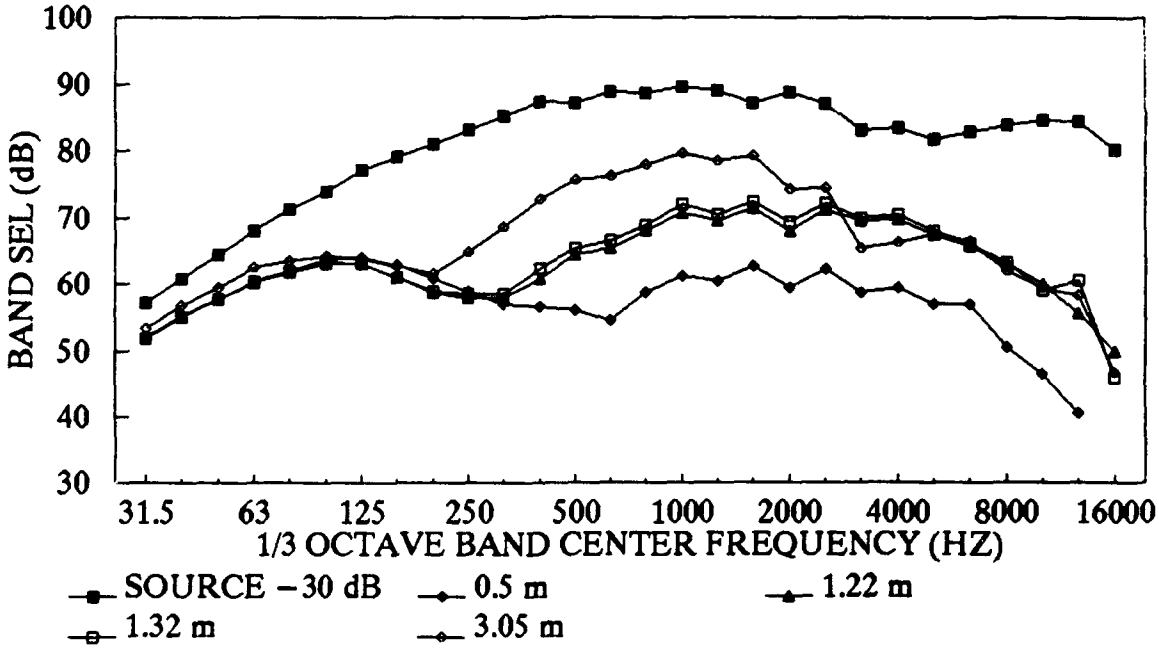

Figure 39. **Spectra for High Gun Over Grass for Various Microphone Heights.**

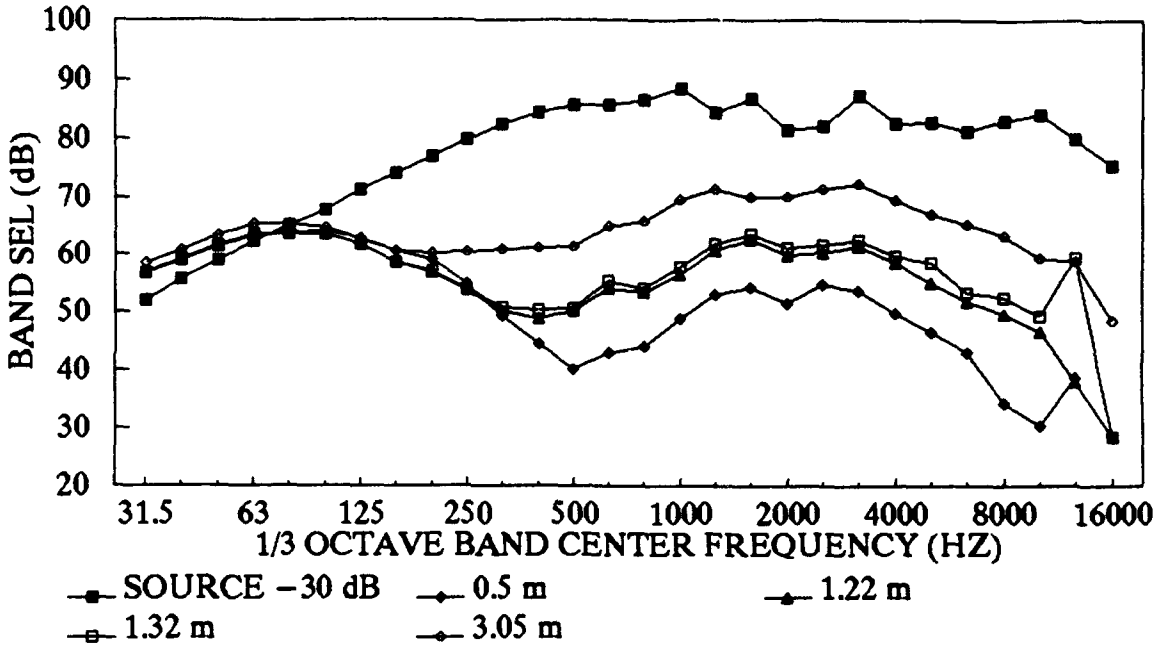

Figure 40. **Spectra for Low Gun Over Grass for Various Microphone Heights.**

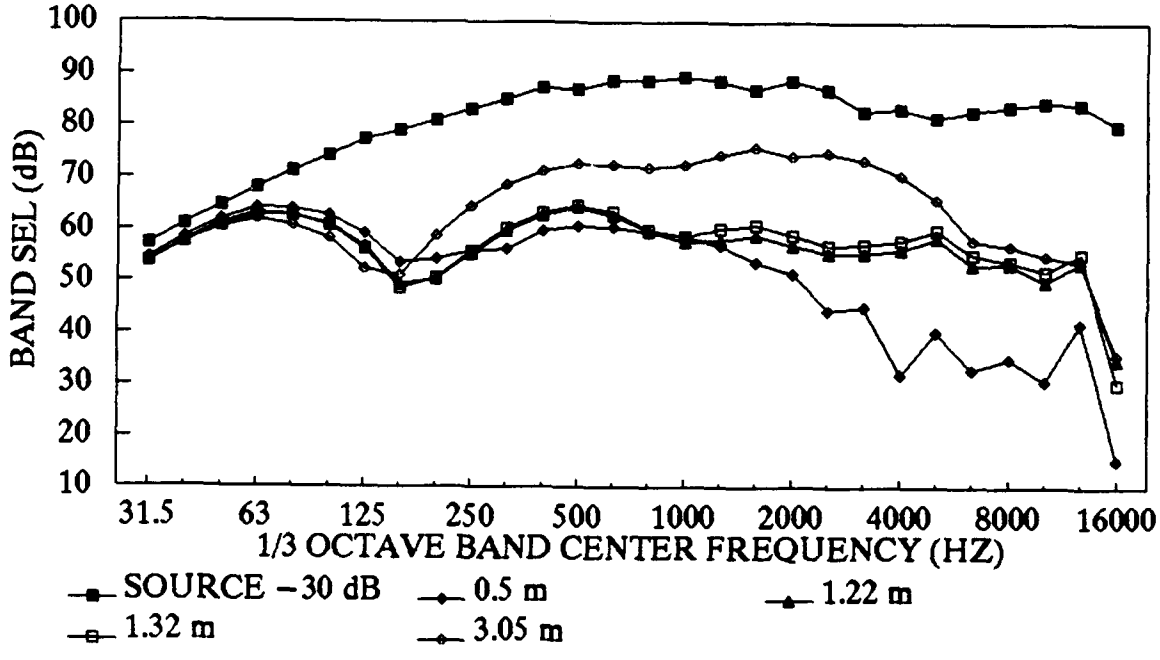

Figure 41. **Spectra for High Gun Over Beans for Various Microphone Heights.**

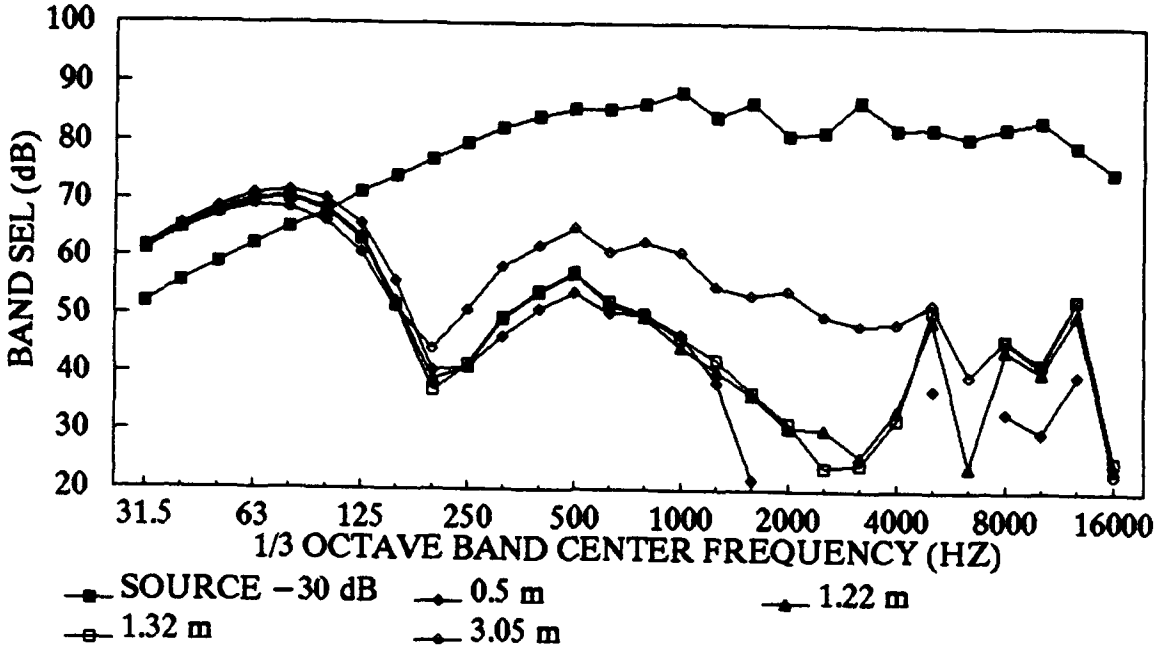

Figure 42. Spectra for Low Gun Over Beans for Various Microphone Heights.

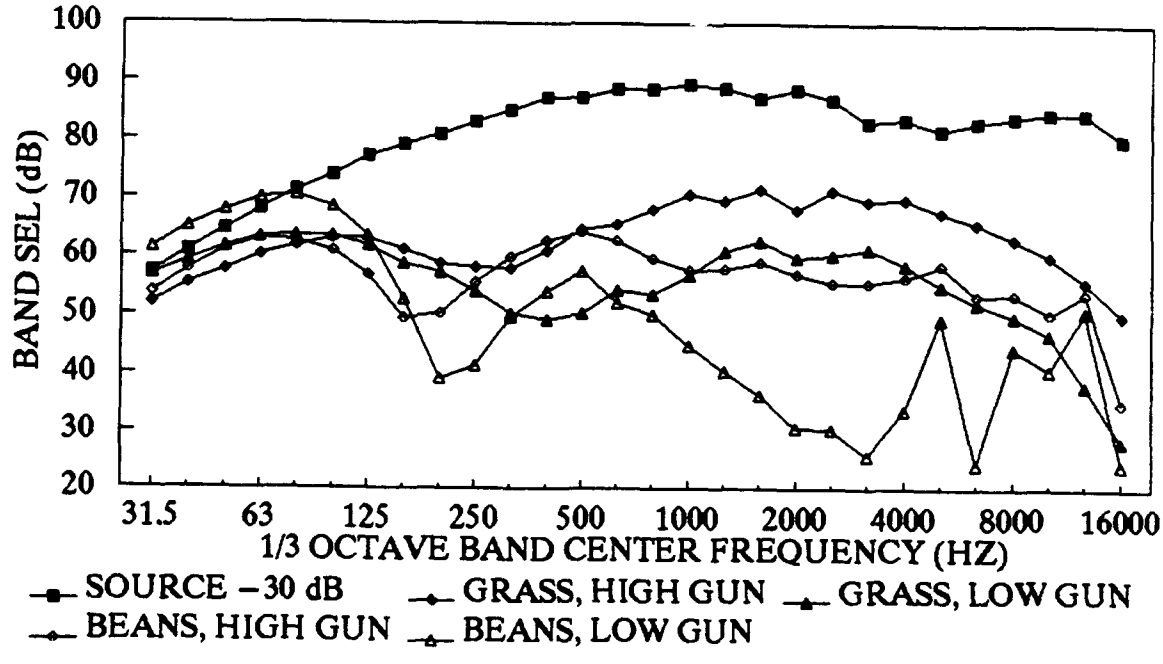

Figure 43. Spectra at 1.22 m Microphone Height for Various Propagation Paths.

Table 15

Overall Summary of Ground Interaction Experimental Results

	Test/Parameters					
Mic Height (m)	Test 3 0703 Grass High Gun	Test 4 0709 Grass Low Gun	Test 10 0834 Beans High Gun	Test 11 0839 Beans Low Gun	Test 14 0912 Grass High Gun	Test 15 0916 Grass Low Gun
FSEL (dB)						
0.5	74.3	74.5	73.4	75.6	72.9	72.1
1.22	79.8	75.2	74.9	75.0	76.5	73.7
1.32	81.6	76.1	76.6	77.1	77.4	73.2
3.05	87.7	81.7	85.1	75.0	87.4	76
ASEL (dB)						
0.5	70.7	64.3	68.0	58.8	65.9	59.2
1.22	78.7	70.3	71.4	62.1	74.6	64.3
1.32	80.6	71.9	73.5	63.9	75.8	63.9
3.05	87.5	80.9	84.7	69.1	87.5	72.0

Expt: Ground Interaction Experiments, Bondville Site.
Date: 8-1-91
Mic @: 90 degrees, 110 meters, various heights
Wind: Near Calm
Gun: 5.56 mm Ruger Mini-14 (M-16)
Height: Low Gun 0.5 m, High Gun 2.88 m

Table 16

Effect of Path Height on Measured Noise Level

Configuration	ASEL (dB)		SEL (dB) (Unweighted)	
Mean height 2.95 m. grass, high gun, 3.05-m Mic.	Test 3: Test 14: Mean:	87.5 87.5 87.5	Test 3: Test 14: Mean:	87.7 87.4 87.6
Mean height 0.86 m. grass, low gun, 1.22-m mic.	Test 4: Test 15: Mean:	70.3 64.3 68.3	Test 4: Test 15: Mean:	75.2 73.7 74.5
Noise level difference (grass).	Test 3-4: Test 14-15: 2 Mean:	17.2 23. 21.2	Test 3-4: Test 14-15: Mean:	12.5 13.7 13.1
Mean height 2.95 m. beans, high gun, 3.05 m mic. (test 10).		84.7		85.1
Mean height 0.86 m. beans, low gun, 1.22 m mic. (test 11).		62.1		75.0
Noise level difference (beans).		22.6		10.1

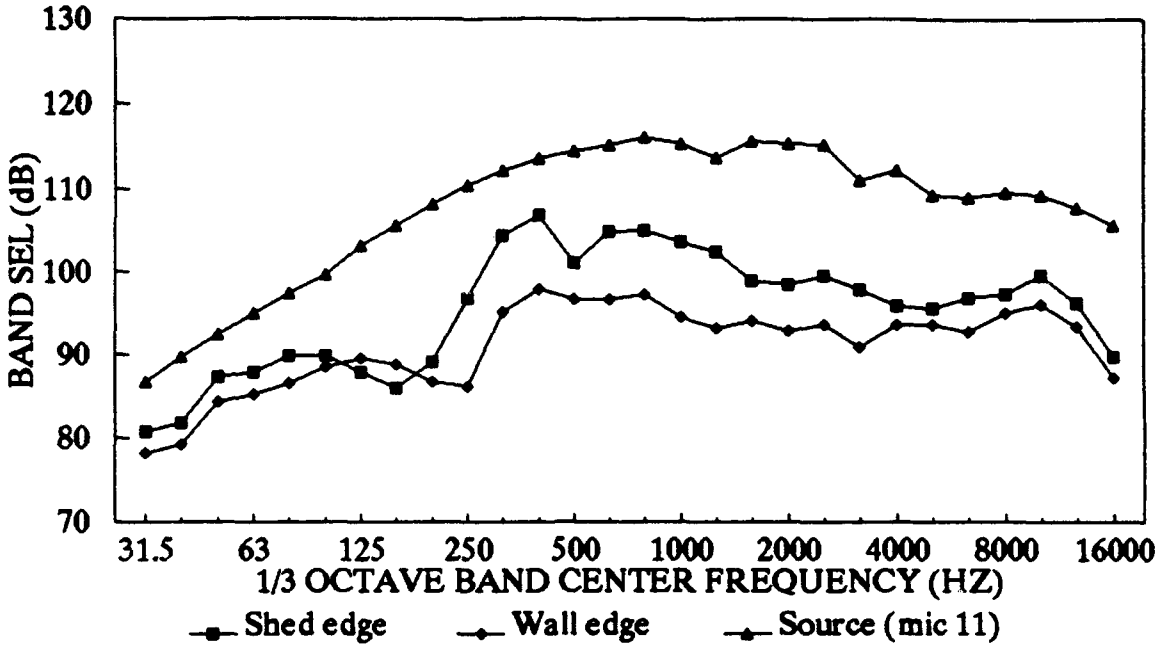

Figure 44. **Source and Barrier Edge Spectra, Ground Reflection Excluded, for Insertion Loss Experiments.**

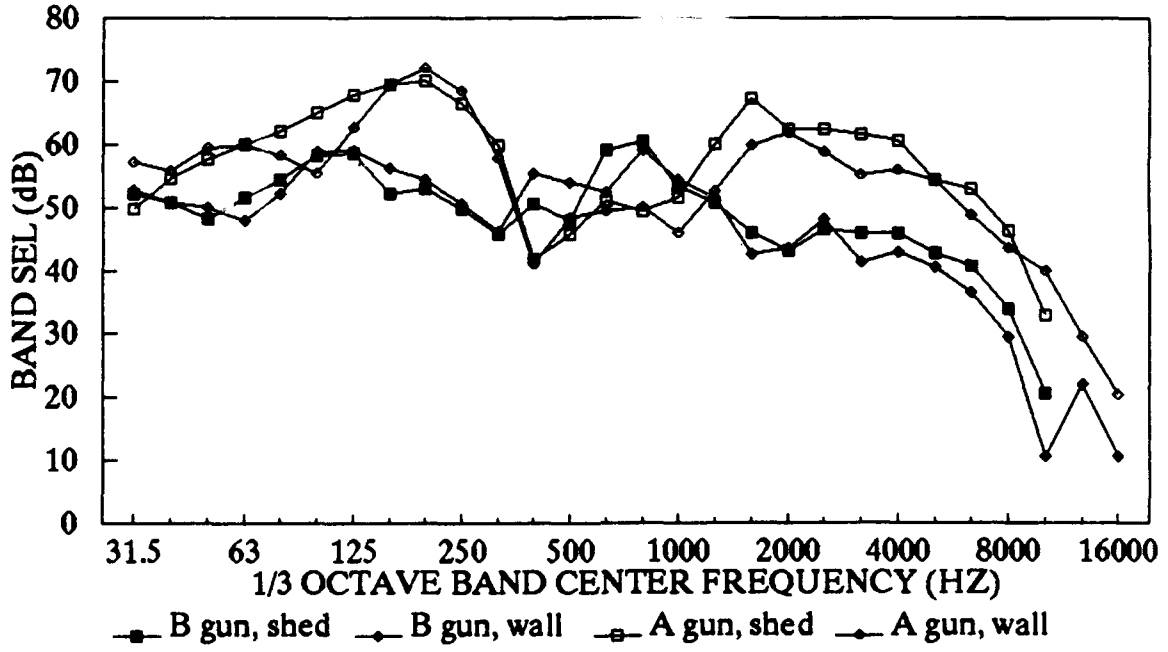

Figure 45. Spectra at 180 Degrees, 80 m.

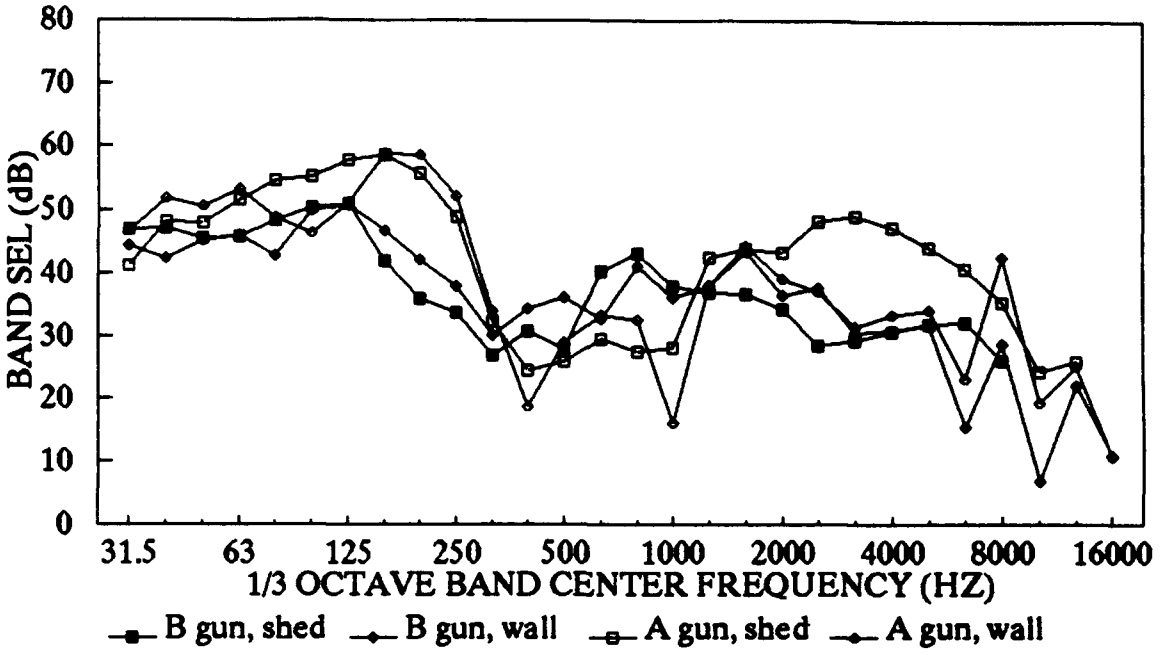

Figure 46. Spectra at 180 degrees, 242 m.

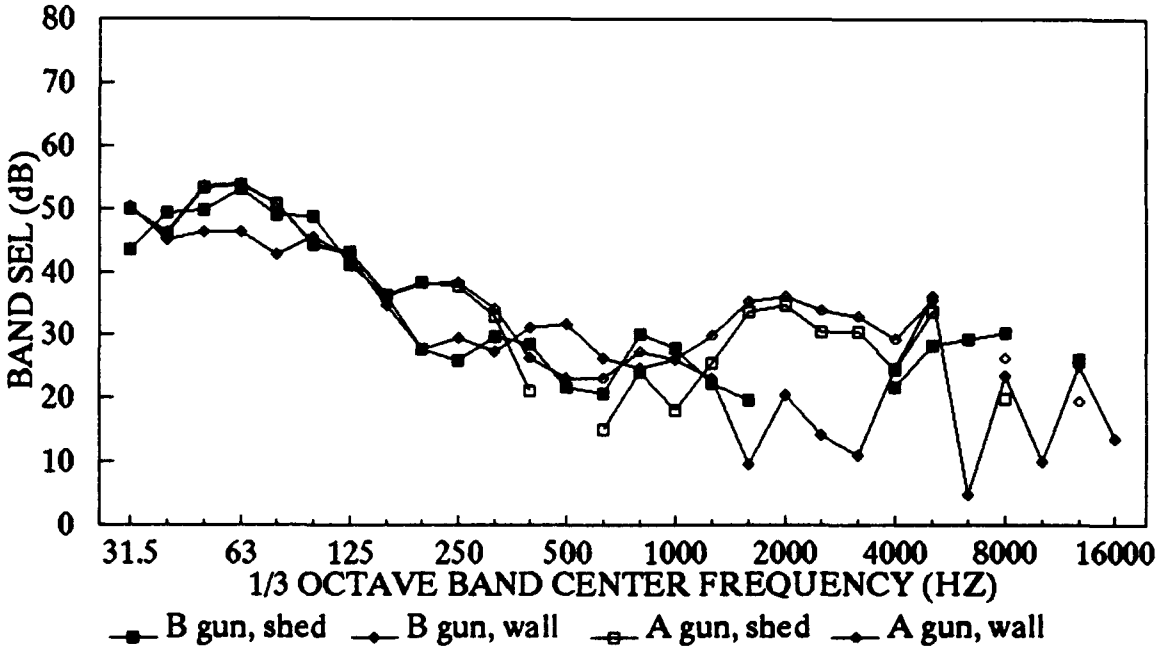

Figure 47. Spectra at 150 degrees, 279 m.

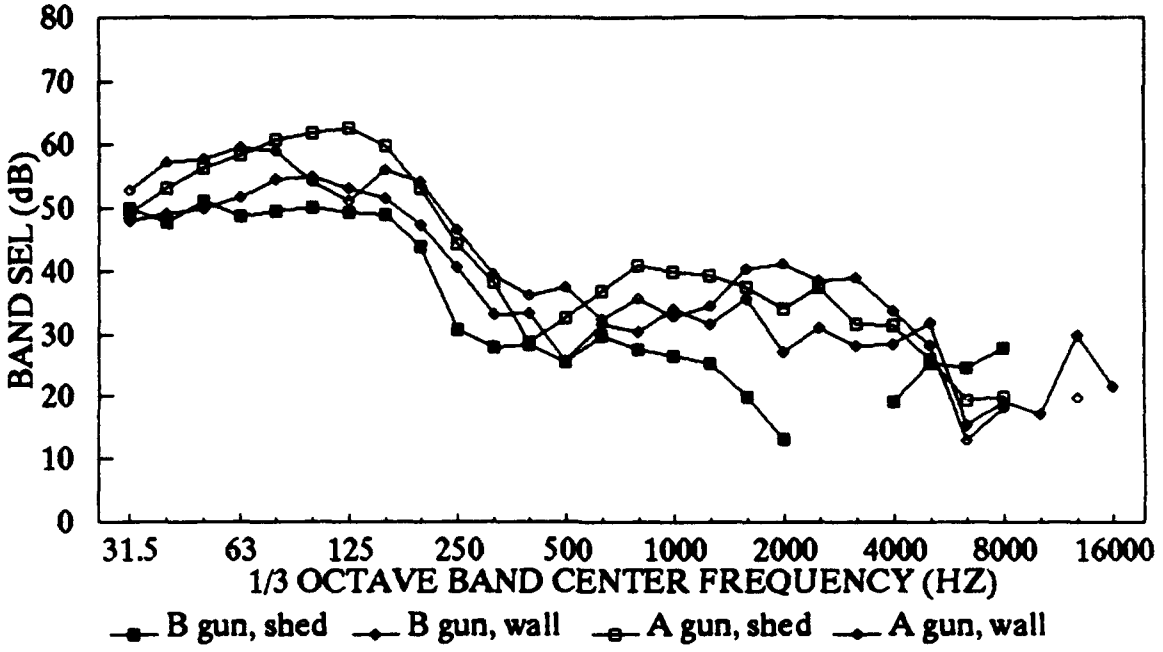

Figure 48. Spectra at 120 degrees, 161 m.

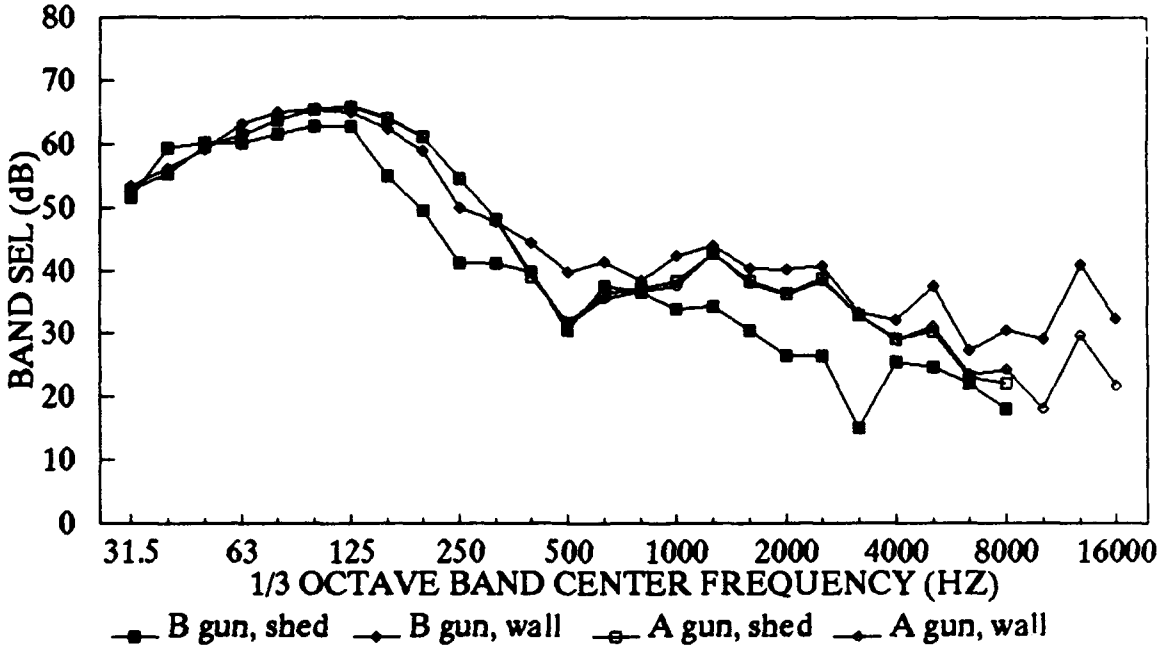

Figure 49. Spectra at 90 degrees, 150 m.

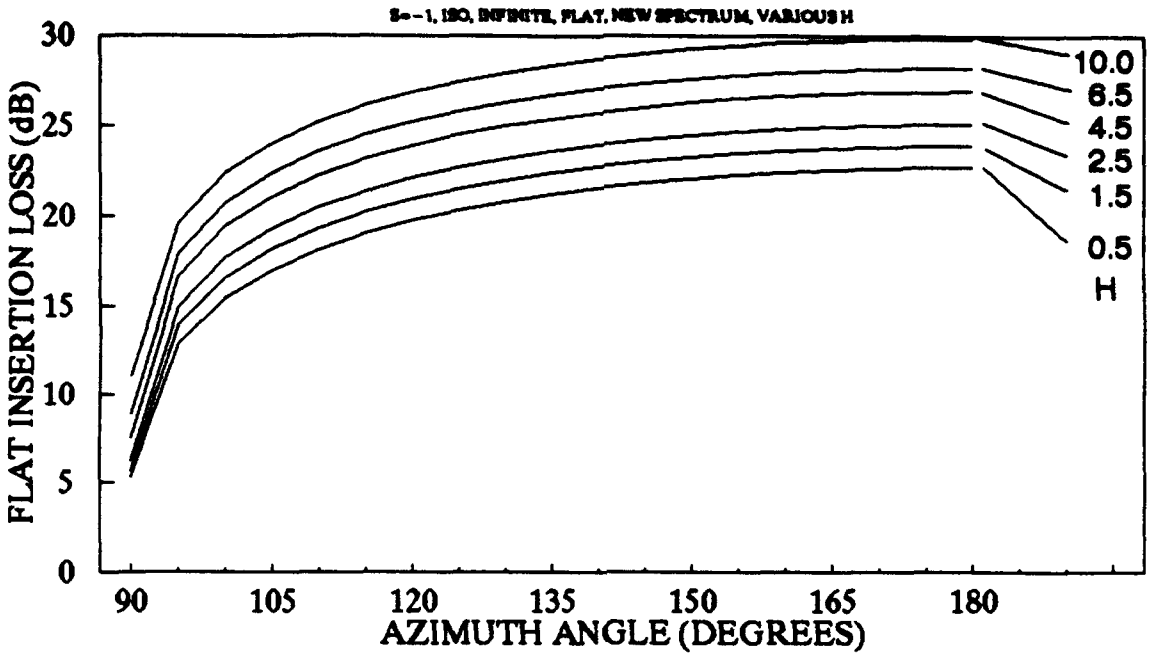

Figure 50. **Calculated Insertion Loss for Various Values of H (Barrier Height Above Source), for a Shed of Infinite Length With an Isotropic Source Located at S = -1 m.**

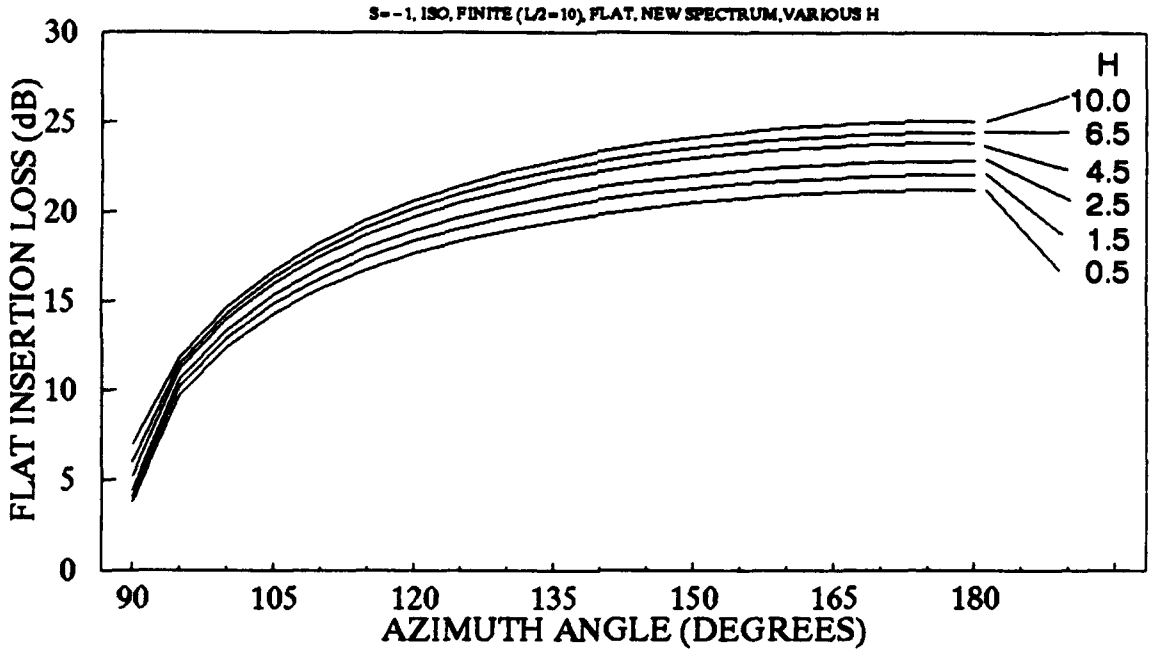

Figure 51. **Calculated Insertion Loss for Various Values of H, for a Shed Length of 20 m With an Isotropic Source Located at S = -1 m.**

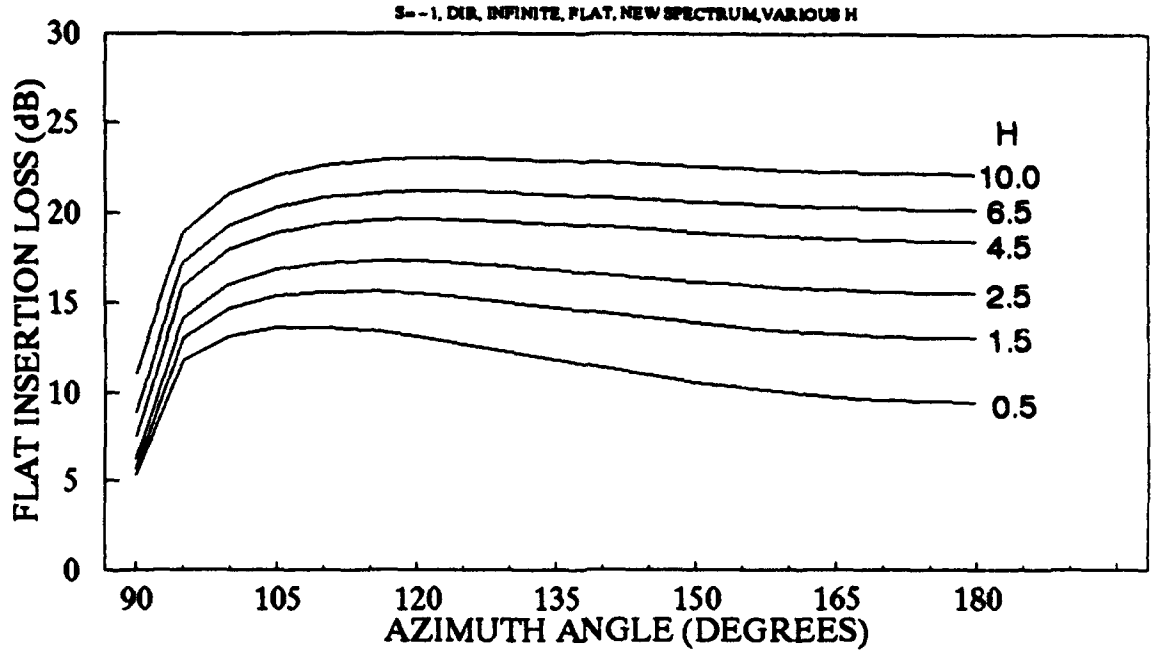

Figure 52. **Calculated Insertion Loss for Various Values of H, for a Shed of Infinite Length With a Gun Located at S = -1 m Firing Normal to the Shed Front.**

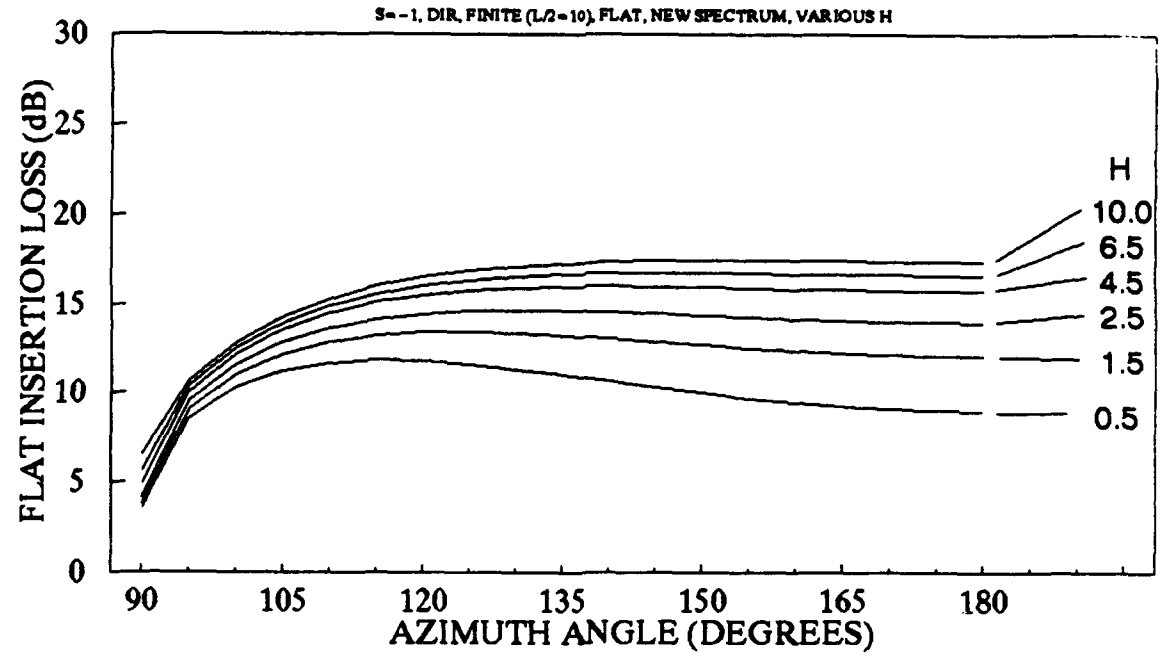

Figure 53. **Calculated Insertion Loss for Various Values of H, for a Shed Length of 20 m With a Gun Located at S = -1 m Firing Normal to the Shed Front.**

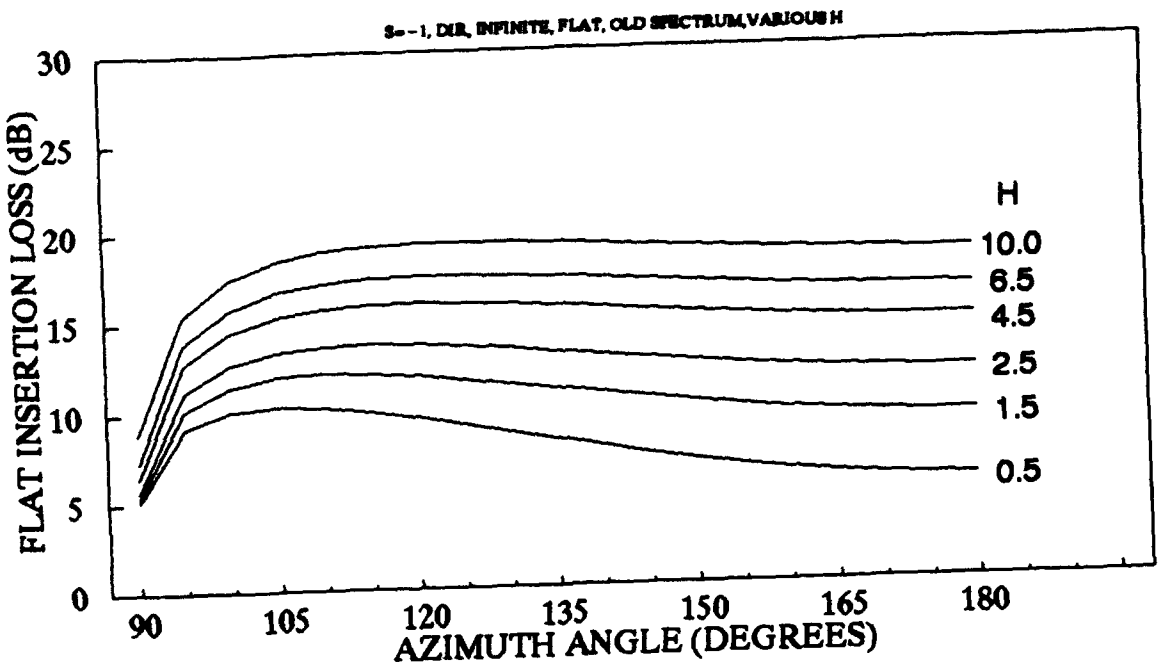

Figure 54. **Calculated Insertion Loss for Various Values of H, for a Shed of Infinite Length With a Gun Located at S = -1 m Firing Normal to the Shed Front.**

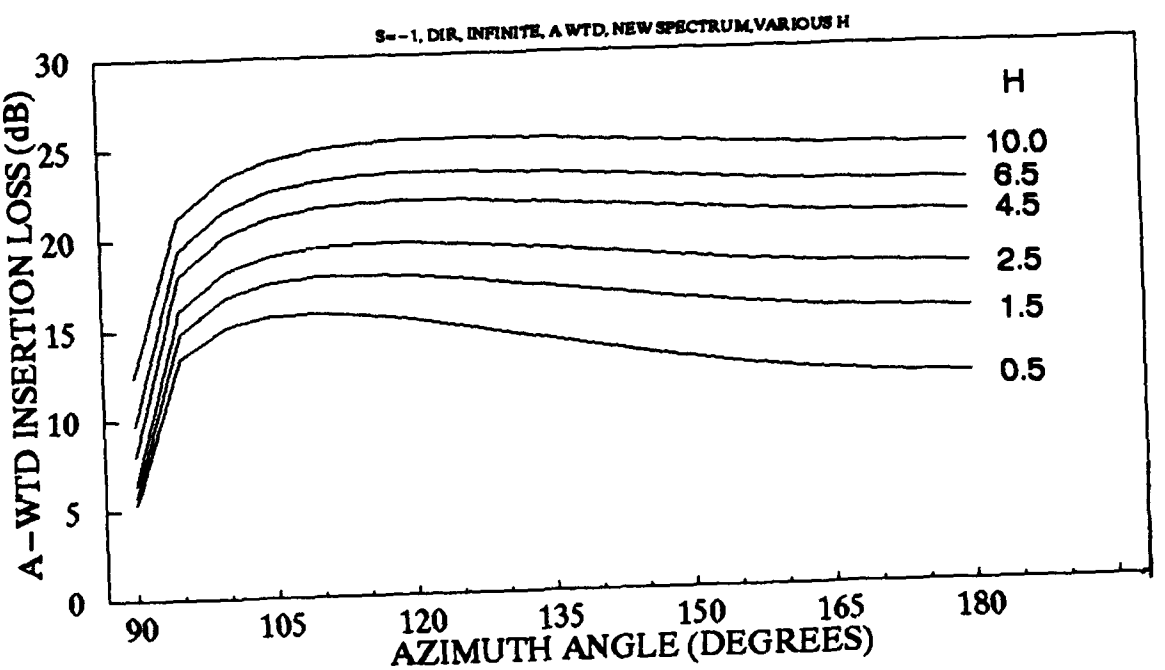

Figure 55. **Calculated A-Weighted Insertion Loss for Various Values of H, for a Shed of Infinite Length With a Gun Located at S = -1 m Firing Normal to the Shed Front.**

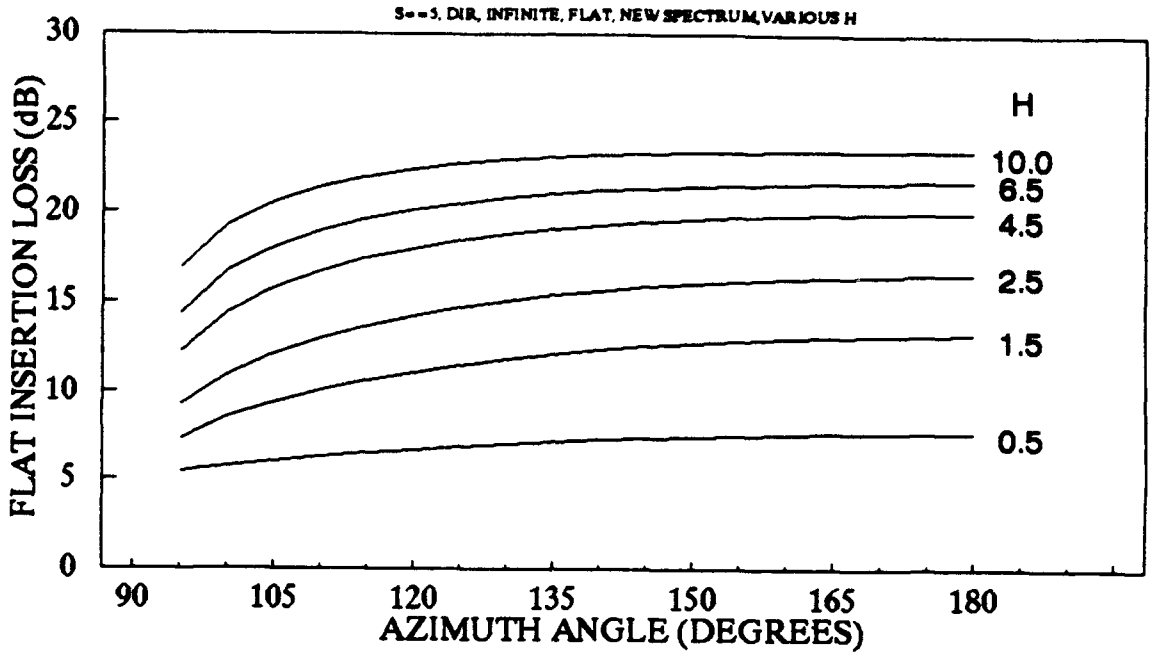

Figure 56. **Calculated Insertion Loss for Various Values of H, for a Wall of Infinite Length With a Gun Located at S = +5 m Firing Normal to the Barrier.**

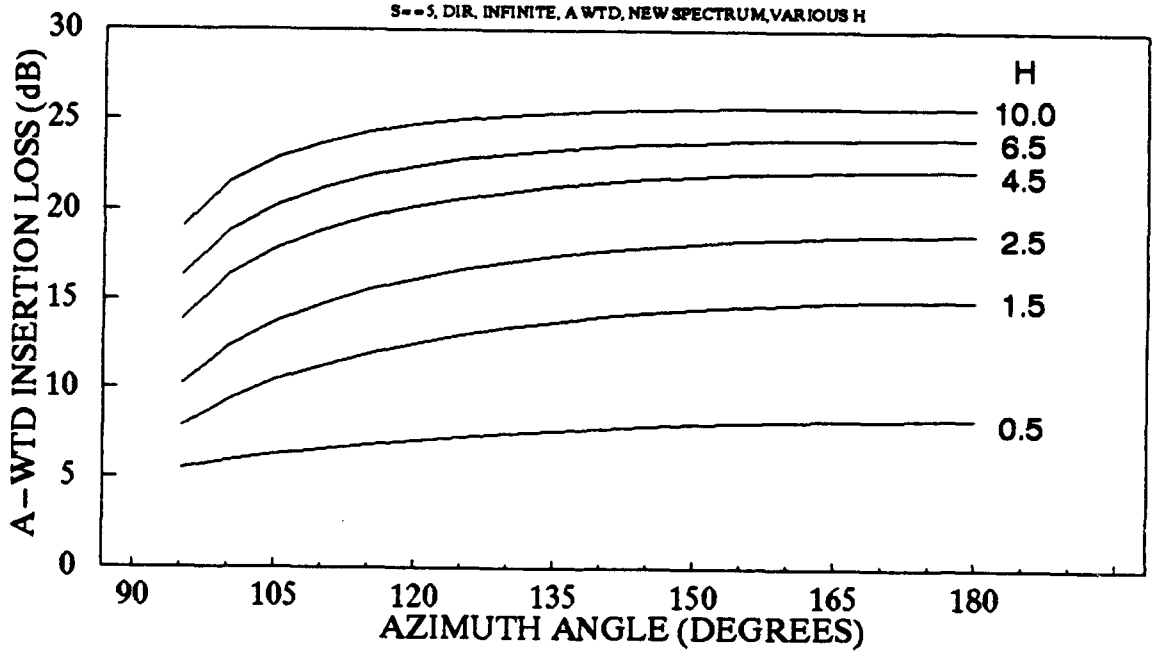

Figure 57. **Calculated A-Weighted Insertion Loss for Various Values of H, for a Wall of Infinite Length With a Gun Located at S = +5 m Firing Normal to the Barrier.**

7 CONCLUSIONS

This study has documented an investigation of the relative noise reduction performance of an open-front firing shed and a simple wall of equal height, both juxtaposed to the firing line in a manner consistent with the design requirements of a military small arms range. The experimental data conclusively show that, in a rifle range scenario, the firing shed and a rear wall, both of 7-m (23-ft) height, are about equally effective in reducing small arms noise in the region to the rear of a rifle range. This is a consequence of the sound field directivity of gun muzzle blast. This result was confirmed by calculations using two radically different analytical diffraction algorithms, both of which were adapted to account for source directivity.

This result contrasts to calculated results for a nondirective source, which show the shed to provide about 4 dB more insertion loss than a simple wall for the geometry considered in this report. Thus the added cost of a firing shed over that of a simple rear wall cannot be justified exclusively on the basis of improved noise reduction to the rear. Calculations indicated that, for the investigated configuration, the optimum wall location (for maximum insertion loss to the rear) is about 5 m behind the gun.

However, calculated results using the algorithm outlined in Appendix A indicate that, for a barrier of more modest height, when the azimuth of primary concern is near 120 degrees (rather than directly to the rear), the shed yields significantly more insertion loss than a wall of equal height, even when both are very long. The calculated results for this exceptional case still need to be proven valid.

The experimental results also conclusively demonstrated that source directivity can have a large effect on insertion loss. This was demonstrated by firing the gun both normal to and parallel to the front of the barrier.

The ground effect experiments conducted during this study clearly demonstrate that interaction between sound waves and the ground can greatly affect achieved insertion loss. It was demonstrated that attenuation is considerably greater for propagation paths nearer to the ground. This can substantially reduce the measured insertion loss of a high structure such as the shed, because the propagation path for the sound diffracted over the top of the structure is substantially higher above the ground than is the propogation path for a comparably unshielded gun. It was also observed that the ground covered by soybeans absorbed more high frequency sound energy that did the ground covered by grass.

For a given noise source and shielding structure combination in a realistic propagation scenario, the sound level and the achieved insertion loss can vary substantially during a day, from day to day, and throughout the year. Such variations occur due to a variety of factors, such as variations in lower atmospheric microstructure (for example, spacial and temporal variations in temperature, wind speed and direction, and turbulence, sometimes due to solar heating) and changes in the interaction between sound waves and the ground (due, for example, to changes in soil conditions and vegetative cover). Successful noise assessment or mitigation needs to account for these factors.

It is concluded that both diffraction algorithms used in this study can provide valuable design information. The conceptually simple algorithm of Appendix A, based on the FHWA barrier design algorithm, was modified to approximately account for source directivity and finite barrier size and shape. The modified algorithm may sometimes yield inaccurate results for cases where it does not apply, for example, in the current study, the case of a gun firing in a direction parallel to the barrier. This algorithm must therefore be used cautiously. The spherical coordinate system analysis of Appendix B rigorously accounts for wave diffraction around a barrier of finite size but is limited in the barrier shapes and source directivity patterns it can model.

When designing barriers, it is necessary but not sufficient to account for the effects of diffraction of sound energy around the edges of the barrier. The methods outlined in this study can help account for the effects of the propagation medium and terrain, and the interactions between sounds waves and the ground to enable a more reliable estimate of actual insertion loss. For an existing firing range, measurements to characterize such effects, made before the barrier is designed, can be useful since it is difficult to estimate ground absorption reliably based on appearance of the ground and ground cover alone.

REFERENCES

American National Standard: Methods for Determination of Insertion Loss of Outdoor Noise Barriers, ANSI S12.8-1987 (American National Standards Institute [ANSI], 1987).

American National Standard: Preferred Frequencies and Band Numbers for Acoustical Measurements, ANS1.6-1967 (ANSI 1967 [rev. 1976]).

American National Standard: Specification for Sound Level Meters, ANSI S1.4-1983 (ANSI, 1983).

Beranek, Leo Leroy, *Noise and Vibration Control* (McGraw Hill, 1971), pp 174-180.

Eldred, K. McK., *Noise Mitigation for Small Arms Ranges*, Report KEE 89-541 (Ken Eldred Engineering, March 1990).

Embleton, T., *Sound Propagation Outdoor–Improved Prediction Schemes for the 80's* (Noise Control Engineering, January-February 1982).

Federal Highway Administration (FHWA), *Noise Barrier Cost Reduction Procedure, STAMINA 2.0/OPTIMA: Users Manual*, Report FHWA/DF-82/001a (FHWA, April 1982).

McBryan, J., *Predicting Noise Impact in the Vicinity of Small-Arms Ranges*, Interim Report N-61/ADA062718 (U.S. Army Construction Engineering Research Laboratories [USACERL], October 1978).

Pater, L., *An Investigation of Small Arms Range Noise Mitigation: Tne Firing Shed and the Interlane Barrier*, TR EAC-92/001/ADA258818 (USACERL, September 1992).

Pater, L., *Gun Blast Far Field Peak Overpressure Contours*, TR 79-442 (U.S. Naval Surface Weapons Center, March 1981).

Schomer, P.D., L.M. Little, A.B. Hunt, *Acoustic Directivity Patterns for Army Weapons*, TR N-60/ADA121665 (USACERL, January 1979).

APPENDIX A: Calculations of Insertion Loss Using a Simple Approximate Barrier Design Algorithm

Description of Algorithm

One method often used to calculate barrier insertion loss is an approximate method that has been adopted by the Federal Highway Administration (FHWA) for design of highway noise barriers (FHWA, April 1982); this algorithm is based on experimental data due to Maekawa. It was chosen for use here because of the relative simplicity with which it can be used for design calculations. As described by Beranek (Beranek 1971, pp 174-180), this barrier insertion loss algorithm "is based on an analytical approximation of experimental data which is consistent with asymptotic results of optical-diffraction theory. In the theory of Fresnel diffraction, only that region of an incident wavefield that is close to the top edge of a barrier contributes appreciably to the wavefield that is diffracted over the barrier. For an observer in the shadow zone of the barrier at some distance away, the diffracted sound field appears to be radiated from a line source along the top edge of the barrier. The strength of this virtual line source is proportional to the strength of the incident wave at the edge of the barrier. The sound pressure in the incident wave, of course, decreases in direct proportion to the distance of the barrier from a point source " and ". . . if the point source is much closer to the edge than is the observer, the strongest section of the virtual line source is very short (as viewed by the observer) . . . ." This indicates that even though the theory strictly applies for barriers of infinite length, if properly used it can give reasonably good results for barriers of finite length. The algorithm includes an empirical adjustment to describe the insertion loss for receivers not shadowed but with a line of sight that passes near a barrier edge.

In this algorithm the amount of insertion loss provided by a barrier depends on the Fresnel number. The Fresnel number is defined as $N = 2\delta/\lambda$ where δ is the difference in propagation distance between the direct path and the diffracted path from source to observer, which can be calculated using plane geometry, and λ is the wavelength of the acoustic radiation. The detailed algorithm for calculating attenuation as a function of Fresnel number is available in references 4 and 12 of this report. Experimental data for continuous noise has shown that the practical upper limit for achievable insertion loss should be taken as 24 dB (Beranek 1971, p 179).

It is important to bear in mind the limitations and assumptions involved in the FHWA algorithm. The algorithm ignores or approximates certain aspects of diffraction that can result in bright spots and variations in intensity within and near the edge of the shadow zone. One should bear in mind that the algorithm was developed for continuous noise but is here being applied to impulse gun blast noise. The Fresnel theory of diffraction on which the algorithm is based does not include consideration of source directivity. Source directivity could modify the field strength distribution along the barrier edge in ways that would degrade the accuracy of the algorithm. It is also not clear whether the algorithm is strictly applicable to the shed when the gun is inside the shed.

The insertion loss was evaluated at octave band center frequencies from 63 to 8000 Hz. These spectral insertion loss values were applied to the source relative spectrum and the resulting spectral levels were summed on an energy basis to obtain the overall insertion loss for the entire spectrum. The "design" source spectrum used for the calculations in the current study is a relative band sound exposure level spectrum that was experimentally obtained for a M-16 rifle at a particular distance and azimuth. Because of a lack of detailed information, it was used for all of the calculations, which ignores the fact that the actual spectrum might vary with distance from the muzzle or with azimuth relative to the line of fire.

The FHWA algorithm does not account for source directivity, that is, variation of field strength or spectral power density distribution with azimuth at a given distance. This is a potentially important issue for a gun because the field strength is known to vary strongly with azimuth angle, and could conceivably have an important effect on insertion loss for some barrier-source orientations. Recalling Beranek's phenomenological description quoted above, it seems clear that directivity could have a significant effect on the strength as viewed by the observer of the virtual line source along the edge of the barrier, depending on where in the source's pressure field the barrier edge is located. A first approximation or estimate, by no means exact, of the effect of directivity on the strength of the virtual line source was made by adjusting the calculated insertion loss according to the difference in source strength for the line of sight to the observer and the line of sight along the path of minimum distance around the barrier to the observer. Gun directivity, expressed as level in decibel units, is modeled according to

$$D = 7\ (1 + \cos\alpha) \qquad \text{[Eq A1]}$$

where α is the angle from line of fire to the direction of interest and D is the amount of directivity expressed in decibels. By this model directivity is referenced to the SEL at 180 degrees, as shown in Figure 2 of the main text, and amounts to 14 dB directly ahead of the gun and lesser amounts in other directions. It should be noted that this correction for directivity is an overall (rather that spectral) level correction. It was adopted because detailed spectral directivity information for the gun is not currently available. It would be desirable to have directivity information at several frequencies throughout the spectrum when assessing the amount of energy that is diffracted around a barrier edge.

Nomenclature

e_i = band sound exposure.

e_r = (arbitrary) reference sound exposure.

$L_i = 10 \log \frac{e_i}{e_r}$ = band level.

subscript i → frequency band.

subscript j → direction to a barrier edge.

subscript o → direction of direct unshielded line-of-sight path from source to observer.

$D_j = 10 \log d_j$ = source directivity for j direction.

$W_i = 10 \log w_i$ = band attenuation of frequency weighting.

$A_{ij} = 10 \log a_{ij}$ = attenuation due to diffraction around barrier edge for band i and direction j.

Algorithm

The insertion loss of a barrier is defined to be

$$IL = L_o - L_d = \text{insertion loss}$$

where L_d is the sound exposure level for the diffracted path and L_o is the sound exposure level for the direct path from source to receiver. The direct path sound exposure level is given by:

$$L_o = D_o + 10 \log \sum_i 10^{(L_i + W_i)/10}$$
$$= D_o + L_O^{ND} \qquad \text{[Eq A2]}$$

where L_0^{ND} denotes the isotropic source contribution, and D_o denotes the contribution due to source directivity, for the direct path. The sound exposure level for the diffracted path, assuming noncoherence, is given by:

$$L_d = 10 \log \sum_j d_j \sum_i e_i w_i a_{ij} / e_r$$
$$= 10 \log \sum_j 10^{D_j/10} \sum_i 10^{(L_i + W_i + A_{ij})/10} \qquad \text{[Eq A3]}$$

Define the diffracted path sound exposure level for an isotropic source to be, for direction j,

$$L_j^{ND} = 10 \log \sum_i 10^{(L_i + W_i + A_{ij})/10} \qquad \text{[Eq A4]}$$

The sound exposure level for the diffracted path can then be written as

$$L_d = 10 \log \sum_j 10^{(D_j + L_j^{ND})/10} \qquad \text{[Eq A5]}$$

and the insertion loss can be written as

$$IL = -10 \log \sum_j 10^{(D_j + L_j^{ND} - D_o - L_o^{ND})/10} \qquad \text{[Eq A6]}$$

For the path direction used to characterize diffraction around one particular edge, the insertion loss is given by:

$$IL_j = L_o^{ND} - L_j^{ND} + D_o - D_j \qquad \text{[Eq A7]}$$

and the total insertion loss from all edges of a finite structure is calculated from:

$$IL = -10 \log \sum_j 10^{IL_j/10} \qquad \text{[Eq A8]}$$

Also note that for an isotropic source $D_o = D_j = O$.

Insertion loss calculations were made for a variety of gun locations relative to the shed, both inside and in front of the shed. For each gun location, three separate insertion loss calculations were made, one for each of the three edges around the shed opening, i.e. for the front edge of the roof and each sidewall. The calculations were carried out for each edge extended to infinity, as an estimate of the broad band insertion loss due to that edge. These calculations were carried out for the line of sight azimuth angle to each microphone location; these involved calculation of spectral insertion loss values which were

then used along with the design source spectrum to obtain a broad band insertion loss value for each azimuth.

An example of the detailed spectral calculations, for the -1 m gun location, is shown in Table A1, which spans several pages. The calculated isotropic source insertion loss, the directivity adjustment and the resultant net (adjusted for directivity) insertion loss are also presented in this table; the insertion loss values are presented as both unweighted and A-weighted values. Each of these quantities is presented, for several different azimuths, for each edge of the structure as well as the overall value for the finite structure. The path length difference used to evaluate Fresnel number in each of these calculations was the shortest path length around the particular barrier edge. Examples of the broad band insertion loss values that resulted from the spectral calculations are presented in Table A2 for a variety of combinations of gun location, direction of fire and frequency weightings. Tables A3 and A4 present insertion loss values at 180-degree azimuth for a wide range of source locations.

Table A1

Calculated Barrier Insertion Loss for the -1 m Gun Location

CALCULATED SHED INSERTION LOSS USING FHWA DIFFRACTION ALGORITHM ADAPTED TO ACCOUNT FOR SOURCE DIRECTIVITY.
SOURCE DIRECTIVITY: ISOTROPIC AND GUN DIRECTIVITY.
RIFLE DIRECTION OF FIRE: PERPENDICULAR TO SHED FRONT.
GUN DIRECTIVITY MODEL: D = 7*(1+COS (THETA))
FREQUENCY WEIGHTING: FLAT AND A

GUN @ (m) = S = -1
BARRIER H (m) = 6.5
WALL L/2 (m) = 10

FIELD POINTS

MIC ANGLE (DEG)	RANGE (M)
90.0	150
120.0	161
150.0	279
180.0	80
180.0	242

DESIGN SOURCE SPECTRUM RELATIVE LEVELS

OCTAVE BAND (HZ)	FLAT LEVEL (dB)
63	-25.8
125	-17.3
250	-11.2
500	-6.8
1000	-5.8
2000	-6.8
4000	-8.7
8000	-10.6

A FREQUENCY WEIGHTING

OCTAVE BAND (HZ)	A WTG ATTEN (dB)
63	-26.2
125	-16.1
250	-8.6
500	-3.2
1000	0.0
2000	1.2
4000	1.0
8000	-1.1

SUMMARY OF RESULTS FOR:
FREQUENCY WEIGHTING: FLAT
GUN LOCATION (m): -1

MIC ANGLE (DEG)	RANGE (M)	********** INSERTION LOSS (dB) ********** OVERALL DIR	OVERALL ISO	TOP ISO	TOP Do-Dj	TOP DIR	LEFT ISO	LEFT Do-Dj	LEFT DIR	RIGHT ISO	RIGHT Do-Dj	RIGHT DIR	MIC ANGLE (DEG)
90	150	8.0	8.6	17.2	-0.1	17.1	9.3	-0.7	8.6	32.4	-0.7	31.7	90
120	161	16.2	20.4	25.5	-4.1	21.4	22.4	-4.2	18.2	32.3	-4.2	28.1	120
150	279	16.8	23.6	27.6	-7.0	20.7	27.2	-6.8	20.5	31.5	-6.8	24.7	150
180	80	16.8	24.7	28.4	-8.1	20.3	30.1	-7.7	22.4	30.1	-7.7	22.4	180
180	242	16.7	24.5	28.3	-8.1	20.2	29.9	-7.7	22.2	29.9	-7.7	22.2	180

Table A1 (Cont'd)

GUN DIRECTIVITY ANGLE BETWEEN LINE OF FIRE AND PATH AROUND BARRIER EDGE.

MIC ANGLE (DEG)	RANGE (m)	TOP EDGE (DEG)	LEFT EDGE (DEG)	RIGHT EDGE (DEG)
90.0	150.0	89.2	84.3	84.3
120.0	161.0	85.3	84.3	84.3
150.0	279.0	82.4	84.3	84.3
180.0	80.0	81.3	84.3	84.3
180.0	242.0	81.3	84.3	84.3

CALCULATION OF PATH LENGTH DIFFERENCE

AZIMUTH (DEG)	R (m)	TOP (m)	LEFT (m)	RIGHT (m)	RCOS−S SQR	RSIN−Y SQR	rsin+y SQR	D	TOP A	RSIN−D SQR	TOP B
90	150	0.58	0.05	20.05	1	19600.00	25600.00	75	75.28778	5625	75.28778
120	161	4.06	2.00	19.26	6642.25	16752.15	22329.35	10.38043	12.28834	16653.81	152.7688
150	279	6.66	6.07	16.03	58864.99	16770.25	22350.25	3.680203	7.536172	18447.02	278.1263
180	80	7.84	11.66	11.66	6561	100.00	100.00	0	6.576473	0	81.26038
180	242	7.66	11.26	11.26	59049	100.00	100.00	0	6.576473	0	243.0669

S =	−1.0
Y =	10
H =	6.5
SQRT(S ^ 2+H ^ 2) =	6.576473

Table A1 (Cont'd)

MIC LOCATION: ANGLE (DEG) = 90.0 RANGE = 150.0
EDGE: RIGHT SIDE WALL GUN @ -1
PATH LENGTH DELTA (m) = 20.05

OCTAVE BAND (HZ)	BAND FRESNEL NO.	BARRIER ATTEN (dB)	SOURCE FLAT LEVEL (dB)	NET FLAT LEVEL (dB)	10^L/10	A WTG (dB)	NET A WT LEVEL (dB)	10^L/10	ARG N2PI^1/2	TANH
63	7.366	-21.7	-25.8	-47.5	0.0000	-26.2	-73.7	0.0000	6.603	0.999996
125	14.616	-24.6	-17.3	-41.9	0.0001	-16.1	-58.0	0.0000	9.583	1
250	29.232	-27.6	-11.2	-38.8	0.0001	-8.6	-47.4	0.0000	13.552	1
500	58.464	-30.7	-6.8	-37.4	0.0002	-3.2	-40.6	0.0001	19.166	1
1000	116.927	-33.7	-5.8	-39.5	0.0001	0.0	-39.5	0.0001	27.105	1
2000	233.854	-36.7	-6.8	-43.5	0.0000	1.2	-42.3	0.0001	38.332	1
4000	467.708	-39.7	-8.7	-48.4	0.0000	1.0	-47.4	0.0000	54.210	1
8000	935.417	-42.7	-10.6	-53.3	0.0000	-1.1	-54.4	0.0000	76.664	1
				SUM =	0.0006		SUM =	0.0003		
				LEVEL =	-32.4		A LEVEL =	-35.2		

MIC LOCATION: ANGLE (DEG) = 120.0 RANGE = 161.0
EDGE: TOP GUN @ -1
PATH LENGTH DELTA (m) = 4.06

OCTAVE BAND (HZ)	BAND FRESNEL NO.	BARRIER ATTEN (dB)	SOURCE FLAT LEVEL (dB)	NET FLAT LEVEL (dB)	10^L/10	A WTG (dB)	NET A WT LEVEL (dB)	10^L/10	ARG N2PI^1/2	TANH
63	1.490	-14.8	-25.8	-40.6	0.0001	-26.2	-66.8	0.0000	3.060	0.995614
125	2.957	-17.7	-17.3	-35.0	0.0003	-16.1	-51.1	0.0000	4.310	0.999639
250	5.914	-20.7	-11.2	-31.9	0.0006	-8.6	-40.5	0.0001	6.096	0.99999
500	11.828	-23.7	-6.8	-30.5	0.0009	-3.2	-33.7	0.0004	8.621	1
1000	23.657	-26.7	-5.8	-32.5	0.0006	0.0	-32.5	0.0006	12.192	1
2000	47.314	-29.7	-6.8	-36.5	0.0002	1.2	-35.3	0.0003	17.242	1
4000	94.628	-32.7	-8.7	-41.4	0.0001	1.0	-40.4	0.0001	24.384	1
	189.256	-35.8	-10.6	-46.4	0.0000	-1.1	-47.5	0.0000	34.484	1
				SUM =	0.0028		SUM =	0.0015		
				LEVEL =	-25.5		A LEVEL =	-28.3		

Table A1 (Cont'd)

MIC LOCATION: ANGLE (DEG) =				150.0		RANGE =	279.0			
EDGE: RIGHT SIDE WALL						GUN @	-1			
PATH LENGTH DELTA (m) =				16.03						
OCTAVE BAND (HZ)	BAND FRESNEL NO.	BARRIER ATTEN (dB)	SOURCE FLAT LEVEL (dB)	NET FLAT LEVEL (dB)	10^L/10	A WTG (dB)	NET A WT LEVEL (dB)	10^L/10	ARG N2PI^1/2	TANH
63	5.890	-20.7	-25.8	-46.5	0.0000	-26.2	-72.7	0.0000	6.063	0.99999
125	11.686	-23.7	-17.3	-41.0	0.0001	-16.1	-57.1	0.0000	8.569	1
250	23.371	-26.7	-11.2	-37.8	0.0002	-8.6	-46.4	0.0000	12.116	1
500	46.743	-29.7	-6.8	-36.5	0.0002	-3.2	-39.7	0.0001	17.137	1
1000	93.485	-32.7	-5.8	-38.5	0.0001	0.0	-38.5	0.0001	24.236	1
2000	186.971	-35.7	-6.8	-42.5	0.0001	1.2	-41.3	0.0001	34.275	1
4000	373.942	-38.7	-8.7	-47.4	0.0000	1.0	-46.4	0.0000	48.472	1
8000	747.884	-41.7	-10.6	-52.4	0.0000	-1.1	-53.5	0.0000	68.550	1
				SUM =	0.0007		SUM =	0.0004		
				LEVEL =	-31.5		A LEVEL =	-34.2		

MIC LOCATION: ANGLE (DEG) =				180.0		RANGE =	80.0			
EDGE: TOP						GUN @	-1			
PATH LENGTH DELTA (m) =				7.84						
OCTAVE BAND (HZ)	BAND FRESNEL NO.	BARRIER ATTEN (dB)	SOURCE FLAT LEVEL (dB)	NET FLAT LEVEL (dB)	10^L/10	A WTG (dB)	NET A WT LEVEL (dB)	10^L/10	ARG N2PI^1/2	TANH
63	2.679	-17.6	-25.8	-43.4	0.0000	-26.2	-69.6	0.0000	4.253	0.999596
125	5.712	-20.5	-17.3	-37.9	0.0002	-16.1	-54.0	0.0000	5.991	0.999997
250	11.424	-23.6	-11.2	-34.7	0.0003	-8.6	-43.3	0.0000	8.472	1
500	22.848	-26.6	-6.8	-33.3	0.0005	-3.2	-36.5	0.0002	11.982	1
1000	45.696	-29.6	-5.8	-35.4	0.0003	0.0	-35.4	0.0003	16.945	1
2000	91.392	-32.6	-6.8	-39.4	0.0001	1.2	-38.2	0.0002	23.963	1
	[illegible]	-35.6	-8.7	-44.3	0.0000	1.0	-43.3	0.0000	33.889	1
			10.6	-49.3	0.0000	-1.1	-50.4	0.0000	47.926	1
				SUM =	[illegible]		SUM =	0.0008		
				[illegible]			[illegible]	-31.1		

Table A1 (Cont'd)

MIC LOCATION: ANGLE (DEG) = 90.0 RANGE = 150.0
EDGE: TOP GUN @ -1
PATH LENGTH DELTA (m) = 0.58

OCTAVE BAND (HZ)	BAND FRESNEL NO.	BARRIER ATTEN (dB)	SOURCE FLAT LEVEL (dB)	NET FLAT LEVEL (dB)	10^L/10	A WTG (dB)	NET A WT LEVEL (dB)	10^L/10	ARG N2PI^1/2	TANH
63	0.211	-8.0	-25.8	-33.8	0.0004	-26.2	-60.0	0.0000	1.153	0.81861
125	0.420	-9.9	-17.3	-27.2	0.0019	-16.1	-43.3	0.0000	1.624	0.925134
250	0.839	-12.4	-11.2	-23.6	0.0044	-8.6	-32.2	0.0006	2.296	0.979939
500	1.678	-15.3	-6.8	-22.0	0.0063	-3.2	-25.2	0.0030	3.247	0.99696
1000	3.356	-16.2	-5.8	-24.0	0.0039	0.0	-24.0	0.0039	4.592	0.999795
2000	6.712	-21.3	-6.8	-28.1	0.0016	1.2	-26.9	0.0021	6.494	0.999995
4000	13.424	-24.3	-8.7	-33.0	0.0005	1.0	-32.0	0.0006	9.184	1
8000	26.848	-27.3	-10.6	-37.9	0.0002	-1.1	-39.0	0.0001	12.988	1
				SUM =	0.0192		SUM =	0.0104		
				LEVEL =	-17.2		A LEVEL =	-19.8		

MIC LOCATION: ANGLE (DEG) = 90.0 RANGE = 150.0
EDGE: LEFT SIDE WALL GUN @ -1
PATH LENGTH DELTA (m) = 0.05

OCTAVE BAND (HZ)	BAND FRESNEL NO.	BARRIER ATTEN (dB)	SOURCE FLAT LEVEL (dB)	NET FLAT LEVEL (dB)	10^L/10	A WTG (dB)	NET A WT LEVEL (dB)	10^L/10	ARG N2PI^1/2	TANH
63	0.020	-5.3	-25.8	-31.2	0.0008	-26.2	-57.4	0.0000	0.351	0.337465
125	0.039	-5.7	-17.3	-23.0	0.0050	-16.1	-39.1	0.0001	0.495	0.457968
250	0.078	-6.3	-11.2	-17.5	0.0180	-8.6	-26.1	0.0025	0.700	0.604154
500	0.156	-7.3	-6.8	-14.1	0.0389	-3.2	-17.3	0.0186	0.989	0.757138
1000	0.312	-9.0	-5.8	-14.8	0.0332	0.0	-14.8	0.0332	1.399	0.885206
2000	0.623	-11.3	-6.8	-18.1	0.0156	1.2	-16.9	0.0206	1.979	0.96251
4000	1.247	-14.0	-8.7	-22.7	0.0054	1.0	-21.7	0.0067	2.799	0.992612
8000	2.493	-17.0	-10.6	-27.6	0.0017	-1.1	-28.7	0.0013	3.956	0.99927
				SUM =	0.1186		SUM =	0.0832		
				LEVEL =	-9.3		A LEVEL =	-10.8		

Table A1 (Cont'd)

MIC LOCATION: ANGLE (DEG) = 150.0 RANGE = 279.0
EDGE: TOP GUN @ -1
PATH LENGTH DELTA (m) = 6.66

OCTAVE BAND (HZ)	BAND FRESNEL NO.	BARRIER ATTEN (dB)	SOURCE FLAT LEVEL (dB)	NET FLAT LEVEL (dB)	10^L/10	A WTG (dB)	NET A WT LEVEL (dB)	10^L/10	ARG N2PI^1/2	TANH
63	2.447	-16.9	-25.8	-42.7	0.0001	-26.2	-68.9	0.0000	3.921	0.999215
125	4.856	-19.8	-17.3	-37.2	0.0002	-16.1	-53.3	0.0000	5.524	0.999968
250	9.712	-22.9	-11.2	-34.0	0.0004	-8.6	-42.6	0.0001	7.812	1
500	19.424	-25.9	-6.8	-32.6	0.0005	-3.2	-35.8	0.0003	11.047	1
1000	38.848	-28.9	-5.8	-34.7	0.0003	0.0	-34.7	0.0003	15.623	1
2000	77.697	-31.9	-6.8	-38.7	0.0001	1.2	-37.5	0.0002	22.095	1
4000	155.394	-34.9	-8.7	-43.6	0.0000	1.0	-42.6	0.0001	31.247	1
8000	310.788	-37.9	-10.6	-48.5	0.0000	-1.1	-49.6	0.0000	44.190	1
				SUM =	0.0017		SUM =	0.0009		
				LEVEL =	-27.6		A LEVEL =	-30.4		

MIC LOCATION: ANGLE (DEG) = 150.0 RANGE = 279.0
EDGE: LEFT SIDE WALL GUN @ -1
PATH LENGTH DELTA (m) = 6.07

OCTAVE BAND (HZ)	BAND FRESNEL NO.	BARRIER ATTEN (dB)	SOURCE FLAT LEVEL (dB)	NET FLAT LEVEL (dB)	10^L/10	A WTG (dB)	NET A WT LEVEL (dB)	10^L/10	ARG N2PI^1/2	TANH
63	2.229	-16.5	-25.8	-42.3	0.0001	-26.2	-68.5	0.0000	3.743	0.998878
125	4.423	-19.4	-17.3	-36.8	0.0002	-16.1	-52.9	0.0000	5.272	0.999947
250	8.846	-22.4	-11.2	-33.6	0.0004	-8.6	-42.2	0.0001	7.455	0.999999
500	17.692	-25.5	-6.8	-32.2	0.0006	-3.2	-35.4	0.0003	10.543	1
1000	35.385	-28.5	-5.8	-34.3	0.0004	0.0	-34.3	0.0004	14.911	1
2000	70.770	-31.5	-6.8	-38.3	0.0001	1.2	-37.1	0.0002	21.087	1
4000	141.539	-34.5	-8.7	-43.2	0.0000	1.0	-42.2	0.0001	29.821	1
8000	283.079	-37.5	-10.6	-48.1	0.0000	-1.1	-49.2	0.0000	42.174	1
				SUM =	0.0019		SUM =	0.0010		
				LEVEL =	-27.2		A LEVEL =	-30.0		

Table A1 (Cont'd)

MIC LOCATION: ANGLE (DEG) = 180.0 RANGE = 242.0
EDGE: TOP GUN @ -1
PATH LENGTH DELTA (m) = 7.66

OCTAVE BAND (HZ)	BAND FRESNEL NO.	BARRIER ATTEN (dB)	SOURCE FLAT LEVEL (dB)	NET FLAT LEVEL (dB)	10^L/10	A WTG (dB)	NET A WT LEVEL (dB)	10^L/10	ARG N2PI^1/2	TANH
63	2.815	-17.5	-25.8	-43.3	0.0000	-26.2	-69.5	0.0000	4.206	0.999555
125	5.586	-20.5	-17.3	-37.8	0.0002	-16.1	-53.9	0.0000	5.924	0.999986
250	11.171	-23.5	-11.2	-34.6	0.0003	-8.6	-43.2	0.0000	8.378	1
500	22.342	-26.5	-6.8	-33.2	0.0005	-3.2	-36.4	0.0002	11.848	1
1000	44.685	-29.5	-5.6	-35.3	0.0003	0.0	-35.3	0.0003	16.756	1
2000	89.369	-32.5	-6.8	-39.3	0.0001	1.2	-38.1	0.0002	23.696	1
4000	178.738	-35.5	-8.7	-44.2	0.0000	1.0	-43.2	0.0000	33.512	1
8000	357.476	-38.5	-10.6	-49.2	0.0000	-1.1	-50.3	0.0000	47.393	1
				SUM =	0.0015		SUM =	0.0008		
				LEVEL =	-28.3		A LEVEL =	-31.0		

MIC LOCATION: ANGLE (DEG) = 180.0 RANGE = 242.0
EDGE: LEFT SIDE WALL GUN @ -1
PATH LENGTH DELTA (m) = 11.26

OCTAVE BAND (HZ)	BAND FRESNEL NO.	BARRIER ATTEN (dB)	SOURCE FLAT LEVEL (dB)	NET FLAT LEVEL (dB)	10^L/10	A WTG (dB)	NET A WT LEVEL (dB)	10^L/10	ARG N2PI^1/2	TANH
63	4.135	-19.1	-25.8	-45.0	0.0000	-26.2	-71.2	0.0000	5.097	0.999925
125	8.204	-22.1	-17.3	-39.4	0.0001	-16.1	-55.5	0.0000	7.180	0.999999
250	16.408	-25.1	-11.2	-36.3	0.0002	-8.6	-44.9	0.0000	10.153	1
500	32.815	-28.1	-6.8	-34.9	0.0003	-3.2	-38.1	0.0002	14.359	1
1000	65.630	-31.2	-5.8	-37.0	0.0002	0.0	-37.0	0.0002	20.307	1
2000	131.260	-34.2	-6.8	-41.0	0.0001	1.2	-39.8	0.0001	28.718	1
4000	262.520	-37.2	-8.7	-45.9	0.0000	1.0	-44.9	0.0000	40.614	1
8000	525.040	-40.2	-10.6	-50.8	0.0000	-1.1	-51.9	0.0000	57.436	1
				SUM =	0.0010		SUM =	0.0005		
				LEVEL =	-29.9		A LEVEL =	-32.7		

Table A1 (Cont'd)

SUMMARY OF RESULTS FOR:
FREQUENCY WEIGHTING: A
GUN LOCATION (m): −1

MIC ANGLE (DEG)	RANGE (M)	INSERTION LOSS (dB) OVERALL DIR	OVERALL ISO	TOP ISO	TOP Do−Dj	TOP DIR	LEFT ISO	LEFT Do−Dj	LEFT DIR	RIGHT ISO	RIGHT Do−Dj	RIGHT DIR	MIC ANGLE (DEG)
90	150	9.1	9.7	19.3	−0.1	19.2	10.3	−0.7	9.6	34.7	−0.7	34.0	90
120	161	18.5	22.7	27.8	−4.1	23.7	24.7	−4.2	20.5	34.5	−4.2	30.3	120
150	279	19.1	25.9	29.9	−7.0	22.9	29.5	−6.8	22.7	33.7	−6.8	27.0	150
180	80	19.1	26.9	30.6	−8.1	22.6	32.3	−7.7	24.6	32.3	−7.7	24.6	180
180	242	18.9	26.8	30.5	−8.1	22.5	32.2	−7.7	24.5	32.2	−7.7	24.5	180

DESIGN SOURCE SPECTRUM RELATIVE LEVELS, FLAT AND A WEIGHTED

OCTAVE BAND (HZ)	REL FLAT LEVEL (dB)	10^L/10	A WTG ATTEN (dB)	BAND F+A	10^L/10	REL A WTD LEVEL (dB)	10^L/10
63	−25.8	0.0026	−26.2	−52.0	0.0000	−51.5	0.0000
125	−17.3	0.0185	−16.1	−33.4	0.0005	−32.9	0.0005
250	−11.2	0.0762	−8.6	−19.8	0.0105	−19.3	0.0119
500	−6.8	0.2103	−3.2	−10.0	0.1007	−9.4	0.1136
1000	−5.8	0.2627	0	−5.8	0.2627	−5.3	0.2965
2000	−6.8	0.2086	1.2	−5.6	0.2750	−5.1	0.3104
4000	−8.7	0.1347	1	−7.7	0.1696	−7.2	0.1915
8000	−10.6	0.0863	−1.1	−11.7	0.0670	−11.2	0.0756
	SUM =	1.0000		SUM =	0.8659	SUM =	1.0000
LOS FLAT LEVEL =		0.00	LOS A WTD LEVEL =		−0.53		0.0000

NOTE: LOS = LINE OF SIGHT, THE DIRECT PATH TO THE UNSHIELDED OBSERVER.

Table A1 (cont'd)

MIC LOCATION: ANGLE (DEG) = 120.0 RANGE = 161.0
EDGE: LEFT SIDE WALL GUN @ -1
PATH LENGTH DELTA (m) = 2.00

OCTAVE BAND (HZ)	BAND FRESNEL NO.	BARRIER ATTEN (dB)	SOURCE FLAT LEVEL (dB)	NET FLAT LEVEL (dB)	10^L/10	A WTG (dB)	NET A WT LEVEL (dB)	10^L/10	ARG N2PI^1/2	TANH
63	0.735	-11.9	-25.8	-37.7	0.0002	-26.2	-63.9	0.0000	2.150	0.97321
125	1.459	-14.7	-17.3	-32.0	0.0006	-16.1	-48.1	0.0000	3.028	0.995324
250	2.919	-17.6	-11.2	-28.8	0.0013	-8.6	-37.4	0.0002	4.282	0.999619
500	5.837	-20.6	-6.8	-27.4	0.0018	-3.2	-30.6	0.0009	6.056	0.999989
1000	11.674	-23.7	-5.8	-29.5	0.0011	0.0	-29.5	0.0011	8.565	1
2000	23.349	-26.7	-6.8	-33.5	0.0004	1.2	-32.3	0.0006	12.112	1
4000	46.697	-29.7	-8.7	-38.4	0.0001	1.0	-37.4	0.0002	17.129	1
8000	93.395	-32.7	-10.6	-43.3	0.0000	-1.1	-44.4	0.0000	24.224	1
				SUM =	0.0057		SUM =	0.0030		
				LEVEL =	-22.4		A LEVEL =	-25.2		

MIC LOCATION: ANGLE (DEG) = 120.0 RANGE = 161.0
EDGE: RIGHT SIDE WALL GUN @ -1
PATH LENGTH DELTA (m) = 19.26

OCTAVE BAND (HZ)	BAND FRESNEL NO.	BARRIER ATTEN (dB)	SOURCE FLAT LEVEL (dB)	NET FLAT LEVEL (dB)	10^L/10	A WTG (dB)	NET A WT LEVEL (dB)	10^L/10	ARG N2PI^1/2	TANH
63	7.075	-21.5	-25.8	-47.3	0.0000	-26.2	-73.5	0.0000	6.667	0.999997
125	14.038	-24.5	-17.3	-41.8	0.0001	-16.1	-57.9	0.0000	9.392	1
250	28.076	-27.5	-11.2	-38.6	0.0001	-8.6	-47.2	0.0000	13.282	1
500	56.153	-30.5	-6.8	-37.2	0.0002	-3.2	-40.4	0.0001	18.783	1
1000	112.305	-33.5	-5.8	-39.3	0.0001	0.0	-39.3	0.0001	26.564	1
2000	224.610	-36.5	-6.8	-43.3	0.0000	1.2	-42.1	0.0001	37.567	1
4000	449.221	-39.5	-8.7	-48.2	0.0000	1.0	-47.2	0.0000	53.128	1
8000	898.441	-42.5	-10.8	-53.2	0.0000	-1.1	-54.3	0.0000	75.134	1
				SUM =	0.0006		SUM =	0.0003		
				LEVEL =	-32.3		A LEVEL =	-35.0		

Table A1 (Cont'd)

MIC LOCATION: ANGLE (DEG) = 180.0 RANGE = 80.0
EDGE: LEFT SIDE WALL GUN @ -1
PATH LENGTH DELTA (m) = 11.66

OCTAVE BAND (HZ)	BAND FRESNEL NO.	BARRIER ATTEN (dB)	SOURCE FLAT LEVEL (dB)	NET FLAT LEVEL (dB)	10^L/10	A WTG (dB)	NET A WT LEVEL (dB)	10^L/10	ARG N2PI^1/2	TANH
63	4.285	-19.3	-25.8	-45.1	0.0000	-26.2	-71.3	0.0000	5.189	0.999938
125	8.502	-22.3	-17.3	-39.6	0.0001	-16.1	-55.7	0.0000	7.309	0.999999
250	17.004	-25.3	-11.2	-36.5	0.0002	-8.6	-45.1	0.0000	10.336	1
500	34.008	-28.3	-6.8	-35.1	0.0003	-3.2	-38.3	0.0001	14.618	1
1000	68.016	-31.3	-5.8	-37.1	0.0002	0.0	-37.1	0.0002	20.673	1
2000	136.033	-34.3	-6.8	-41.1	0.0001	1.2	-39.9	0.0001	29.236	1
4000	272.066	-37.3	-8.7	-46.0	0.0000	1.0	-45.0	0.0000	41.345	1
8000	544.132	-40.3	-10.6	-51.0	0.0000	-1.1	-52.1	0.0000	58.471	1
				SUM =	0.0010		SUM =	0.0005		
				LEVEL =	-30.1		A LEVEL =	-32.9		

MIC LOCATION: ANGLE (DEG) = 180.0 RANGE = 80.0
EDGE: RIGHT SIDE WALL GUN @ -1
PATH LENGTH DELTA (m) = 11.66

OCTAVE BAND (HZ)	BAND FRESNEL NO.	BARRIER ATTEN (dB)	SOURCE FLAT LEVEL (dB)	NET FLAT LEVEL (dB)	10^L/10	A WTG (dB)	NET A WT LEVEL (dB)	10^L/10	ARG N2PI^1/2	TANH
63	4.285	-19.3	-25.8	-45.1	0.0000	-26.2	-71.3	0.0000	5.189	0.999938
125	8.502	-22.3	-17.3	-39.6	0.0001	-16.1	-55.7	0.0000	7.309	0.999999
250	17.004	-25.3	-11.2	-36.5	0.0002	-8.6	-45.1	0.0000	10.336	1
500	34.008	-28.3	-6.8	-35.1	0.0003	-3.2	-38.3	0.0001	14.618	1
1000	68.016	-31.3	-5.8	-37.1	0.0002	0.0	-37.1	0.0002	20.673	1
2000	136.033	-34.3	-6.8	-41.1	0.0001	1.2	-39.9	0.0001	29.236	1
4000	272.066	-37.3	-8.7	-46.0	0.0000	1.0	-45.0	0.0000	41.345	1
8000	544.132	-40.3	-10.6	-51.0	0.0000	-1.1	-52.1	0.0000	58.471	1
				SUM =	0.0010		SUM =	0.0005		
				LEVEL =	-30.1		A LEVEL =	-32.9		

Table A1 (Cont'd)

MIC LOCATION: ANGLE (DEG) =				180.0		RANGE =	242.0			
EDGE: RIGHT SIDE WALL						GUN @	-1			
PATH LENGTH DELTA (m) =				11.26						
OCTAVE BAND (HZ)	BAND FRESNEL NO.	BARRIER ATTEN (dB)	SOURCE FLAT LEVEL (dB)	NET FLAT LEVEL (dB)	10^L/10	A WTG (dB)	NET A WT LEVEL (dB)	10^L/10	ARG N2PI^1/2	TANH
63	4.135	-19.1	-25.8	-45.0	0.0000	-26.2	-71.2	0.0000	5.097	0.999925
125	8.204	-22.1	-17.3	-39.4	0.0001	-16.1	-55.5	0.0000	7.180	0.999999
250	16.408	-25.1	-11.2	-36.3	0.0002	-8.6	-44.9	0.0000	10.153	1
500	32.815	-28.1	-6.8	-34.9	0.0003	-3.2	-38.1	0.0002	14.359	1
1000	65.630	-31.2	-5.8	-37.0	0.0002	0.0	-37.0	0.0002	20.307	1
2000	131.260	-34.2	-6.8	-41.0	0.0001	1.2	-39.8	0.0001	28.718	1
4000	262.520	-37.2	-8.7	-45.9	0.0000	1.0	-44.9	0.0000	40.614	1
8000	525.040	-40.2	-10.6	-50.8	0.0000	-1.1	-51.9	0.0000	57.436	1
				SUM =	0.0010		SUM =	0.0005		
				LEVEL =	-29.9		A LEVEL =	-32.7		

Table A2

Summary of Calculated Results for Various Combinations of Gun Location, Direction of Fire and Frequency Weighting

FIRING SHED FOR SMALL ARMS
CALCULATED BARRIER INSERTION LOSS USING FHWA DIFFRACTION ALGORITHM,
WITH CORRECTION FOR SOURCE DIRECTIVITY, GUN FIRING SOUTH.
GUN DIRECTIVITY: D = 14*(1+COS (THETA))/2 re 180 DEG FROM LINE OF FIRE.
GUN LOCATION (m): −1 FREQUENCY WEIGHTING: FLAT

MIC ANGLE (DEG)	RANGE (M)	********** INSERTION LOSS (dB) ********** OVERALL DIR	OVERALL ISO	TOP ISO	TOP Do−Dj	TOP DIR	LEFT ISO	LEFT Do−Dj	LEFT DIR	RIGHT ISO	RIGHT Do−Dj	RIGHT DIR	MIC ANGLE (DEG)
90	150	8.0	8.6	17.2	−0.1	17.1	9.3	−0.7	8.6	32.4	−0.7	31.7	90
120	161	16.2	20.4	25.5	−4.1	21.4	22.4	−4.2	18.2	32.3	−4.2	28.1	120
150	279	16.8	23.6	27.6	−7.0	20.7	27.2	−6.8	20.5	31.5	−6.8	24.7	150
180	80	16.8	24.7	28.4	−8.1	20.3	30.1	−7.7	22.4	30.1	−7.7	22.4	180
180	242	16.7	24.5	28.3	−8.1	20.2	29.9	−7.7	22.2	29.9	−7.7	22.2	180

FIRING SHED FOR SMALL ARMS
CALCULATED BARRIER INSERTION LOSS USING FHWA DIFFRACTION ALGORITHM,
WITH CORRECTION FOR SOURCE DIRECTIVITY, GUN FIRING SOUTH.
GUN DIRECTIVITY: D = 14*(1+COS (THETA))/2 re 180 DEG FROM LINE OF FIRE.
GUN LOCATION (m): −1 FREQUENCY WEIGHTING: A

MIC ANGLE (DEG)	RANGE (M)	********** INSERTION LOSS (dB) ********** OVERALL DIR	OVERALL ISO	TOP ISO	TOP Do−Dj	TOP DIR	LEFT ISO	LEFT Do−Dj	LEFT DIR	RIGHT ISO	RIGHT Do−Dj	RIGHT DIR	MIC ANGLE (DEG)
90	150	9.1	9.7	19.3	−0.1	19.2	10.3	−0.7	9.6	34.7	−0.7	34.0	90
120	161	18.5	22.7	27.8	−4.1	23.7	24.7	−4.2	20.5	34.5	−4.2	30.3	120
150	279	19.1	25.9	29.9	−7.0	22.9	29.5	−6.8	22.7	33.7	−6.8	27.0	150
180	80	19.1	26.9	30.6	−8.1	22.6	32.3	−7.7	24.6	32.3	−7.7	24.6	180
180	242	18.9	26.8	30.5	−8.1	22.5	32.2	−7.7	24.5	32.2	−7.7	24.5	180

FIRING SHED FOR SMALL ARMS
CALCULATED BARRIER INSERTION LOSS USING FHWA DIFFRACTION ALGORITHM,
WITH CORRECTION FOR SOURCE DIRECTIVITY, GUN FIRING WEST.
GUN DIRECTIVITY: D = 14*(1+COS (THETA))/2 re 180 DEG FROM LINE OF FIRE.
GUN LOCATION (m): -1 FREQUENCY WEIGHTING: FLAT

MIC ANGLE (DEG)	RANGE (M)	********** INSERTION LOSS (dB) ********** OVERALL DIR	OVERALL ISO	TOP ISO	TOP Do-Dj	TOP DIR	LEFT ISO	LEFT Do-Dj	LEFT DIR	RIGHT ISO	RIGHT Do-Dj	RIGHT DIR	MIC ANGLE (DEG)
90	150	8.2	8.6	17.2	-0.0	17.2	9.3	-0.0	9.2	32.4	-14.0	18.5	90
120	161	17.1	20.4	25.5	-0.1	25.3	22.4	0.9	23.3	32.3	-13.0	19.2	120
150	279	19.8	23.6	27.6	-0.1	27.6	27.2	3.5	30.7	31.5	-10.5	21.0	150
180	80	21.8	24.7	28.4	0.0	28.4	30.1	7.0	37.0	30.1	-7.0	23.1	180
180	242	21.7	24.5	28.3	0.0	28.3	29.9	7.0	36.9	29.9	-7.0	23.0	180

FIRING SHED FOR SMALL ARMS
CALCULATED BARRIER INSERTION LOSS USING FHWA DIFFRACTION ALGORITHM,
WITH CORRECTION FOR SOURCE DIRECTIVITY, GUN FIRING WEST.
GUN DIRECTIVITY: D = 14*(1+COS (THETA))/2 re 180 DEG FROM LINE OF FIRE.
GUN LOCATION (m): -1 FREQUENCY WEIGHTING: A

MIC ANGLE (DEG)	RANGE (M)	********** INSERTION LOSS (dB) ********** OVERALL DIR	OVERALL ISO	TOP ISO	TOP Do-Dj	TOP DIR	LEFT ISO	LEFT Do-Dj	LEFT DIR	RIGHT ISO	RIGHT Do-Dj	RIGHT DIR	MIC ANGLE (DEG)
90	150	9.4	9.7	19.3	-0.0	19.3	10.3	-0.0	10.2	34.7	-14.0	20.7	90
120	161	19.4	22.7	27.8	-0.1	27.6	24.7	0.9	25.6	34.5	-13.0	21.5	120
150	279	22.0	25.9	29.9	-0.1	29.8	29.5	3.5	33.0	33.7	-10.5	23.3	150
180	80	24.1	26.9	30.6	0.0	30.6	32.3	7.0	39.3	32.3	-7.0	25.4	180
180	242	24.0	26.8	30.5	0.0	30.5	32.2	7.0	39.2	32.2	-7.0	25.2	180

Table A2 (Cont'd)

FIRING SHED FOR SMALL ARMS
CALCULATED BARRIER INSERTION LOSS USING FHWA DIFFRACTION ALGORITHM,
WITH CORRECTION FOR SOURCE DIRECTIVITY, GUN FIRING WEST.
GUN DIRECTIVITY: D = 14*(1+COS (THETA))/2 re 180 DEG FROM LINE OF FIRE.
GUN LOCATION (m): 5 FREQUENCY WEIGHTING: FLAT

MIC ANGLE (DEG)	RANGE (M)	********** INSERTION LOSS (dB) ********** OVERALL DIR	OVERALL ISO	TOP ISO	TOP Do-Dj	TOP DIR	LEFT ISO	LEFT Do-Dj	LEFT DIR	RIGHT ISO	RIGHT Do-Dj	RIGHT DIR	MIC ANGLE (DEG)
90	150	0.0	0.0	0.0	0.0	0.0	0.0	0.0	0.0	0.0	0.0	0.0	90
120	161	7.2	7.3	21.9	-0.1	21.8	7.5	0.2	7.7	31.9	-12.3	19.5	120
150	279	17.9	19.6	24.0	-0.0	23.9	22.3	2.8	25.0	30.2	-9.8	20.5	150
180	80	19.7	21.8	24.8	0.0	24.8	27.8	6.3	34.0	27.8	-6.3	21.5	180
180	242	19.4	21.5	24.6	0.0	24.6	27.5	6.3	33.7	27.5	-6.3	21.2	180

FIRING SHED FOR SMALL ARMS
CALCULATED BARRIER INSERTION LOSS USING FHWA DIFFRACTION ALGORITHM,
WITH CORRECTION FOR SOURCE DIRECTIVITY, GUN FIRING WEST.
GUN DIRECTIVITY: D = 14*(1+COS (THETA))/2 re 180 DEG FROM LINE OF FIRE.
GUN LOCATION (m): 5 FREQUENCY WEIGHTING: A

MIC ANGLE (DEG)	RANGE (M)	********** INSERTION LOSS (dB) ********** OVERALL DIR	OVERALL ISO	TOP ISO	TOP Do-Dj	TOP DIR	LEFT ISO	LEFT Do-Dj	LEFT DIR	RIGHT ISO	RIGHT Do-Dj	RIGHT DIR	MIC ANGLE (DEG)
90	150	0.0	0.0	0.0	0.0	0.0	0.0	0.0	0.0	0.0	0.0	0.0	90
120	161	7.9	7.9	24.1	-0.1	24.1	8.0	0.2	8.2	34.1	-12.3	21.8	120
150	279	20.2	21.9	26.2	-0.0	26.2	24.5	2.8	27.3	32.5	-9.8	22.7	150
180	80	21.9	24.0	27.1	0.0	27.1	30.0	6.3	36.3	30.0	-6.3	23.8	180
180	242	21.7	23.8	26.8	0.0	26.8	29.7	6.3	36.0	29.7	-6.3	23.5	180

Table A3

Insertion Loss at 180° vs Source Location, for Structure of Infinite Length, Structure Height 7 m, Source Height 0.5m

SOURCE LOCATION S (m)	INSERTION LOSS AT 180°, 242 meters. FLAT DIR (dB)	FLAT ISO (dB)	A WTD DIR (dB)	A WTD ISO (dB)	DIR EFFECT (dB)
−30	23.4	37.2	25.7	39.5	−13.8
−25	22.7	36.5	25.0	38.7	−13.8
−20	21.9	35.6	24.2	37.8	−13.7
−15	21.0	34.4	23.2	36.6	−13.4
−10	20.0	32.8	22.2	35.1	−12.9
−9	19.8	32.5	22.0	34.7	−12.7
−8	19.6	32.1	21.9	34.3	−12.4
−7	19.5	31.6	21.8	33.9	−12.1
−6	19.4	31.2	21.7	33.4	−11.7
−5	19.4	30.6	21.6	32.9	−11.3
−4	19.4	30.1	21.7	32.4	−10.7
−3	19.6	29.5	21.8	31.8	−9.9
−2	19.8	28.9	22.1	31.2	−9.1
−1	20.2	28.3	22.5	30.5	−8.1
0	20.6	27.6	22.9	29.9	−7.0
1	21.0	26.9	23.3	29.2	−5.9
2	21.4	26.3	23.6	28.6	−4.9
3	21.6	25.7	23.9	28.0	−4.1
4	21.8	25.1	24.0	27.4	−3.3
5	21.9	24.6	24.1	26.8	−2.7
6	21.8	24.1	24.1	26.4	−2.3
7	21.8	23.6	24.0	25.9	−1.9
8	21.7	23.2	23.9	25.5	−1.6
9	21.5	22.8	23.8	25.1	−1.3
10	21.3	22.5	23.6	24.7	−1.1
15	20.4	21.0	22.7	23.3	−0.6
20	19.6	20.0	21.8	22.2	−0.3
25	18.9	19.2	21.1	21.4	−0.2
30	18.4	18.5	20.5	20.7	−0.2
35	17.9	18.0	20.0	20.1	−0.1
40	17.5	17.5	19.6	19.7	−0.1

Table A4

Insertion Loss at 180° vs. Source Location, for Structure Length of 20 m, Structure Height 0.5 m

SOURCE LOCATION S (m)	INSERTION LOSS AT 180°, 242 meters. FLAT DIR (dB)	FLAT ISO (dB)	A WTD DIR (dB)	A WTD ISO (dB)	DIR EFFECT (dB)
−30	18.8	32.5	21.1	34.8	−13.7
−25	18.2	31.8	20.4	34.0	−13.6
−20	17.5	30.9	19.7	33.1	−13.4
−15	16.7	29.8	19.0	32.0	−13.0
−10	16.1	28.4	18.3	30.6	−12.3
−9	16.0	28.0	18.2	30.3	−12.1
−8	15.9	27.7	18.1	29.9	−11.8
−7	15.8	27.3	18.1	29.5	−11.5
−6	15.8	26.9	18.1	29.1	−11.1
−5	15.9	26.5	18.1	28.7	−10.6
−4	16.0	26.0	18.2	28.3	−10.0
−3	16.1	25.5	18.4	27.8	−9.4
−2	16.4	25.0	18.6	27.3	−8.7
−1	16.7	24.5	18.9	26.8	−7.9
0	17.0	24.0	19.3	26.3	−7.0
1	17.3	23.5	19.6	25.7	−6.1
2	17.6	23.0	19.9	25.2	−5.3
3	17.9	22.4	20.1	24.7	−4.6
4	18.1	22.0	20.3	24.2	−3.9
5	18.2	21.5	20.4	23.8	−3.3
6	18.2	21.1	20.5	23.3	−2.9
7	18.2	20.7	20.5	22.9	−2.5
8	18.2	20.3	20.4	22.6	−2.1
9	18.1	19.9	20.4	22.2	−1.8
10	18.0	19.6	20.3	21.9	−1.6
15	17.4	18.3	19.6	20.5	−0.9
20	16.7	17.2	18.9	19.5	−0.5
25	16.1	16.4	18.3	18.7	−0.4
30	15.5	15.8	17.7	18.0	−0.3
35	15.1	15.3	17.3	17.5	−0.2
40	14.7	14.8	16.9	17.0	−0.1

APPENDIX B:

An Evaluation of Insertion Loss
by a Rigorous Diffraction Algorithm

University of Illinois at Urbana-Champaign and Environmental Acoustics Team, U.S. Army Construction Engineering Research Lab, P.O. Box 9005, Champaign IL 61866-9005

INTRODUCTION

Community annoyance due to rifle fire on military bases has long been a subject of concern. It has been suggested that a shelter erected near the gun could effectively reduce blast noise in specific regions behind the shelter. A series solution for the field intensities exists for a spherical shelter with a semicircular aperture, which is assumed to be a reasonable model for a more practical, rectilinear structure of the same general dimensions. This solution then allows comparison of shelter effectiveness for various shelter configurations, while considering source spectral power distribution and directivity. This paper shows the results of computations for two structures, using a model sound source typical of rifle fire noise.

THEORY

To evaluate the effectiveness of such a structure, several simplyfying assumptions are made. The model investigated is hemispherical shell with a portion of its surface vibrating, which is representative of the sound source, and a rigid section representative of the shelter itself (see Figure B1.) Although a spherical shelter may be impractical for actual construction, investigation of such a structure should yield results similar to those achieved from a rectilinear structure, as sound diffraction around an object depends more on the general dimensions of the structure than the actual details of construction. Further, the ground is assumed to be perfectly reflecting, so that by symmetry this case can be treated as if it were in unbounded space.

This spherical diffraction problem was solved for special cases more than 100 years ago and has been described by many authors; this paper presents an extension of that solution. The sound source is described as an axially symmetric function of radial particle velocities at the surface of the shell; these velocities are zero everywhere except for a constant velocity u_0 from zero degrees to the azimuthal angle of the aperture θ_0 (the dashed lines in Figure B1):

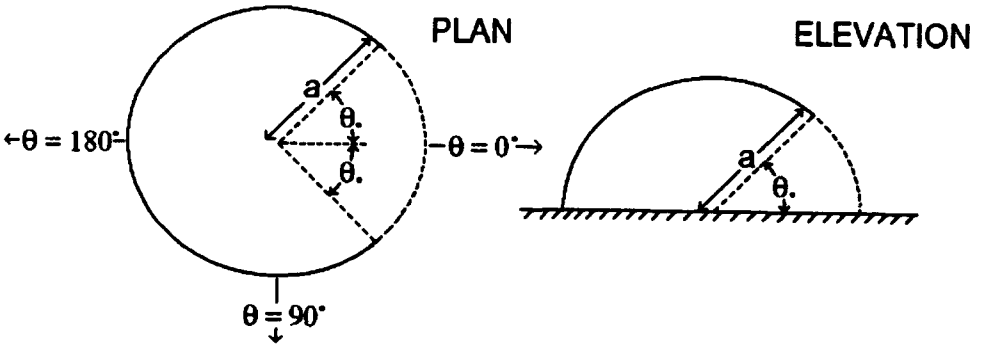

Figure B1. Plan and Elevation Diagrams of a Spherical Acoustic Shelter.

$$U(\theta)=\begin{cases} u_0, & 0\le\theta<\theta_0 \\ 0, & \theta_0<\theta\le\pi \end{cases} \qquad \text{[Eq B1]}$$

The surface velocity function is expanded into a series of Legendre functions:

$$U(\theta)=\sum_{m=0}^{\infty} U_m P_m(\cos\theta) \qquad \text{[Eq B2]}$$

where the coefficients U_m are found from the integral

$$U_m=(m+1/2)\int_0^{\pi} U(\theta)\, P_m(\cos\theta)\sin\theta\, d\theta\,. \qquad \text{[Eq B3]}$$

For the velocity function given by [Eq 2], this integral has the value

$$U_m=\frac{1}{2}u_0\left[P_{m-1}(\cos\theta_0)-P_{m+1}(\cos\theta_0)\right]. \qquad \text{[Eq B4]}$$

The radiated pressure wave is described by the axially symmetric spherical wavefunction. This wavefunction may be separated into radial and azimuthal components, which are Hankel functions and Legendre functions, respectively, and expanded as a series of these functions:

$$p=\sum_{m=0}^{\infty} A_m P_m(\cos\theta)\, h_m(kr)\, e^{-i\omega t} \qquad \text{[Eq B5]}$$

The expansion coefficients A_m are found from the U_m by utilizing the boundary condition of particle velocity at the surface of the sphere, found from the gradient of the pressure:

$$u_a=\frac{-i}{\rho\omega}\sum_{m=0}^{\infty} A_m P_m(\cos\theta)\,\frac{d}{dr}h_m(kr)\Big|_{r=a}\, e^{-i\omega t} \qquad \text{[Eq B6]}$$

where

$$\frac{d}{dr}h_m(kr)=\frac{k}{2m+1}\left[m\,h_{m-1}(kr)-(m+1)h_{m+1}(kr)\right] \qquad \text{[Eq B7]}$$

Equating the surface velocity [Eq 2] and particle velocity [Eq 6] series term by term yields an expression for the expansion coefficients A_m in [Eq 5]:

$$A_m=i\rho c U_m\frac{(2m+1)}{m\,h_{m-1}(ka)-(m+1)\,h_{m+1}(ka)} \qquad \text{[Eq B8]}$$

To obtain results for a specific gun, field intensities for each one-third octave band center frequency component in the spectrum are calculated and superimposed, weighted according to the spectrum. The spectrum used in the examples in this paper is shown in Figure B2, and is assumed to be representative of rifle fire.

To simulate source directivity, the velocity function $U(\theta)$ was modified to correspond to a typical rifle directivity pattern (shown in Figure B3, expressed in terms of normalized particle velocity.) The directivity pattern was approximated by 10 constant velocity sections to facilitate the computation of the U_m in [Eq 3].

As the source frequency increases, the pressure wave [Eq 5] must be calculated to higher orders to maintain a desired level of accuracy. The order of calculation was determined by observing the approximate order past which the results were stable. Summations involving from 25 to 1000 terms were

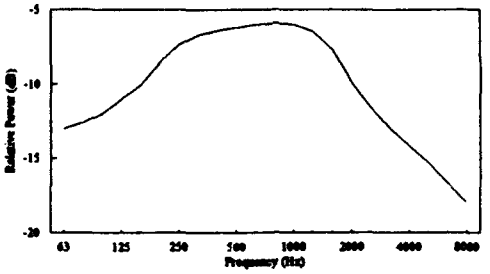

Figure B2. Assumed small arms spectrum.

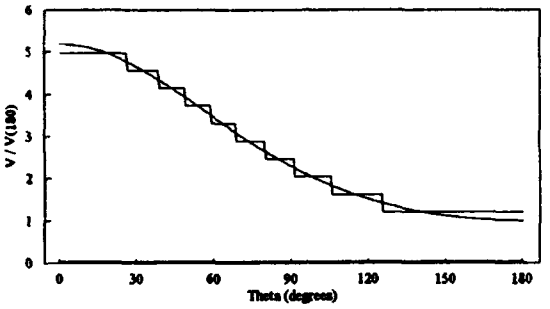

Figure B3. Assumed rifle directivity pattern and step approximations.

needed, which necessitated the careful computation of the intrinsic functions involved in the calculations. The computations were performed on a 80386-based microcomputer with a math coprocessor operating at 16 MHz; up to 6 hours were required for the broad spectrum, high frequency cases.

The results are plotted in two ways: as directivity patterns obtained by plotting the field intensities in dB, normalized to the maximum intensity in each case; and as insertion loss for each structure. The insertion loss may be found by utilizing field intensities calculated for a structure with a 180 degree aperture, representative of an open source. With the assumptions that the inside of the structure investigated is perfectly absorbing and that the source is unaffected by the addition of the shelter, insertion loss is calculated as the ratio of the field intensities for the open source and the source/structure combination. In the plots, 0 degrees is directly downrange and 180 degrees is in the rearward direction.

RESULTS

Two types of structures were investigated. The first was a quarter sphere (aperture angle of 90 degrees) with a radius of 7 m, referred to in the figures as the *Enclosure*. This is roughly representative of an open shed 7 m high and 14 m wide, which are the dimensions of an existing structure for which field data is available. For comparison, the second was a structure with an aperture angle of 125.5 degrees and a radius of 8.6 m, which roughly models a wall 7 m high and 14 m wide, and is referred to as the *Wall*.

Figures B4 and B5 show the composite results for an isotropic and a directional source, respectively, using third octave frequencies between 63 Hz and 8 kHz weighted according to Figure B2. Results from both the structures are shown together for direct comparison. The results are plotted as a directivity pattern of intensity radiating from the shed; the values are normalized to the maximum sound intensity for each case and presented on a dB scale.

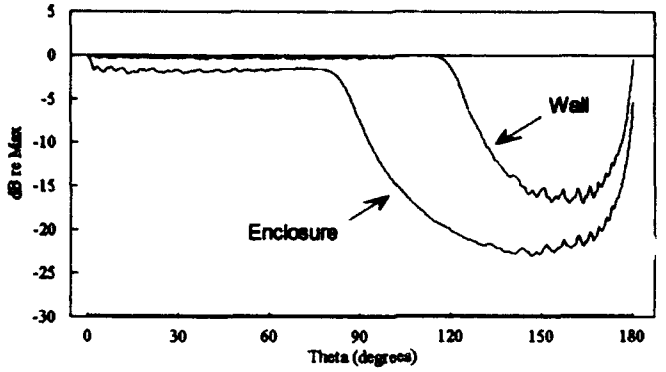

Figure B4. Structural directivity patterns for the composite isotropic source.

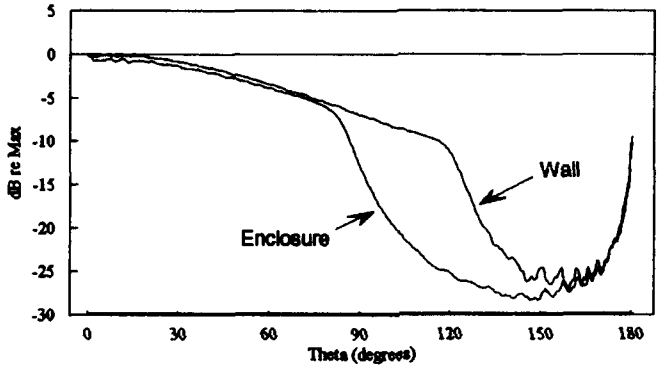

Figure B5. Structural directivity patterns for the composite directional source.

For the isotropic source inside the enclosure, the greatest sound reduction from maximum is about 23 dB around 145 degrees, and for the wall, intensities are down by a maximum of 17 dB at about 160 degrees. For the directional source, the enclosure performs better than the wall by only about 1 dB, with a greatest reduction of 28 dB at 150 degrees. The directive source/wall combination has a maximum reduction of 27 dB at 160 degrees.

Plots of structural insertion loss calculated in the manner described above are shown in Figures B6 and B7 for an isotropic source and a directional source, respectively. As was indicated in the structure directivity plots, the enclosure significantly outperforms the wall in terms of insertion loss for the isotropic source. The enclosure offers a maximum of 21 dB protection around 145 degrees, while the maximum reduction for the wall is 17 dB at about 160 degrees. For the directional source, however, the best performance of the two structures differs by only about 1 dB. The enclosure shows a maximum insertion loss of 15 dB at 145 degrees, and the wall's best performance is 14 dB around 160 degrees. It is perhaps not intuitively obvious that source directivity should greatly alter the relative performance of the two structures. However, similar results have been found from field measurements,[1] which suggests that source directivity must be considered to effectively model noise mitigation potential.

Although maximum protection for a directional source is approximately the same for both structures, it should be noted that the enclosure shields a broader range of angles than the wall. For the enclosure, insertion loss is above 10 dB from 100 degrees to 170 degrees. For the wall, such protection exists only from 100 degrees to 135 degrees.

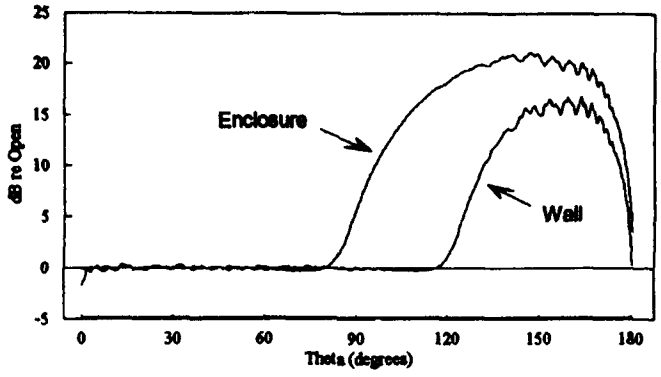

Figure B6. Structural insertion loss for the isotropic source.

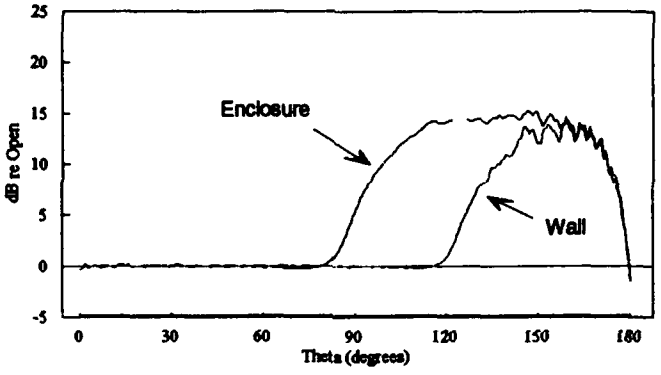

Figure B7. Structural insertion loss for the directional source.

CONCLUSIONS

This mathematical solution is a powerful tool for analysis of the relative noise reduction potential of various acoustical shelter configurations. Since it allows the consideration of the source power distribution spectrum and the source directivity, a specific situation can be effectively modeled, which should prove useful in designing and positioning acoustic shelters.

ACKNOWLEDGEMENT

This work was performed at the U.S. Army Construction Engineering Research Laboratory. The problem was suggested by Dr. Larry L. Pater, and Prof. G.W. Swenson, Jr. outlined the theoretical approach. Hong C. Zuang performed some initial computations.

REFERENCES

1. Lord Rayleigh, *Theory of Sound*, Vol 2 (Dover Publications, New York, 1945).

2. P.M. Morse, *Vibration and Sound*, (McGraw-Hill, New York, 1936).

3. L.L. Pater, unpublished data, (USACERL, P.O. Box 9005, Champaign IL).

APPENDIX C: Effect of Atmospheric Absorption on the Source Spectrum

Absorption of sound energy by the atmosphere affects spectrum shape because the atmosphere more strongly attenuates higher frequencies. The degree to which a spectrum is modified can be estimated by means of a standardized algorithm[1]. The amount of attenuation depends on frequency, distance from the source, and ambient barometric pressure, air temperature and relative humidity. Table C1 shows the amount of attenuation for each octave band for conditions similar to those of the experiments described in this report. The effect on these attenuation values on the source spectrum is shown in Figure C1. Experimental source to microphone distances ranged from 80 to 284 meters. It is seen that the effect of atmospheric absorption is small for all octave bands below the 8000 Hz band.

[1] *American National Standard: Method for the Calculation of the Absorption of Sound by the Atmosphere*, ANSI S1.26-1978 (American National Standards Institute, 1978).

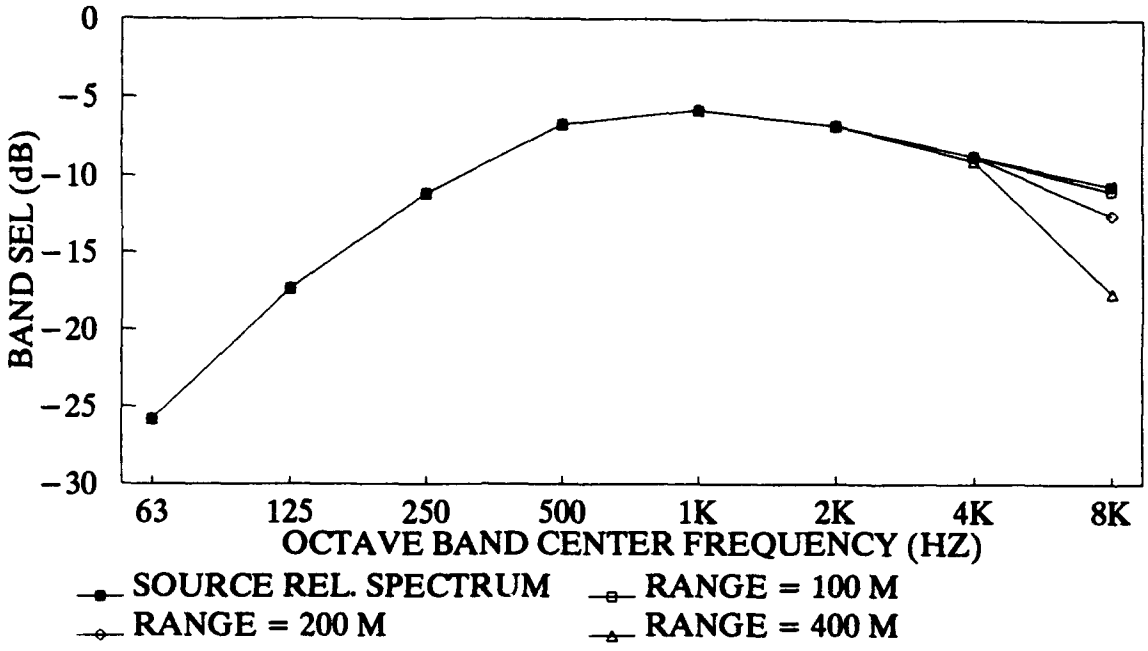

Figure C1. Effect of Atmospheric Absorption on Source Spectrum at Several Distances.

Table C1

Attenuation Due to Atmospheric Absorption for Several Propogation Distances, T= 20 °C, 70% Relative Humidity, Standard Sea Level Pressure.

OCTAVE BAND (HZ)	ATTENUATION (dB) AT		
	100 M	200 M	400 M
63	0.0	0.0	0.0
125	0.0	0.0	0.0
250	0.0	0.0	0.0
500	0.0	0.0	0.0
1K	0.0	0.0	0.0
2K	0.0	0.0	0.0
4K	0.0	0.0	0.3
8K	0.3	1.9	7.0

USACERL DISTRIBUTION

Chief of Engineers
ATTN: CEHEC-IM-LH (2)
ATTN: CEHEC-IM-LP (2)
ATTN: CECG
ATTN: CERD-M
ATTN: CECC-P
ATTN: CERD-L
ATTN: CECW-P
ATTN: CECW-PR
ATTN: CEMP-E
ATTN: CEMP-C
ATTN: CECW-O
ATTN: CECW
ATTN: CERM
ATTN: CEMP
ATTN: CERD-C
ATTN: CEMP-M
ATTN: CEMP-R
ATTN: CERD-ZA
ATTN: DAEN-ZCE
ATTN: DAIM-FDP

CECPW
ATTN: CECPW-F 22060
ATTN: CECPW-TT 22060
ATTN: CECPW-ZC 22060
ATTN: DET III 79906

US Army Engr District
ATTN: Library (40)

US Army Engr Division
ATTN: Library (13)

US Army Europe
ATTN: AEAEN-EH 09014
ATTN: AEAEN-ODCS 09014
29th Area Support Group
ATTN: AERAS-FA 09054
100th Support Group
ATTN: AETT-EN-DPW 09114
222d Base Battalion
ATTN: AETV-BHR-E 09034
235th Base Support Battalion
ATTN: Unit 28614 Ansbach 09177
293d Base Support Battalion
ATTN: AEUSG-MA-AST-WO-E 09086
409th Support Battalion (Base)
ATTN: AETTG-DPW 09114
412th Base Support Battalion 09630
ATTN: Unit 31401
Frankfurt Base Support Battalion
ATTN: Unit 25727 09242
CMTC Hohenfels 09173
ATTN: AETTH-DPW
Mainz Germany 09185
ATTN: BSB-MZ-E
21st Support Command
ATTN: DPW (10)
US Army Berlin
ATTN: AEBA-EH 09235
ATTN: AEBA-EN 09235
SETAF
ATTN: AESE-EN-D 09613
ATTN: AESE-EN 09630
Supreme Allied Command
ATTN: ACSGEB 09703
ATTN: SHIHB/ENGR 09705

INSCOM
ATTN: IALOG-I 22060
ATTN: IAV-DPW 22186

USA TACOM 48090
ATTN: AMSTA-XE

Defense Distribution Region East
ATTN: DDRE-WI 17070

HQ XVIII Airborne Corps 28307
ATTN: AFZA-DPW-EE

4th Infantry Div (MECH)
ATTN: AFZC-FE

US Army Materiel Command (AMC)
Alexandria, VA 22333-0001
ATTN: AMCEN-F
Installations: (19)

FORSCOM
Forts Gillem & McPherson 30330
ATTN: FCEN
Installations: (23)

6th Infantry Division (Light)
ATTN: APVR-DE 99505
ATTN: APVR-WF-DE 99703

TRADOC
Fort Monroe 23651
ATTN: ATBO-G
Installations: (20)

Fort Belvoir 22060
ATTN: CETEC-IM-T
ATTN: CECC-R 22060
ATTN: Engr Strategic Studies Ctr
ATTN: Water Resources Support Ctr
ATTN: Australian Liaison Office

USA Natick RD&E Center 01760
ATTN: STRNC-DT
ATTN: DRDNA-F

US Army Materials Tech Lab
ATTN: SLCMT-DPW 02172

USARPAC 96858
ATTN: DPW
ATTN: APEN-A

SHAPE 09705
ATTN: Infrastructure Branch LANDA

Area Engineer, AEDC-Area Office
Arnold Air Force Station, TN 37389

HQ USEUCOM 09128
ATTN: ECJ4-LIE

AMMRC 02172
ATTN: DRXMR-AF
ATTN: DRXMR-WE

CEWES 39180
ATTN: Library

CECRL 03755
ATTN: Library

USA AMCOM
ATTN: Facilities Engr 21719
ATTN: AMSMC-EH 61299
ATTN: Facilities Engr (3) 85613

USAARMC 40121
ATTN: ATZIC-EHA

Military Traffic Mgmt Command
ATTN: MTEA-GB-EHP 07002
ATTN: MT-LOF 20315
ATTN: MTE-SU-FE 28461
ATTN: MTW-IE

Fort Leonard Wood 65473
ATTN: ATSE-DAC-LB (3)
ATTN: ATZA-TE-SW
ATTN: ATSE-CFLO
ATTN: ATSE-DAC-FL

Military Dist of WASH
Fort McNair
ATTN: ANEN 20319

USA Engr Activity, Capital Area
ATTN: Library 22211

US Army ARDEC 07806
ATTN: SMCAR-ISE

Engr Societies Library
ATTN: Acquisitions 10017

Defense Nuclear Agency
ATTN: NADS 20305

Defense Logistics Agency
ATTN: DLA-WI 22304

Walter Reed Army Medical Ctr 20307

National Guard Bureau 20310
ATTN: NGB-ARI

US Military Academy 10966
ATTN: MAEN-A
ATTN: Facilities Engineer
ATTN: Geography & Envr Engrg

Naval Facilities Engr Command
ATTN: Facilities Engr Command (8)
ATTN: Division Offices (11)
ATTN: Public Works Center (8)
ATTN: Naval Constr Battalion Ctr 93043
ATTN: Naval Civil Engr Service Center 93043

8th US Army Korea
ATTN: DPW (12)

USA Japan (USARJ)
ATTN: APAJ-EN-ES 96343
ATTN: HONSHU 96343
ATTN: DPW-Okinawa 96376

416th Engineer Command 60623
ATTN: Gibson USAR Ctr

US Army HSC
Fort Sam Houston 78234
ATTN: HSLO-F
Fitzsimons Army Medical Ctr
ATTN: HSHG-DPW 80045

Tyndall AFB 32403
ATTN: HQAFCESA Program Ofc
ATTN: Engrg & Srvc Lab

USA TSARCOM 63120
ATTN: STSAS-F

American Public Works Assoc. 64104-1806

US Army Envr Hygiene Agency
ATTN: HSHB-ME 21010

US Gov't Printing Office 20401
ATTN: Rec Sec/Deposit Sec (2)

Nat'l Institute of Standards & Tech
ATTN: Library 20899

Defense Tech Info Center 22304
ATTN: DTIC-FAB (2)

284
2/94

☆ U.S. GOVERNMENT PRINTING OFFICE: [illegible]510-S/00029